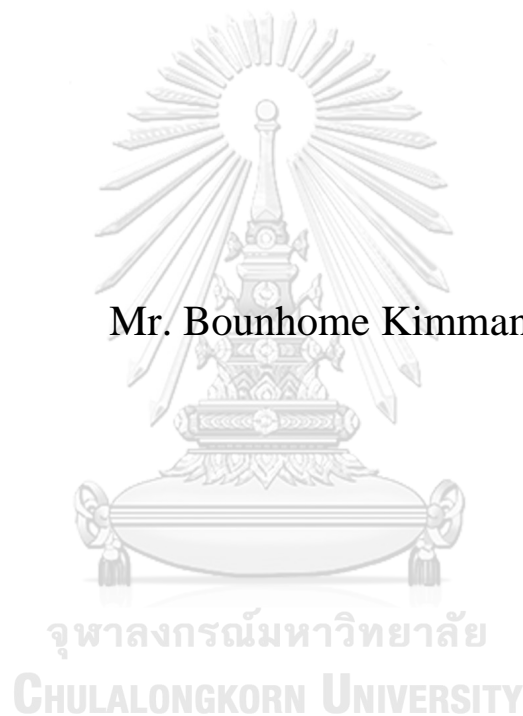


Optimal multi-reservoir system operations under inflow
scenarios in Nam Ngum River Basin, Lao PDR



A Dissertation Submitted in Partial Fulfillment of the Requirements
for the Degree of Doctor of Engineering in Water Resources Engineering
Department of Water Resources Engineering
FACULTY OF ENGINEERING
Chulalongkorn University
Academic Year 2021
Copyright of Chulalongkorn University

การหาค่าที่เหมาะสมสำหรับงานปฏิบัติการระบบอ่างเก็บน้ำ ภายใต้สถานการณ์การน้ำไหลเข้าอ่าง
เก็บน้ำในกลุ่มน้ำจิม สปป. ลาว



วิทยานิพนธ์นี้เป็นส่วนหนึ่งของการศึกษาตามหลักสูตรปริญญาวิศวกรรมศาสตรดุษฎีบัณฑิต
สาขาวิชาวิศวกรรมแหล่งน้ำ ภาควิชาวิศวกรรมแหล่งน้ำ
คณะวิศวกรรมศาสตร์ จุฬาลงกรณ์มหาวิทยาลัย
ปีการศึกษา 2564
ลิขสิทธิ์ของจุฬาลงกรณ์มหาวิทยาลัย

Thesis Title	Optimal multi-reservoir system operations under inflow scenarios in Nam Ngum River Basin, Lao PDR
By	Mr. Bounhome Kimmany
Field of Study	Water Resources Engineering
Thesis Advisor	Assistant Professor Supattra Visessri, Ph.D.
Thesis Co Advisor	Assistant Professor PIYATIDA RUANGRASSAMEE, Ph.D.

Accepted by the FACULTY OF ENGINEERING, Chulalongkorn University
in Partial Fulfillment of the Requirement for the Doctor of Engineering

..... Dean of the FACULTY OF
ENGINEERING
(Professor SUPOT TEACHAVORASINSKUN, D.Eng.)

DISSERTATION COMMITTEE

..... Chairman
(Associate Professor TUANTAN KITPAISALSAKUL,
D.Eng.)

..... Thesis Advisor
(Assistant Professor Supattra Visessri, Ph.D.)

..... Thesis Co-Advisor
(Assistant Professor PIYATIDA RUANGRASSAMEE,
Ph.D.)

..... Examiner
(Assistant Professor Anurak Sriariyawat, Ph.D.)

..... Examiner
(Assistant Professor Pongsak Suttinon, D.Eng.)

..... External Examiner
(Associate Professor Chaiyuth Sukhsri)

CHULALONGKORN UNIVERSITY

บุญโฮม กิมมณี : การหาค่าที่เหมาะสมสำหรับงานปฏิบัติการระบบอ่างเก็บน้ำ ภายใต้สถานการณ์การน้ำไหลเข้าอ่างเก็บน้ำ
ในลุ่มน้ำจิม สปป. ลาว. (Optimal multi-reservoir system operations under inflow
scenarios in Nam Ngum River Basin, Lao PDR) อ.ที่ปรึกษาหลัก : ผศ. ดร.สุภัทรา วิเศษศรี, อ.ที่
ปรึกษาร่วม : ผศ. ดร.ปิยธิดา เรืองรัมย์

ลุ่มน้ำจิมเป็นหนึ่งในลุ่มน้ำหลักที่สำคัญของประเทศลาวที่มีทรัพยากรน้ำอุดมสมบูรณ์ ด้วยเหตุนี้โครงการผลิตกระแสไฟฟ้าพลังน้ำหลายแห่งจึงถูกพัฒนาขึ้นและได้ดำเนินการผลิตกระแสไฟฟ้าจนถึงปัจจุบัน นอกจากนี้ยังมีอีกหลายโครงการที่อยู่ระหว่างการก่อสร้าง และอยู่ระหว่างการวางแผนการก่อสร้าง โครงการผลิตกระแสไฟฟ้าเหล่านี้มีการบริหารจัดการโดยหน่วยงานที่แตกต่างกันและเป็นอิสระต่อกัน ซึ่งอาจนำไปสู่ความขัดแย้งในการดำเนินงานและเป็นอุปสรรคต่อการพัฒนาประเทศ งานวิจัยนี้จึงถูกพัฒนาขึ้นโดยมีวัตถุประสงค์หลักของการวิจัยคือ การพัฒนาแบบจำลองการบริหารระบบอ่างเก็บน้ำเพื่อเพิ่มประสิทธิภาพในการผลิตไฟฟ้าในลุ่มน้ำจิมให้ได้สูงสุดภายใต้ผลกระทบของการเปลี่ยนแปลงสภาพภูมิอากาศ การศึกษานี้ยังได้พิจารณาถึงผลกระทบที่อาจเกิดขึ้นจากการเพิ่มการผลิตไฟฟ้าให้สูงสุดซึ่งอาจนำไปสู่ท่วมได้ แบบจำลองการหาค่าเหมาะสมที่สุดสำหรับการปฏิบัติการระบบอ่างเก็บน้ำภายใต้ข้อจำกัดซึ่งเป็นการศึกษาหลักของวิทยานิพนธ์นี้ได้รับการพัฒนาโดยอิงจากปัญหาแบบไม่เชิงเส้นจำนวนผสม (Mixed-Integer Nonlinear Programming, MINLP) ผ่านระบบการสร้างแบบจำลองพีชคณิตทั่วไป (General Algebraic Modeling System, GAMS) และแก้ไขปัญหาคด้วยโปรแกรมเครื่องมือ Basic Open-source Nonlinear Mixed Integer programming, BONMIN การประเมินผลกระทบของการเปลี่ยนแปลงสภาพอากาศจะใช้ข้อมูลฝนจากแบบจำลองภูมิอากาศระดับภูมิภาค (Regional Climate Models, RCMs) ภายใต้สถานการณ์ต่างๆ ที่ได้รับการปรับแก้ความเอนเอียงเชิงสถิติแล้ว เนื่องจากข้อจำกัดทางด้านข้อมูลปริมาณน้ำท่า จึงต้องใช้แบบจำลองทางอุทกวิทยา (Integrated Flood Analysis System, IFAS) เพื่อจำลองปริมาณน้ำท่าที่ไหลเข้าอ่างเก็บน้ำในปัจจุบันและอนาคต ผลการวิจัยพบว่า การบริหารอ่างเก็บน้ำแบบเดี่ยวสามารถเพิ่มการผลิตไฟฟ้ารายปีได้ 12.2% เมื่อเทียบกับข้อมูลการบริหารจริง ในขณะที่การบริหารอ่างเก็บน้ำแบบเป็นระบบสามารถเพิ่มการผลิตไฟฟ้าพลังน้ำรายปีโดยเฉลี่ยได้ 20.2% (6.0% จากโครงการผลิตกระแสไฟฟ้าน้ำจิม 1 และ 14.2% จากโครงการผลิตกระแสไฟฟ้าน้ำจิม 2) แบบจำลองการหาค่าเหมาะสมที่สุดสามารถลดจำนวนวันน้ำท่วมได้ นอกจากนี้ยังสามารถลดปริมาณน้ำท่าสูงสุด ปริมาณน้ำที่ไหลออกจากเขื่อน และปริมาณน้ำที่ไหลผ่านทางระบายน้ำล้นโดยเฉลี่ยประมาณ 4.8% 3.6% และ 4.7% ตามลำดับ ปริมาณน้ำฝนรายปีในอนาคตภายใต้ภาพฉายการปล่อยก๊าซเรือนกระจก (RCP) 4.5 และ 8.5 เพิ่มขึ้นโดยเฉลี่ยประมาณ 8.2% และ 17.4% ตามลำดับเมื่อเทียบกับข้อมูลสถานีตรวจวัด การเพิ่มขึ้นของปริมาณน้ำฝนอาจนำไปสู่การเพิ่มขึ้นของปริมาณน้ำท่าในอนาคต และมีความเป็นไปได้ว่าในอนาคตอาจเกิดเหตุการณ์อุทกภัยที่มีความรุนแรงมากขึ้น และอาจยาวนานกว่าที่เคยเป็นมา โค้งปฏิบัติการอ่างเก็บน้ำ (Indicative reservoir operating curves) ในปัจจุบันและในอนาคตได้รับการพัฒนาจากข้อมูลระดับน้ำสูงสุดและต่ำสุดของอ่างเก็บน้ำโดยอิงตามข้อมูลปริมาณน้ำที่ปล่อยจากแบบจำลอง ผลการวิจัยชี้ให้เห็นว่า การประยุกต์ใช้แบบจำลองการหาค่าเหมาะสมที่สุดมีส่วนช่วยในการควบคุมการปล่อยน้ำออกจากอ่างเก็บน้ำได้ดีขึ้นภายใต้เงื่อนไขที่กำหนดในการศึกษานี้ สำหรับการวิจัยในอนาคตควรพิจารณาความไม่แน่นอนจากภาพฉายการเปลี่ยนแปลงสภาพภูมิอากาศและการพัฒนาทางเศรษฐกิจและสังคมด้วย

สาขาวิชา วิศวกรรมแหล่งน้ำ
ปีการศึกษา 2564

ลายมือชื่อนิสิต
ลายมือชื่อ อ.ที่ปรึกษาหลัก
ลายมือชื่อ อ.ที่ปรึกษาร่วม

6071423121 : MAJOR WATER RESOURCES ENGINEERING

KEYWORD: Optimization model, Reservoir operation, Nam Ngum River Basin, GAMS, MINLP, IFAS, Reservoir operating curves

Bounhome Kimmany : Optimal multi-reservoir system operations under inflow scenarios in Nam Ngum River Basin, Lao PDR. Advisor: Asst. Prof. Supattra Visessri, Ph.D. Co-advisor: Asst. Prof. PIYATIDA RUANGRASSAMEE, Ph.D.

The Nam Ngum River is one of the main rivers in Lao PDR. Many hydropower projects are currently operated, under construction, and in the planning stage within the Nam Ngum River Basin (NNRB). These hydropower projects are managed by different organizations which could lead to conflict in operation and hinder the achievement of national developments. The main objective of this research is therefore to develop an optimization model for maximizing hydropower production in the NNRB through optimal reservoir operation under the impact of climate change. The potential consequence of maximizing hydropower production that could lead to flooding was also considered in this study. The optimization model for the optimal multi-reservoir operation with the specified constraints is the main focus of this thesis. It was developed based on mixed-integer nonlinear programming (MINLP) through the General Algebraic Modeling System (GAMS). The optimization problems were solved by Basic Open-source Nonlinear Mixed-Integer (BONMIN) optimizer. To assess the impacts of climate change, the biased corrected precipitation projection under different scenarios obtained from the regional climate models (RCMs) was used. Due to the limitation of streamflow data, the Integrated Flood Analysis System (IFAS) model was used to simulate the present and future streamflow in the NNRB. The results showed that the optimal single reservoir operation using the optimization model could increase the annual hydropower production by 12.2% compared to the actual operation. When the optimization model was applied to the multi-reservoir system, it could increase the annual hydropower production by 20.2% (6.0% from NN1 and 14.2% from NN2) on average. It was also found that the optimization model could reduce the flooding days and also flood peak, amount of outflow volume, flow-through spillway by approximately 4.8%, 3.6%, and 4.7%, respectively on average. The future annual precipitation based on RCP4.5 and RCP8.5 scenarios increase by approximately 8.2% and 17.4% on average, respectively when compared to the observation. The increase of precipitation could lead to an increase in the future streamflow under both RCPs and the large flood events could occur and probably last longer than what occurred in the past. The present and future indicative reservoir operating curves were developed from maximum and minimum storage levels based on the optimal release for maximizing hydropower production and could be used to support decision-making on the release. The results suggest that the application of the optimization model could potentially contribute to better control of the release with the specified constraints in this study. For further research, the uncertainties from climate change scenarios and socio-economic development scenarios should be considered.

Field of Study: Water Resources Engineering
Academic Year: 2021

Student's Signature
Advisor's Signature
Co-advisor's Signature

ACKNOWLEDGEMENTS

Undertaking this research has been a genuinely life-changing experience for me and it would not have been successful without guidance, suggestions, and support from many respected people and government agencies during my Ph.D. study at Chulalongkorn University.

Foremost, I gratefully acknowledge the scholarship support through the JICA Project for ASEAN University Network/Southeast Asia Engineering Education Development Network (AUN/SEED-Net) during my Ph.D. study.

I would like to express my special appreciation to my academic supervisors Asst. Prof. Dr. Supattra Visessri and Asst. Prof. Dr. Piyatida Ruangrassamee for providing excellent guidance, encouragement, and support for my study and thesis. This research has also greatly benefited from their valuable suggestions, comments, and constant feedback which have contributed to the improvement of the research.

Besides my supervisors, I also would like to express my gratitude to the research committee: Assoc. Prof. Dr. Tuantan Kitpaisalsakul, Assoc. Prof. Chaiyuth Sukhsri, Asst. Prof. Dr. Anurak Sriariyawat, and Asst. Prof. Dr. Pongsak Suttinon for providing insightful comments and recommendations on my research.

I am very grateful to all students and official staff in the Department of Water Resources Engineering, Faculty of Engineering, Chulalongkorn University for their assistance during my Ph.D. study. The experience I have received is memorable and invaluable.

Special thanks to Professor Yasuto Tachikawa, Assoc. Prof. Yutaka Ichikawa, and Assoc. Prof. Kazuaki Yorozu in Hydrology and Water Resources Research laboratory, and Assoc. Prof. Sunmin Kim in International Management of Civil Infrastructure laboratory, Department of Civil and Earth Resources Engineering, Kyoto University, Japan for their warm welcome and valuable comments and suggestions on my research during the Short-Term Study in Japan Program supported by the JICA Project for AUN/SEED-Net. I also would like to thank the researchers and students in the lab for all discussions and support.

I also would like to thank the Department of Meteorology and Hydrology and Department of Geology and Minerals, Lao PDR for supporting the data; and also thank the Meteorological Research Institute (MRI), Japan Meteorological Agency (JMA) for providing the NHRCM data.

Finally, I would like to acknowledge my family always provides the greatest support and constant encouragement to me.

Bounhome Kimmany

TABLE OF CONTENTS

	Page
ABSTRACT (THAI)	iii
ABSTRACT (ENGLISH)	iv
ACKNOWLEDGEMENTS	v
TABLE OF CONTENTS	vi
LIST OF FIGURES	x
LIST OF TABLES	xii
CHAPTER 1 INTRODUCTION	1
1.1. Background	1
1.2. Research objectives	3
1.3. Scope of research and assumptions	3
1.4. Research contributions	4
1.5. Expected outcomes	4
1.6. Organization of the thesis	5
CHAPTER 2 LITERATURE REVIEW	8
2.1. Optimal reservoir operation	8
2.1.1. GAMS	9
2.1.2. MINLP	9
2.1.3. Previous studies on reservoir operation	10
2.2. Climate model	11
2.2.1. Global Climate Models (GCMs)	12
2.2.2. Regional Climate Model (RCMs)	13
2.2.3. Climate model selection	13
2.2.4. Bias correction of RCM precipitation	19
2.3. Streamflow prediction	21
2.3.1. IFAS model	22

2.3.2.	Model parameter sensitivity analysis.....	24
2.3.3.	Model parameter calibration and validation	24
2.3.4.	Previous studies on streamflow simulation	24
CHAPTER 3 STUDY AREA		27
3.1.	Background of the NNRB	27
3.2.	Hydropower development	28
3.3.	Existing reservoir operation	31
3.4.	Geographical features	32
3.4.1.	Topography.....	32
3.4.2.	Land use.....	33
3.4.3.	Soil type.....	34
3.5.	Meteorological and hydrological conditions	36
3.5.1.	Rainfall	38
3.5.2.	Evaporation.....	40
3.5.3.	Streamflow.....	41
3.6.	Population status.....	42
3.7.	Water use	43
3.7.1.	Domestic water usage.....	43
3.7.2.	Irrigation water usage.....	44
3.8.	Flood problem	46
CHAPTER 4 METHODOLOGY		47
4.1.	Data collection and preliminary analysis	47
4.1.1.	Observed data	48
4.1.2.	RCMs data	48
4.1.3.	Spatial data	49
4.1.4.	Physical reservoir characteristic data.....	49
4.2.	Optimization model development	49
4.2.1.	Input data requirement.....	51
4.2.2.	Objective function	52

4.2.3.	Constraints	52
4.2.4.	Solver tool.....	55
4.3.	Optimization model under flood condition	55
4.4.	The indicative reservoir operating curves development.....	55
4.5.	Optimization model development procedure	56
CHAPTER 5 RESULTS AND DISCUSSION		58
5.1.	Optimal single reservoir operations.....	58
5.1.1.	Monthly hydropower production.....	58
5.1.2.	Annual hydropower production.....	59
5.2.	Optimal multi-reservoir operation for present.....	59
5.2.1.	Monthly hydropower production.....	59
5.2.2.	Annual hydropower production.....	61
5.3.	Optimal reservoir operation under future climate change scenarios	62
5.3.1.	Monthly hydropower production under climate change scenarios 62	
5.3.2.	Annual hydropower production under climate change scenarios.	65
5.4.	Optimal reservoir operation with and without flood conditions.....	67
5.4.1.	Optimal reservoir operation without river capacity constraint	68
5.4.2.	Optimal reservoir operation with river capacity constraint	72
5.5.	Indicative reservoir operating curves	74
5.5.1.	Indicative reservoir operating curves for present	74
5.5.2.	Indicative reservoir operating curves under climate change scenarios	76
5.6.	Summary.....	78
CHAPTER 6 CONCLUSIONS AND RECOMMENDATIONS		80
6.1.	Conclusions	80
6.1.1.	RCM analysis	80
6.1.2.	Streamflow prediction	81
6.1.3.	Optimal reservoir operation.....	82

6.1.4. The optimal reservoir operation with and without river capacity constraints.....	83
6.1.5. Indicative reservoir operating curves.....	84
6.2. Recommendations	85
REFERENCES	87
APPENDIX.....	94
Appendix A Consistency of the observed rainfall data	95
Appendix B Impact of climate change scenarios.....	98
B.1. RCM selection.....	98
B.2. Bias correction	101
B.3. MQM verification	108
B.4. Future precipitation scenarios	110
Appendix C Streamflow prediction	113
C.1. Model setup.....	114
C.2. Parameter sensitivity analysis	115
C.3. Model calibration and validation	115
C.4. Results of streamflow prediction	124
C.4.1. Parameter sensitivity analysis.....	124
C.4.2. Model calibration results	125
C.4.3. Model validation results	128
C.4.4. Model application	130
C.4.5. Future streamflow scenarios	131
VITA.....	135

LIST OF FIGURES

Figure 1-1 Nam Ngum River Basin (a) location and (b) schematic of existing hydropower and river system.....	6
Figure 1-2 Research procedure	7
Figure 2-1 Description of the GCM and RCM.	12
Figure 2-2 The schematic of quantile mapping technique.....	20
Figure 2-3 Schematic figure of distributed hydrological model.....	22
Figure 2-4 (a) Surface tank, (b) Groundwater tank, (c) River channel tank.....	23
Figure 3-1 The Nam Ngum River Basin map.....	28
Figure 3-2 Location of hydropower plant in the NNRB.....	31
Figure 3-3 Distribution of surface elevation map.....	33
Figure 3-4 Land use distribution map of the NNRB.....	34
Figure 3-5 Soil distribution map of the NNRB.....	36
Figure 3-6 Locations of the meteorological and hydrological observed stations in the NNRB	38
Figure 3-7 Isohyetal annual rainfall over the NNRB in period of 1990-2015.....	39
Figure 3-8 Monthly average rainfall over the NNRB in period of 1990-2015.....	39
Figure 3-9 Annual rainfall pattern over the NNRB in period of 1990-2015	40
Figure 3-10 Monthly average evaporation loss over the NNRB in period of 2007-2015	40
Figure 3-11 Annual streamflow pattern at Pakkayoung station in period of 1990-2015	41
Figure 3-12 Monthly mean streamflow at Pakkayoung station in period of 1990-2015	41
Figure 3-13 Distribution of population in village in the NNRB	42
Figure 3-14 Existing irrigation areas in the NNRB region 2015	45
Figure 4-1 Overall research methodology flowchart	47
Figure 4-2 Schematic of the optimal reservoir operations.....	50
Figure 4-3 Num Ngum 1 hydropower project	53
Figure 4-4 Components of a hydropower plant	53
Figure 4-5 Schematic of sideflow system and sub-basin in the NNRB.....	57
Figure 5-1 Comparison of average monthly hydropower production of NN1 between the optimization and observation.....	58
Figure 5-2 Comparison of annual hydropower production of NN1 between the MINLP model and the observation.....	59
Figure 5-3 Comparison of average monthly hydropower production of NN1 from the multi-reservoir optimization and the observation.	60
Figure 5-4 Comparison of average monthly hydropower production of NN2 from the multi-reservoir optimization and the observation.	61
Figure 5-5 Comparison of average monthly hydropower production of NN1 and NN2 from the multi-reservoir optimization and the observation.....	61

Figure 5-6 Annual hydropower from the MINLP model compared to the observation of NN1 and NN2.	62
Figure 5-7 Future monthly hydropower production of NN1 HPP under RCP4.5 and RCP8.5 inflow scenarios.....	63
Figure 5-8 Comparison of future average monthly hydropower production of NN1 HPP under RCP4.5 and RCP8.5 inflow scenarios.	63
Figure 5-9 Future monthly hydropower production of NN2 HPP under RCP4.5 and RCP8.5 inflow scenarios.....	64
Figure 5-10 Comparison of future average monthly hydropower production of NN2 HPP under RCP4.5 and RCP8.5 inflow scenarios.	64
Figure 5-11 Future monthly hydropower production of NN3 HPP under RCP4.5 and RCP8.5 inflow scenarios.....	65
Figure 5-12 Comparison of future average monthly hydropower production of NN3 HPP under RCP4.5 and RCP8.5 inflow scenarios.	65
Figure 5-13 Annual hydropower production from NN1, 2, and 3 HPPs under climate change of RCP4.5 scenario.	66
Figure 5-14 Annual hydropower production from NN1, 2, and 3 HPPs under climate change of RCP8.5 scenario.	67
Figure 5-15 Total annual hydropower production from NN1, 2, and 3 HPPs under RCP4.5 and RCP8.5 inflow scenarios.....	67
Figure 5-16 The monthly hydropower production from optimization and observation without river capacity constraint.	68
Figure 5-17 Observed daily outflow from NN1 reservoir at flood control point.	69
Figure 5-18 Optimized daily outflow without river capacity constraint scenario at flood control point.	70
Figure 5-19 Future daily outflow without river capacity constraint at flood control point under RCP4.5 scenario.	71
Figure 5-20 Future daily outflow without river capacity constraint at flood control point under RCP8.5 scenario.	71
Figure 5-21 The monthly hydropower production from optimization and observation with river capacity constraint.	73
Figure 5-22 Optimized daily outflow with river capacity constraint scenario at flood control point.....	73
Figure 5-23 Indicative optimal reservoir operating curves for NN1 reservoir	74
Figure 5-24 Indicative optimal reservoir operating curves for NN2 reservoir	75
Figure 5-25 Indicative the future reservoir operating curves for NN1 HPP under climate change scenarios.....	77
Figure 5-26 Indicative the future reservoir operating curves for NN2 HPP under climate change scenarios.....	77
Figure 5-27 Indicative the future reservoir operating curves for NN3 HPP under climate change scenarios.....	78

LIST OF TABLES

Table 2-1 The various GCMs with spatial resolution.....	14
Table 2-2 The characteristics of RCMs model	16
Table 2-3 Cell type characteristics.....	22
Table 3-1 The area size of province within the NNRB	27
Table 3-2 Project features of hydropower plant in the NNRB	30
Table 3-3 Characteristic of NN1, NN2, and NN3 hydropower plants.....	30
Table 3-4 Land use distribution in the NNRB	34
Table 3-5 Soil distribution in the NNRB	35
Table 3-6 Hydrological observed stations within the NNRB	37
Table 3-7 Meteorological observed stations within the NNRB.....	37
Table 3-8 Population distribution within the NNRB region 2019.....	43
Table 3-9 The estimated monthly amount of water usage within the NNRB region ..	44
Table 3-10 The irrigation areas and water use in the NNRB.....	45
Table 3-11 Flood and flood damage in Laos (1966-2011)	46
Table 4-1 Physical data requirement for optimization model.....	51
Table 4-2 Time series data requirement for optimization model.....	51
Table 5-1 Annual hydropower production.....	59
Table 5-2 Summary of annual hydropower production from optimization and observation without river capacity constraint.	69
Table 5-3 Summary of annual outflow volume, flow through spillway, and flood period without river capacity constraint.....	70
Table 5-4 Summary of annual hydropower production from optimization and observation with river capacity constraint.....	73
Table 5-5 Summary of annual outflow volume and flow through spillway with river capacity constraint.	74

CHAPTER 1

INTRODUCTION

This chapter introduces the rationale behind the research of optimal multi-reservoir system operations under reservoir inflow scenarios using optimization model. This chapter begins with the background of the Nam Ngum River Basin (NNRB) and multi-reservoir operation problems followed by objectives and scope of the study. Research contribution and outcomes are highlighted. Thesis organization is provided to facilitate acquisition of reading comprehension.

1.1. Background

Lao PDR has large potential of hydropower generation, so the government of Lao PDR is striving to become the "Battery of Asia" by exporting the hydropower to boost the country's economy. As of 2018, there are total of 516 hydropower power projects (HPPs) under operation and planning in Laos. Of these, 61 HPPs have been operated; 52 HPPs are under construction; 148 HPPs are expected to construct and finish in 2030; and 255 projects are agreed to be constructed based on the signed MoU. These HPPs are expected to produce 34,452 MW, 22,566 MW (65.5%) of which for export and the rest for domestic use. During the period of 2005-2015, the peak load has been continuously increased by 13% per year in average. Also, in 2015, the hydropower demand from Greater Mekong Subregion (GMS) increased to 148,371 MW higher than the total power generation from operated HPPs. By the year of 2025, the hydropower demand was forecasted to increase approximately by 14% a year in average (Ministry of Energy and Mines, 2018b).

The Nam Ngum River is one of significant and important rivers in Laos with plentiful water resources. There are 6 HPPs that are currently operated in NNRB; 2 HPPs are under construction, and other 3 HPPs are in the planning stage (Figure 1-1). The reservoir operation is based on the existing operating rule curves. The reservoir operating rule curves used for Nam Ngum 1 HPP were developed in 1990s (Villa et al., 2016). The renewal of operating rule curves is necessary, and it is high time to renew them by expanding the data to develop operating curves that are more suitable for current operations.

Also, the government of Lao PDR has persistently determined to find methods to obtain the maximum benefit from the hydropower, which is expected to increase significantly in the future through effective reservoir operations (Ministry of Energy and Mines, 2018a). However, the NNRB has faced several operational problems caused by natural variability such as the flood and management of water supply such as lacking cooperation between stakeholders in the upstream and downstream (Keophila et al., 2018). Even though, many optimization and simulation models have

been developed and applied over the past several decades, the new techniques are needed to increase the effectiveness on reservoir operations. Jayasekera et al. (2016a) discussed that the conventional reservoir operation method (WEAP) is often not adequate for establishing optimal operation decisions, especially when integrated operation of multipurpose multi-reservoirs is considered. To achieve the optimal multi-purpose of reservoir operation, Taesoon et al. (2008) illustrated that it is very difficult and complex task due to conflict of the multiple objectives.

The flood damages in the NNRB were mostly occurred in the downstream which belongs to Vientiane Province and Vientiane Capital. The downstream of the Nam Ngum River before joining to the Mekong River is narrow; the bed slope is very mild, and the influence of the Mekong River level causes difficulty in draining the flooded area. In addition, there are also many low-lying areas in the Vientiane Plain, which are easily inundated by small floods. Even though many hydropower projects were established, the flood at downstream area still occurred. The recent flood records suggest that the NNRB is prone to significant flood events with recurrence interval of 6 years in average. Reservoir operation and flood control in the NNRB is complicated by the changing climate, extremely heavy rain in the late monsoon season.

The effect of climate change on reservoir operation has become an important part of much research in water resources system. Changing in the amount and timing of reservoir inflow and precipitation are the most important aspects of climate change for the reservoir operation. It could be useful for future operations if the impact of climate change on inflow is considered in deriving the operation rule system (Jayasekera et al., 2016b). One of concerns in reservoir operations for hydropower generation is existing hydrological variability and operation without considering the impact of climate change (Piman et al., 2015). Henceforth, optimal reservoir operations need to incorporate plans to assess hydrological uncertainty caused by climate change. Due to these, different ensembles of Regional Climate Models (RCMs) should be considered to estimate future streamflow that can be used as input for optimal reservoir operations.

According to the problems of reservoir operations in NNRB, the optimization model possibly provides necessary solution to improve reservoir operations for NNRB under various inflows. Therefore, this study aims to optimize water release to maximize the hydropower production while meeting domestic and irrigation demand as well as minimizing flooding in the downstream of NN1. The Integrated Flood Analysis System (IFAS) with observed and projected precipitation from Regional Climate Models (RCMs) are used in this study. The RCM product, Max-Planck-Institute Earth System Model (MPI-ESM), from SEACLID-CORDEX under Representative Concentration Pathway (RCP)4.5 and RCP8.5 are selected for assessing future scenarios. The General Algebraic Modeling System (GAMS) is

applied as optimization model to optimize the reservoir operation under different inflow scenarios.

1.2. Research objectives

1) To develop the optimal reservoir operation model for maximizing hydropower production in NNRB with and without flood constraints at downstream of NN1 reservoir.

2) To assess the impact of climate change on reservoir operation under different Representative Concentration Pathway (RCP) scenarios.

1.3. Scope of research and assumptions

The whole scope of this research is presented in Figure 1-2, and the details of the scope are listed below.

1) The study area is the NNRB which is in the middle of Lao PDR, and it is one of major tributaries of the Mekong River as presented in Figure 1-1.

2) The main purposes of the NN1 reservoir commonly include ecosystem, hydropower production, water supply for domestic and irrigation, and flood reduction. In the study area, the water demand for domestic and irrigation uses are relatively small and the minimum streamflow from NN1 HPP is sufficient for retaining the ecosystem, irrigation, and water supply for domestic. Therefore, the main purpose of reservoir optimization focused on maximizing hydropower production in the NNRB.

3) This study performed optimization in present and future scenarios. The present scenario is optimized on NN1 and NN2 HPPs, while the future scenario is optimized on NN1, NN2, and NN3 HPPs. The Nam Lik 1/2 and NN5 HPPs are not considered for this study.

4) This study optimized both of single and multiple reservoirs operations. The single reservoir operation is performed only for NN1. The multi-reservoirs operations are divided into two cases including the present case optimized on NN1 and NN2, and the future case optimized on NN1, NN2, and NN3 HPPs.

5) Both single and multiple reservoirs operations are optimized with and without flood condition at downstream of NN1 HPP.

6) Both daily and monthly time scale are considered in the optimization model. The monthly time scale is considered for both present (2012-2015) and future (20 years) scenarios. While the daily time scale is considered for wet years in both present and future scenarios to assess the flood peak and duration at the downstream of NN1.

7) Flood issue is considered only at the downstream of NN1 HPP after the joining between Nam Ngum and Nam Lik rivers, and the flood duration is monitored at the flood control point.

8) The sideflows including the flows from Nam Bak, Nam Sane, Nam Phay, Nam Song, and upper Ngum rivers are considered. The

9) To assess the impacts of climate uncertainty on reservoir operations, the RCMs projected by SEACLID/CORDEX Southeast Asia and NHRCM projected by MRI are analyzed under RCP 4.5 and RCP8.5 scenarios.

10) The MINLP solver tool in GAMS was used to maximize the hydropower production of NNRB in all scenarios.

11) The observed rainfall and streamflow data from 1990 to 2015 are used for present scenario optimization. For future scenario, projected RCM data are used to assess the impact of climate change on reservoir operations.

1.4. Research contributions

Optimization models have widely been applied in a large number of studies. However, the study or use of optimization for reservoir operations in Lao PDR is very few. Lao PDR positioned itself as the Battery of Asia. Efficient reservoir operation is crucial to achieving this goal. In this study, the optimization model is developed for optimal multi-reservoir system operation to maximize the hydropower production.

This study uses high spatial resolution of different Regional Climate Models (RCM) products to simulate reservoir inflow under different RCM scenarios. SEACLID/CORDEX Southeast Asia and NHRCM under RCP4.5 and RCP8.5 climate scenarios are used for assessing the impact of climate change. To the best of the author's knowledge, these products have not been used for assessing inflow uncertainty in reservoir operation in Lao PDR.

The NNRB is mountainous area and covered by 81% of forest. The hydrological observed stations are limited. This study area can be considered an ungauged basin. The application of optimization model in ungauged basin involves a number of challenges. A relatively small number of studies attempt to address the optimal reservoir system operation in the ungauged basin in Lao PDR. There remains a challenge to develop and improve reservoir operation in Lao PDR. Moreover, the studies on the impact of climate change on reservoir operation and hydropower development within the basin are quite limited.

1.5. Expected outcomes

- 1) Optimization modelling for single and multi-reservoir operation in the NNRB.
- 2) The assessment of the effect of reservoir inflow uncertainty on reservoir operation in the NNRB.
- 3) Recommended reservoir operating curves for maximizing hydropower production in the NNRB and others reservoir system with similar characteristics.

4) Improved understanding of the impact of climate change on reservoir operation in the NNRB.

1.6. Organization of the thesis

The thesis is organized into six chapters. A brief overview of the thesis organization in each chapter is given below.

Chapter 1 introduces the rationale behind the research of optimal multi-reservoir system operations under reservoir inflow scenarios using optimization model. This chapter provides the overview of the study.

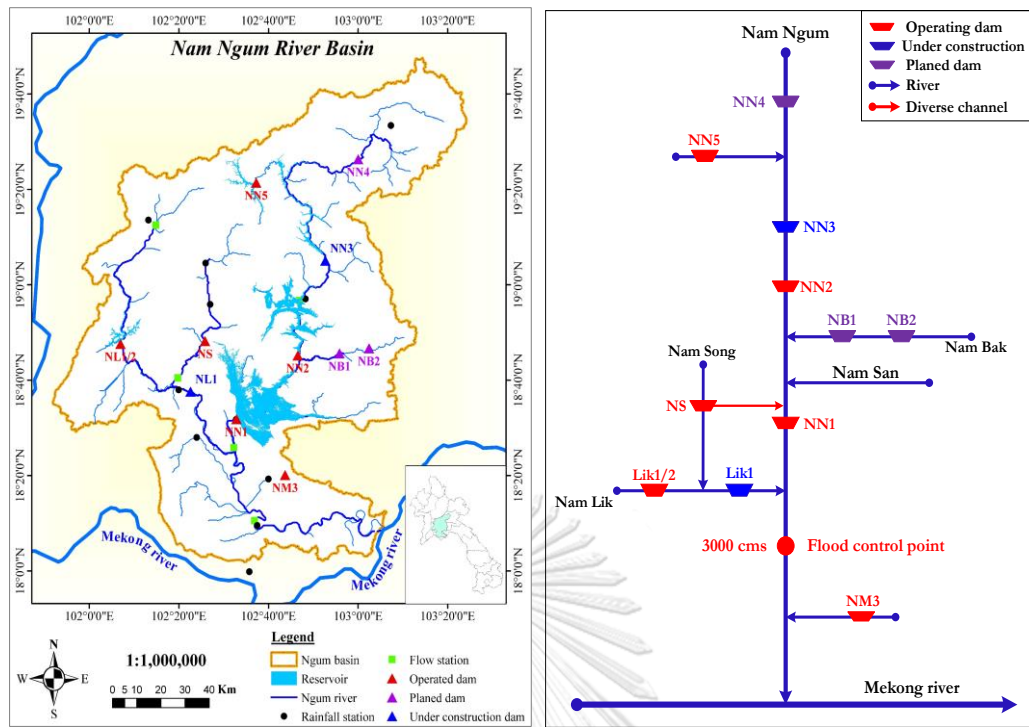
Chapter 2 introduces and reviews the progression of ideas in the domain of streamflow prediction and reservoir operations. In line with the focus of this thesis, the literature of rainfall-runoff model for reservoir inflow prediction, optimization model for optimal reservoir operation, impacts of climate change on reservoir operations, and bias correction technique are reviewed.

Chapter 3 focuses on the characteristics of the NNRB selected as the study area. The climate, geography, river network, hydrological conditions, and hydropower condition are explained to establish understanding of the river basin.

Chapter 4 presents the methodology of the research. To achieve the desired objectives mentioned in the earlier section, this chapter is divided into four parts. The chapter starts with the data collection and preliminary analysis followed by the RCM data processing and RCM bias correction. Then, the process of reservoir inflow prediction is presented using rainfall-runoff model. The final part of this chapter is presented the process of the optimization model development based on the objective function of maximizing hydropower production is presented.

Chapter 5 presents the results and discussions of the research. The first section shows the results of the optimal single reservoir operation followed by the optimal multi-reservoir operations. The third and fourth section presents the optimal reservoir operations under future climate change and flood condition, respectively. The final section discusses on the recommended reservoir operating curves.

Chapter 6 presents the conclusions and recommendations of the research. This chapter starts with the conclusions of the optimal reservoir operation including single, multiple reservoirs for present and future scenarios. The reservoir operating curves are also recommended in this section. The final section presents the recommendations for further research.



(a) location

(b) schematic of river system

Figure 1-1 Nam Ngum River Basin (a) location and (b) schematic of existing hydropower and river system.

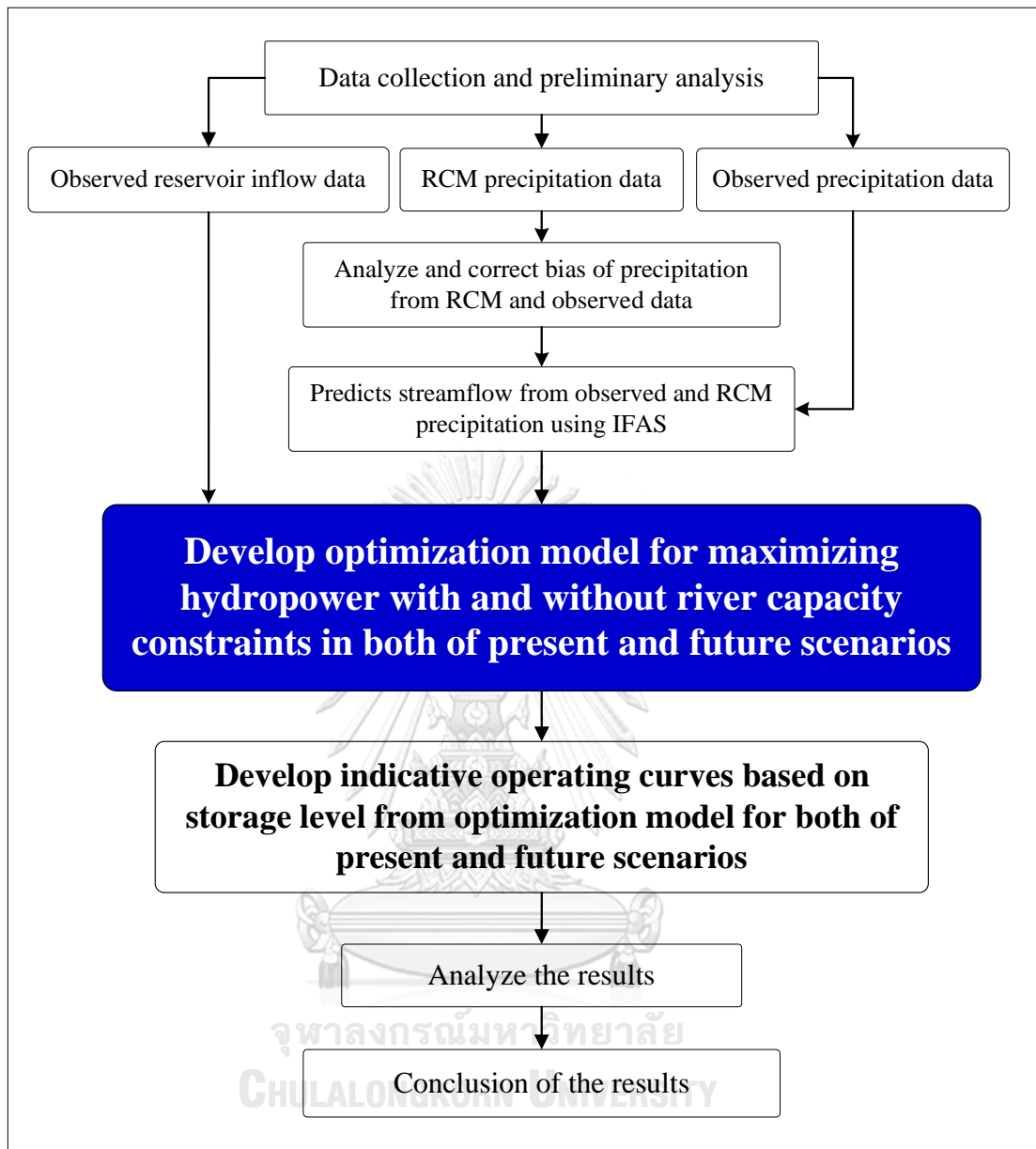


Figure 1-2 Research procedure

CHAPTER 2

LITERATURE REVIEW

This chapter focuses on the review of the development of ideas in the domain of optimization for optimal reservoir operation. Related literature including climate modelling and rainfall-runoff modelling are also reviewed.

2.1. Optimal reservoir operation

Reservoir operation may refer to the storing of water in a reservoir and then supply to multiple purposes. Generally, releasing or storing water in reservoirs is controlled by upper and lower rule curves (Jothiprakash and Arunkumar, 2014). Many reservoir operation approaches were applied to find the suitable rule curves to use for the operating guideline. Reservoir operations can be divided into single and multi-reservoir operations. The multi-reservoir systems operation is more complex and challenging than single reservoir operation. The complexity of multi-reservoir operation may arise from various objectives each reservoir is serving, operations controlled by different organizers, which easily results in conflicts (Ahmadi et al., 2014). In recent years, many researchers have developed methods to solve these challenges and complexity in reservoir operations. Zhang et al. (2014) suggested that the complexities of reservoir system operations problems might be achieved by optimization techniques.

Optimization for multi-reservoir operations relates to many objectives, variables, and uncertainty. The optimal reservoir system operation must be considered of minimizing cost and loss or maximizing benefits using optimal strategies. Optimization techniques are based on defining objective functions, control decision criteria, and constraints as limitations during optimization states. Objective functions should be incorporated measures such as efficiency, survivability, and sustainability. The constraints should be defined based on the problems (Ahmad and El-Shafie, 2014). Some constraints in optimal reservoir operation are defined including conservation of mass, minimum and maximum storage, release and water requirements as well as hydropower generation limitations, and other hydrological and hydraulic constraints (Jothiprakash and Arunkumar, 2014).

There are many optimization techniques that have been developed to operate different types of reservoir system from basic to advances including hedging policy (Rittima, 2009), Standard Operation Policy (SOP) (Rohde and Naparaxawong, 1981), Linear Programming (LP) (Ginting et al., 2017), Nonlinear Programming (NLP) (Arunkumar and Jothiprakash, 2012), chance constraint (Birhanu et al., 2014), neural network (Chang et al., 2005), and Genetic Algorithm (GA) (Karamouz et al., 2002).

Although different optimization models have been developed to serve multi-reservoir systems, achieving more efficiency is still a major concern among researchers when dealing with the complexity of water resources management. This study discussed the Mixed-Integer Non-Linear Programming (MINLP) technique for optimal multi-reservoir operation through General Algebraic Modeling System (GAMS) software.

2.1.1. GAMS

This study, GAMS is considered as the optimization model to maximize the hydropower production in NNRB. GAMS refers to the high-level modeling system for solving complex problems including linear, nonlinear, and mixed integer optimization problems. GAMS contains several optional solver programming and model types with different characteristics and performances. MINLP is considered as a model to solve the optimization problems with binary condition. MINLP is an optimization modelling includes both mixed-integer linear programming and nonlinear programming as subproblems. The solver programming applied in MINLP to carry out the local optimization is Basic Open-source Nonlinear Mixed Integer programming (BONMIN). BONMIN is an open-source solver for MINLP problems developed by P. Bonami under cooperation between Canegie Mellon University and IBM research (Bonami et al., 2008). BONMIN uses nonlinear branch-and-bound (B&B) and outer approximation algorithms to search the optimal solutions in feasible regions. This solver is guarantee local optimization only. B&B, originally solve for mixed-integer linear programming (MILP) and it can also apply for mixed-integer nonlinear problems. The B&B approach can be described in terms of a tree search. The tree search is performed in space of integer variables and this solution can also solve the MINLP problems. Initially, B&B method selects one integer variable that non-integer value and branches on them. Then, branching generates new NLP subproblems and one of these subproblems will be selected and solved. The solution of subproblems generates the upper bound for subproblems in new nodes of the tree. The process will continue until the upper bound exceeds the best known solution, then the subproblem is infeasible. The searching process stops when there are no more nodes in space to explore (Androulakis, 2009).

2.1.2. MINLP

MINLP refers to optimization problems with nonlinear function and discrete and continuous variables in the objective function and constraints. MINLP can be applied to the various field including engineering, finance, and manufacturing. The Mixed-Integer (MI) term is used to solve binary variables for various purposes (Belotti et al., 2013). The general formula of MINLP is defined as:

$$\begin{array}{ll}
 \text{Maximize} & f(x, y) \\
 \text{Subject to} & g(x, y) > 0 \\
 & L \leq x, y \leq U
 \end{array} \tag{2-1}$$

where: $f(x, y)$ is nonlinear objective function, $g(x, y)$ is nonlinear constraint function, x, y are the decision variables, L, U are Lower and Upper bounds.

MINLP technique is a solver tool developed through the GAMS language. The GAMS software was originally developed by a group of economists from the World Bank in order to facilitate the resolution of large and complex non-linear models on a personal computer. The MINLP technique can be defined as mathematical programming with continuous and discrete variables and nonlinearities in the objective function and constraints. The MINLP is widely used for formulating problems that were necessary to simultaneously optimize the system structure discrete and continuous parameters. Upper and lower bounds can be obtained from any feasible point for searching for a solution. According to (Schl et al., 2008), it was explained that MINLP problems are difficult to solve because they combine all the difficulties of natural mixed integer programming (MIP) and the difficulty in solving nonlinear programming (NLP). Many open-sourced solvers that available for MINLP have been designed in GAMS for solving optimization problems; in particular, they are AMPL, BDMLP, BONMIN, COUENNE solvers and many solvers are limited access (Rosenthal, 2008). In this study, the Basic Open-source Nonlinear Mixed-Integer optimizer is used for solving optimization problems. It is an open-source solver tool available for MINLP in GAMS without purchasing a license approved by the open-source initiative (Bonami and Lee, 2011).

2.1.3. Previous studies on reservoir operation

Because the problems related to water release from reservoirs were not met with the water demand and complexities. In recent year, there are many researchers studied reservoir operation to solve these problems. Examples of related previous studies are summarized below:

Soltani (2008) applied the optimization of reservoir operation rules by using the differential evolutionary algorithm with stochastic inflow scenarios to model the Zayandehrud reservoir in Isfahan, Iran. The results showed the uncertainty band of inflow which is narrowed in demand which supplies through optimal reservoir operation planning.

Rittima (2009) simulated reservoir operation by using a hedging policy that was applied at the Mun Bon and Lam Chae reservoirs. The results were compared with the standard operating policy and probability-based rule curve. The results showed that two-point and three-point hedging performed well for all components of

reservoir behavior compared with the standard operating policy and other hedging policies.

Arunkumar and Jothiprakash (2012) applied Non-linear programming (NLP) to derive optimal operational rules for maximizing the hydropower production of Koyna reservoir, India under three different inflow conditions, representing wet, normal, and dry years. From different scenarios, it was observed that more hydropower could be generated for various dependable inflow conditions if the restrictions on releases are slightly relaxed. The study showed that the Koyna hydropower plant had the potential to generate more hydropower.

Jayasekera et al. (2016b) developed a Water Evaluation and Planning System (WEAP21) modeling framework for the Nam Ngum River Basin with incorporating the climate change driven hydrologic cycle and water infrastructures operations, such as reservoirs for hydropower, water storage, and diversions for irrigation. The results from the study showed the uncertainty affects reservoir inflow and water allocation, these led to complexity in reservoir operation. However, the reservoir simulation method does not guarantee to yield the optimal rule curves because of arbitrary decision of engineers.

Bangsulin et al. (2017) studied the reservoir operation management for simulation electricity production, reservoir control, and water supply the downstream of Namkhan River, north of Laos. The simulation software used in the research was HEC-ResSim. The results showed that electricity generation increased 3.53% in normal water year.

Keophila et al. (2018) applied HEC-ResSim model to assess effectiveness of cascade reservoir for the flood control operation and electricity production in the NNRB. The simulation results showed that the flooding days in the flood years were close to the actual recorded data. Direct benefit of water control was the increase of electricity production.

2.2. Climate model

Climate model is a tools for investigating the climate system for making climate predictions on various time scales and for future climate projections based on the set of equations derived from chemical, physical, and biological laws (Abiodun and Adedoyin, 2016). The climate models simulate the large set of physical climate system characteristics such as ocean and atmosphere circulation, precipitation, temperature, relative fluxes, cloudiness, snow, and sea-ice cover. Climate models are usually classified from simple energy balance models to complex earth system model which requires high computational resources and sophisticated numerical techniques (G. Flato et al., 2013). The climate models are also known as general circulation

model or global climate model (GCMs) and regional climate model (RCMs). These models are considered to produce simulations and predictions of future climates which are useful for planning purposes (Eden et al., 2014). The main differences between GCMs and RCMs are their domains as shown in Figure 2-1 (Souverijns, 2019).

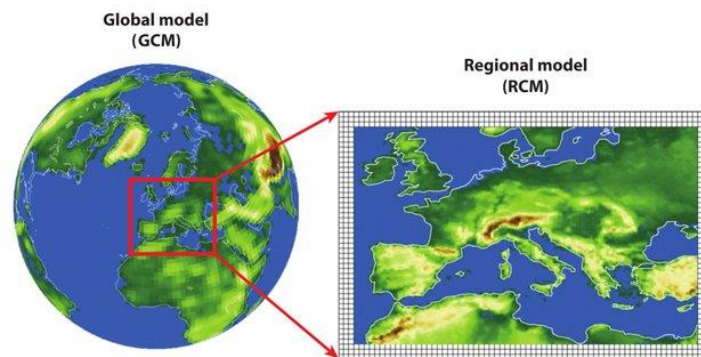


Figure 2-1 Description of the GCM and RCM.

2.2.1. Global Climate Models (GCMs)

The GCM is a mathematical model that describes the process of mass and energy circulation between global climate system (atmosphere, ocean, and land surface) set by Intergovernmental Panel on climate change (IPCC) based on Navier-Stokes equation in order to be used in weather simulation throughout the world (Mechoso and Arakawa, 2015). The GCMs were originated from weather simulation models but some can be applied in both climate and weather simulations. The most recognized applications of GCMs are the projection of future climate uncertainty under various ensembles and scenarios of increasing atmospheric carbon dioxide (CO₂) emission. There are several types of GCMs widely used at present for climate research e.g., simple global climate models (SGCMs), atmospheric global climate models (AGCMs), oceanic global climate models (OGCMs), and couple atmospheric-ocean global climate models (AOGCMs). For more details of each type of GCMs please refer to (IPCC, 2013). These models are crucial tools for improving understanding of climate behavior on various time scales in historical, present, and future periods. However, the limitation arises from computing power that frequently affects spatial resolution. In general, the GCMs do not resolve small spatial resolution scales since their spatial resolution is approximately 100 km at the best (Ganopolski, 2019). The lower spatial resolution or large-scale models might produce large errors and uncertainties when the outputs of climate data from GCMs were applied to regional scale (Kerkhoff et al., 2012). In order to reduce the error and uncertainty, high-resolution climate models or RCMs are needed to simulate climate phenomena at smaller or local scale.

2.2.2. Regional Climate Model (RCMs)

Compared to GCM, RCM is a relatively high-resolution model in limited area. The RCMs were developed on the basis of physical atmospheric processes related to topography that is projected to be affected by climate change. The RCMs are downscaled using initial global data set from GCMs as boundary conditions to increase spatial resolution and accuracy over the specific area of interest. The RCMs are also used the complex local factors such as precipitation, temperature, wind, and waves to simulate the future regional or national climate (Samadi et al., 2010). Hence, the spatial resolution of RCMs is always higher than the global climate data set. Two main techniques to downscale from GCMs to RCMs are statistic and dynamic downscaling methods. The discussion on GCM downscaling techniques are beyond the scope of this study, more details on GCMs can be found on references (Chokkavarapu and Mandla, 2019; Liang et al., 2008; Wilby and Wigley, 1997). The RCM outputs can be used for hydrological analysis to represent the effects of climate change on evaporation, precipitation (Trenberth, 2011), streamflow (Xizhi et al., 2019), flood risk assessment (Akter et al., 2018), and global warming. There are many available RCM experiments constructed from different scenarios. The RCM selection is therefore essential to obtain the suitable RCM products for certain area.

2.2.3. Climate model selection

There are a large number of available climate models and the number of new climate models increases rapidly (Akhter, 2017). The outputs from Couple Model Intercomparison Project Phase 3 (CMIP3) used in fourth Assessment Report (AR4) of Intergovernmental Panel on Climate Change's (IPCC) contains 25 different climate models. Whereas the outputs from CMIP5 used in AR5 of IPCC contains 61 different climate models (Lutz et al., 2016). Usually, these climate models have multiple ensemble and variable dataset (Ullah and Shrestha, 2012) over the coarse spatial resolution as shown in Table 2-1. Decision on which variable should be considered depends on the objective of climate change impact assessment (Ruane and McDermid, 2017). GCMs from CMIP5 under 20 climate modeling groups around the world with historical and projected simulations from 1950-2005, and 2006-2100, respectively are completely simulated and available in CMIP5.

Table 2-1 The various GCMs with spatial resolution.

GCM	Research center	Resolution (Degree Lon. x Lat.)
BCC-CSM1-1	Beijing Climate Center, China Meteorological Administration, China	2.8 x 2.8
BCC-CSM1-1-M		1.12 x 1.12
BNU-ESM	College of Global Change and Earth System Science, Beijing Normal University, China	2.8 x 2.8
CanESM2	Canadian Center for Climate Modelling and Analysis, Canada	2.8 x 2.8
CCSM4	National Center of Atmospheric Research, USA	1.25 x 0.94
CESM1-BGC	Community Earth System Model Contributors, USA	1.25 x 0.94
CESM1-CAM5		1.25 x 0.94
CESM1-FASTCHEM	Community Earth System Model Contributors, USA	1.25 x 0.94
CESM1-WACCM		2.5 x 1.89
CMCC-CESM	Centro Euro-Mediterraneo per I Cambiamenti Climatici, Italy	3.75 x 7.71
CMCC-CM		3.75 x 7.71
CMCC-CMS		1.88 x 1.87
CMCC-CMS		1.88 x 1.87
CNRM-CM5	National Center of Meteorological Research, France	1.4 x 1.4
CNRM-CM5-2		1.4 x 1.4
CSIRO-Mk3-6	Commonwealth Scientific and Industrial Research Organization/Queensland Climate Change Center of Excellence, Australia	1.88 x 1.87
EC-EARTH	EC-EARTH consortium, (Netherlands/Ireland)	1.13 x 1.12
FGOALS-g2	LASG, Institute of Atmospheric Physics, Chinese Academy of Sciences, China	2.8 x 2.8
FIO-ESM	The First Institute of Oceanography, SOA, China	2.81 x 2.79
GFDL-CM3	NOAA Geophysical Fluid Dynamics Laboratory, USA	2.5 x 2.0
GFDL-ESM2G		2.5 x 2.0
GFDL-ESM2M		2.5 x 2.0
GISS-E2-H	NASA Goddard Institute for Space Studies, USA	2.5 x 2.0
GISS-E2-H-CC		2.5 x 2.0
GISS-E2-R		2.5 x 2.0
GISS-E2-R-CC		2.5 x 2.0
HadCM3	Met Office Hadley Center, UK	3.75 x 2.5
HadGEM2-AO		1.88 x 1.25
HadGEM2-CC		1.88 x 1.25
HadGEM2-ES		1.88 x 1.25
INMCM4	Institute for Numerical Mathematics, Russia	2.0 x 1.5
IPSL-CM5A-LR	Institute Pierre Simon Laplace, France	3.75 x 1.8
IPSL-CM5A-MR		2.5 x 1.25
IPSL-CM5B-LR		3.75 x 1.8

GCM	Research center	Resolution (Degree Lon. x Lat.)
MIROC5	Atmosphere and Ocean Research Institute (University of Tokyo), National Institute for Environmental Studies, and Japan Agency for Marine-Earth Science and Technology	1.4 × 1.4
MIROC-ESM		2.8 × 2.8
MIROC-ESM-CHEM		2.8 × 2.8
MPI-ESM-LR	Max Planck Institute for Meteorology, Germany	1.88 × 1.87
MPI-ESM-MR		1.88 × 1.87
MRI-CGCM3	Meteorological Research Institute, Japan	1.1 × 1.1
NorESM1-M	Norwegian Climate Center, Norway	2.5 × 1.9

Many researchers study on the selection criteria of climate model to obtain the suitable one for climate change impact assessment. According to (Smith and Hulme, 1998) four different types of criteria which should be considered to select the most suitable RCM.

Vintage: in general, the new RCMs were more reliable than the old RCMs. This might be because the complexities; physical system of climate and higher spatial resolution were considered.

Resolution of model: the resolution of some GCMs may not be sufficient for scenario construction, especially in the regional scale where RCMs might be better. As mentioned in the Vintage criteria, more recent RCMs are generally of higher resolution, but this does not mean that the model is necessarily better than the earlier one.

Validity: the reproducibility of RCMs to simulate historical climate is used as a criterion to select models. Different climate variables and patterns can be considered based on the objective of the climate change impact assessment. However, different models could have good performance in predicting certain variables or patterns and are likely to produce different predictions. The intercomparison projects facilitate the present conditions for the models to be compared reasonably (Fu et al., 2005).

Representativeness of results: The results from RCMs can be much different in estimating regional climate change. When several RCMs are needed to be selected, a prudent approach must be conducted. RCMs predicting similar range of changes and in line with the observed climate variable should be selected. Therefore, some criteria which can be used for RCMs model selection include physical plausibility and realism, consistency, appropriateness, and accessibility.

In this research, the climate models are obtained from SEACLID/CORDEX-SEA. SEACLID/CORDEX-SEA which is a project aiming to downscale a number of GCMs from CMIP5 for Southeast Asia region through the task-sharing among the

countries involved. The GCMs were downscaled to the regional climate model (RCMs) in high-resolution climate scenarios of $25 \text{ km} \times 25 \text{ km}$ (Tuyet et al., 2019). Three RCMs including ICHEC-EC-EARTH, IPSL-CM5A, and MPI-ESM are considered for this study. These RCMs were downscaled by Ramkhamhaeng University Center of Regional Climate change Renewable Energy (RU-CORE). Another RCM also considered for this study is Non-Hydrostatic Regional Climate Model (NHRCM). NHRCM was developed by the Japan Meteorological Agency/Meteorological Research Institute (JMA/MRI), Japan with a high-resolution of $5 \text{ km} \times 5 \text{ km}$ (Cruz and Sasaki, 2017). The climate model selection criteria used for this study is based on the resolution of model and the accessibility of the data as mentioned in representativeness of model. These RCM outputs would be analyzed and compared with the observation data. The RCM with best values of performance indices would be selected. The regional climate models used in this study are summarized in Table 2-2.

Table 2-2 The characteristics of RCMs model

Feature	RCM characteristics			
Research Institute	SEACLID/CORDEX-SEA and RU-CORE			JMA/MRI
Products	MPI-ESM-MR	IPSL-CM5A-LR	ICHEC-EC-EARTH	NHRCM
Spatial resolution	$25\text{km} \times 25\text{km}$	$25\text{km} \times 25\text{km}$	$25\text{km} \times 25\text{km}$	$5\text{km} \times 5\text{km}$
Scenarios	Historical: 1970-2005 RCP4.5: 2006-2100 RCP8.5: 2006-2100	Historical: 1970-2005 RCP4.5: 2006-2100 RCP8.5: 2006-2100	Historical: 1970-2005 RCP4.5: 2006-2100 RCP8.5: 2006-2100	Historical: 1970-2000 RCP8.5: 2001-2100

There are many studies that used the RCMs from SEACLID/CORDEX-SEA and MRI to study the climate change impact assessment, which presented as follows.

1) Previous studies on SEACLID/CORDEX-SEA

Aldrian et al. (2004) simulated long-term precipitation over Indonesia using MPI regional climate model. Three different lateral boundaries forcing have been performed through the regional climate model simulation. The simulation results were compared with the observation data. In general, the climate model performed well in simulating spatial pattern of monthly and seasonal precipitation over the land area, but overestimated precipitation over the sea. Regional climate model also reproduced variability well during El Nino, however; model fails to show good simulation during wet and dry monsoon.

Ngo-Duc et al. (2016) evaluated the performance of RegCM4 in rainfall simulations over Southeast Asia under different combinations of air-sea flux and deep-convection parameterization schemes under SEACLID/CORDEX Southeast Asia. Four different datasets of gridded rainfall were used for the model performance assessment. Over the Southeast Asia, simulation produced unrealistic rainfall responses to surface temperature. The model resulted that atmospheric force to the processing of the land surface compared to the observation. The robust system was designed to rank the simulation based on their performance in different rainfall characteristics. The result suggested that the air-sea flux scheme performed better overall than the rest of the simulation.

Fredolin Tangang et al. (2018) simulated the annual precipitation over the Southeast Asia under 2°C of global warming based on the model simulations of SEACLID/CORDEX Southeast Asia. In this study, four indices of extreme rainfall were considered including annual total rainfall, consecutive dry day, frequency of rainfall exceeding 50 mm/day, and intensity of extreme rainfall. The results illustrated that the most changes during the period of 2031-2051 were significant largely. The result also showed that in the northern part of Southeast Asia is suggested that the area might face more serious effect than other region in Southeast Asia.

Fredolin Tangang et al. (2019) used both of GCMs and RCMs for climate change impact assessment over Thailand for three periods of 2011-2040, 2041-2070, and 2071-2099. Seven members of six GCMs and three RCMs are used to estimate ensemble mean. The results showed that the mean precipitation has good relationship with observation over Thailand during period of 1976-2005. Moreover, the ensemble mean of projected precipitation under both of RCPs gave contrast results between the northern and southern part of Thailand during dry months. During the historical period, magnitude changed up to 15% depending on the projection period and sub-region. In contrast, the projected precipitation during wet season for both of RCPs reduced by 10% in the same area. These changes were related to regional circulation change in winter and summer monsoon.

Oeurng et al. (2019) applied hydrologic model to assess impact of climate change on 11 river flows in Tonle Sap Basin, Cambodia. Precipitation from three GCMs (GFDL-CM3, GISS2-R-CC, and IPSL-CM5A-MR) were used for streamflow simulation. The result demonstrated that the projected streamflow was likely to decrease in both dry and wet seasons. The mean annual projected streamflow of 2030s, 2060s, and 2090s decreased in the range of 9-29%, 10-35%, and 7-41%, respectively. Moreover, the increase in extreme streamflow could reduce flood magnitude and increase drought events over the basin. This study provided

understanding for water resources adaptation and planning strategies in streamflow decreasing situation.

2) Previous studies on NHRCM

Yukimoto et al. (2012) developed a new global climate model, MRI-CGCM3 from MRI-CGCM2 series. The simulation of present-day mean climate in the historical experiment was evaluated by comparing it with observation including reanalysis. The result showed that model could reasonably produce the overall mean climate, seasonal variation in the atmosphere and ocean. The simulated climate variability was also evaluated, and it was found to be realistic. However, the simulated sea surface temperature indicated generally warm bias in the southern and cold bias in the northern, and the simulated sea ice expanded excessively in the northern in winter.

Cruz and Sasaki (2017) simulated the present climate over Southeast Asia to evaluate the performance of the Non-hydrostatic Regional Climate (NHRCM) for determining its downscaling applicability in the region. The boundary conditions of ECMWF ERA-Interim dataset over the region in 25 km resolution in period of 1989-2008 were used for the simulation. The results showed that NHRCM can reduce the overestimated precipitation and improve in spatial patterns, especially over Philippine and Maritime Continent. On the other hand, NHRCM had tendency to underestimate daily precipitation, particularly over Laos and Cambodia, while overestimate daily precipitation over northeast of Thailand. The result also suggested that NHRCM can improve the potential applicability in present and projection climate scenarios for the region.

Anwar Tinumbang Aulia et al. (2018) applied the simulation result of NHRCM 5 km resolution to evaluate river discharge over Thailand region using SiBUC and 1K-FRM models which are land surface and flow routing model, respectively. The runoff was simulated using SiBUC, while the river discharge was simulated using 1K-FRM and they were compared with the observation data. The result indicated that the NHRCM 5 km showed underestimated precipitation over most of Thailand, except in the northern part that the NHRCM gave better accuracy. For the discharge simulation, the 1K-FRM performed well in upper Bhumibol reservoir.

Ngai et al. (2020) simulated present and future precipitation over Malaysia using NHRCM 5 km under the RCP8.5 scenario to investigate the extreme precipitation projection. Overall, the result demonstrated that the model was capable to simulate the historical precipitation. On the other hand, NHRCM precipitation tended to underestimate in high and mean precipitation intensity over Malaysia.

However, the NHRCM showed that the number of hotspots was identified with significant projected increases in extreme, mean, and consecutive dry day up to 80, 30, and 20%, respectively.

2.2.4. Bias correction of RCM precipitation

The RCMs are outstanding tool for prediction of future climate under various assumptions. Although RCMs can represent regional scale of climate conditions, such outputs still have statistical bias and uncertainty when compared with the observed data (Berg et al., 2012). Therefore, when the RCMs data are applied without bias adjustment for hydrological model analysis at a basin scale, it may affect the reliability of the model results (Nguyen et al., 2016). Thus, bias correction is a crucial step to reduce systematic error of model and offers more reliable outputs of climate data from RCM simulations before applying them to impact assessment of climate change applications (Argueso et al., 2013).

Several different bias adjustment approaches have been developed and improved for regional climate impact studies (Ngai et al., 2017). These techniques include e.g. multiple linear regression (Hay and Clark, 2003), quantile mapping (Cannon et al., 2015; Switanek et al., 2017), gamma-gamma transformation (Sharma et al., 2007), distribution mapping (Ines and Hansen, 2006), local intensity scaling (Luo et al., 2018), and delta change method (Räty et al., 2014). Quantile Mapping (QM) technique has been widely used in bias correction for RCMs data due to its good performance in many areas (Switanek et al., 2017). QM technique is used to adjust the cumulative distribution function (CDF) of simulated precipitation data with the CDF of rain gaged data using transfer function (Cannon et al., 2015). The study of Trinh et al. (2019) found that the application of the QM technique can be explored to correct the bias on precipitation derived from the model simulations under framework of SEACLID/COREDEX-Southeast Asia (Trinh et al., 2019). Cannon et al. (2015) illustrated that the QM technique can capture the variation of precipitation and match all statistical moments. Moreover, QM technique aims to correct the RCMs data toward identical population feature such as mean, variance, skewness etc. with the observation (Ringard et al., 2017). As a result, the QM technique is a preferred method to be used in this research study. The schematic of QM method is shown in Figure 2-2, and transformation function is formulated as shown in Equation 2-2.

$$P_{bc} = F_{obs}^{-1} \left(F_{sim} \left(P_{sim} \right) \right), \quad (2-2)$$

where P_{bc} is adjusted precipitation, P_{sim} is precipitation from RCM, F_{sim} is cumulative distribution function (CDF) of P_{sim} , and F_{obs}^{-1} is invert of the cumulative distribution function of P_{obs} .

The cumulative distribution function (CDF) from the observed and RCM precipitation data can be estimated through the following equation:

$$CDF_t = \frac{1}{n+1} + CDF_{t-1} \text{ or } CDF = \frac{m}{n+1} \gg CDF_0 = 0, \quad (2-3)$$

where CDF_t is the cumulative distribution function at time t , CDF_{t-1} is the cumulative distribution function at time $t-1$, m is the order number of data, and n is the total number of data.

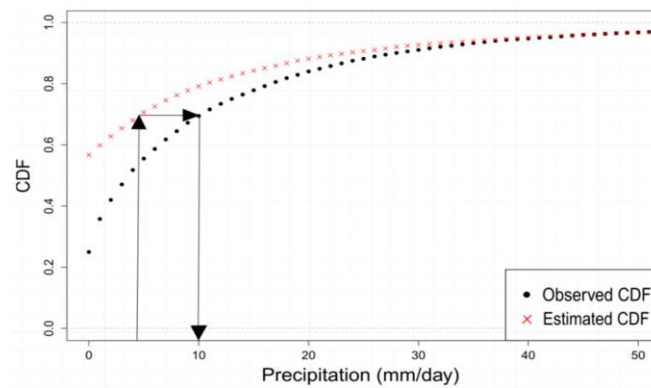


Figure 2-2 The schematic of quantile mapping technique

Several studies used QM technique for bias correction of RCMs are presents as follow:

Cannon et al. (2015) used QM bias correction algorithm to correct distributional bias in precipitation from climate models. The projected daily precipitation from CMIP5 over Canada was considered to adjust the corrected biases. Performance of QM method was evaluated based on extreme precipitation index. The bias correction showed that the adjusted precipitation projection was close to the observation data. The result also showed that QM method provided good ability in reducing bias of raw precipitation from climate model.

Ngai et al. (2017) applied QM method to adjust the bias of RCM and GCM simulated for daily surface mean temperature and precipitation over Southeast Asia Region based on dataset from APHRODITE. Four different RCM outputs in CORDEX-EA were used to correct bias adjustment. The results illustrated that the RCM biases were comparable with the GCM biases. Generally, QM technique can improve biases of both precipitation from RCM and GCM. However, the bias correction technique provided better performance for daily surface temperature than for daily precipitation. Overall, this study demonstrated that QM method was acceptable for RCM and GCM daily precipitation over CORDEX-EA.

Enayati et al. (2020) compared the abilities of bias correction method (QM) for assessing the performance of bias correction technique under various conditions. The raw GCM and RCM outputs (ICHEC and NOAA-ESM) from CORDEX dataset were selected to be applied over the Karkheh River basin in Iran. The results showed that the performance of bias correction depended on transfer function, topographic condition, and parameter sets. This study suggested that QM method could provide improved results for both temperature and precipitation variables.

Amsal et al. (2019) applied statistical bias correction technique to correct bias of the raw climate projection outputs (RegCM) from downscaled CMIP5 GCM climate simulation over Indonesian region. The bias correction method was based on the initial assumption of Gamma distribution. The results illustrated that QM method could generally improve skill in simulating precipitation over Indonesia and it was an essential tool for further regional climate model studies.

Heo et al. (2019) applied two-shape parameter distribution in QM method to correct bias of precipitation for climate model under climate change scenario. The impact on frequency analysis of extreme precipitation in future period was also investigated using Burr XII and Kappa distributions. The results demonstrated that two-shape parameter distribution in QM method led to better performance in reproducing the observed precipitation compared to other distributions. This study suggested that the Kappa distribution was considered as the best distribution.

2.3. Streamflow prediction

In terms of sustainable water resources management planning, streamflow time series data are of high important yet many catchments across the world as well as in Laos are poorly gauged or ungauged (Chiew et al., 2018). This presented the need for reliable hydrologic model for streamflow simulation in poorly gauged or ungauged catchments (Vasiliades, 2014). Streamflow simulation studies involve the process of transferring the model parameters form gauged to poorly gauged or ungauged catchments (Razavi and Coulibaly, 2016). There are many hydrological models that have widely been used for continuous streamflow simulation and assessment of the effect of climate change on optimal reservoir operations in the river basins (Hosseini et al., 2014). In this study, Integrated Flood Analysis System (IFAS) is reviewed for continuous streamflow simulation in NNRB. The NNRB can be considered as ungauged or poorly gauged basin because most area is mountainous and meteorological and hydrological stations are very limited. The IFAS has interface for the local data and global data that can be downloaded from website as the input, which is suitable for the NNRB. Moreover, IFAS performed well in predicting streamflow for the Nam Song River which is one of tributaries of the Nam Ngum River. IFAS is expected to perform well in NNRB (Kimmany et al., 2016).

2.3.1. IFAS model

IFAS model was developed by a collaborative research team of International Centre for Water Hazard and Risk Management (ICHARM), the Public Works Research Institute (PWRI) (Fukami et al., 2009). IFAS is a succinct tool with a Graphic User Interface (GUI) for building analysis distributed rainfall-runoff model. The model comprises of distributed hydrological model based on the tank model and routing model and also based on kinematic wave hydraulic model. There are several tank models contained in IFAS including surface tank, groundwater tank, and river channel tank models as showing in Figure 2-3.

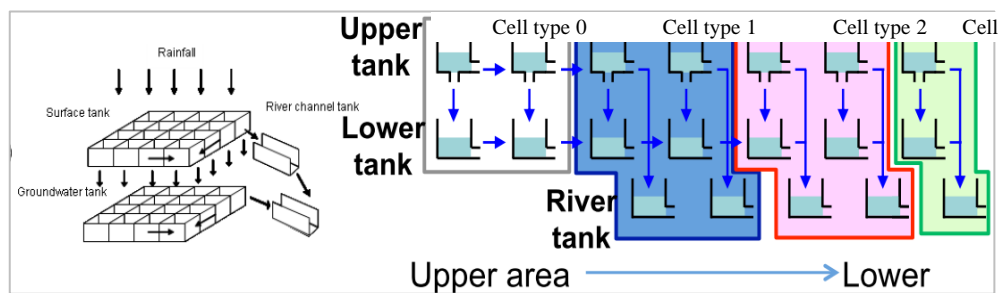


Figure 2-3 Schematic figure of distributed hydrological model.

IFAS adopts cell type to set runoff process in upper, middle reach and downstream area and assuming that the upstream is the area near the end of the drainage course of each river tributary. The upstream or downstream watersheds contain four cell types as present in Table 2-3. The vertical and horizontal flows in IFAS model structure are based on three forms as shown in Figure 2-4. The mechanism of the three forms of tank including surface tank, groundwater tank, and river channel tank can briefly be explained in the following paragraphs (Fukami et al., 2009).

Table 2-3 Cell type characteristics

Cell type	Characteristics
Cell type 0	The cell which water flows only into surface tank and aquifer tank, without river channel tank
Cell type 1	The cell which water flows into aquifer tank and river channel tank from surface tank
Cell type 2	The cell which water flows from aquifer tank into river channel tank
Cell type 3	The cell of river tank, which executes channel routing based on kinematic wave method.

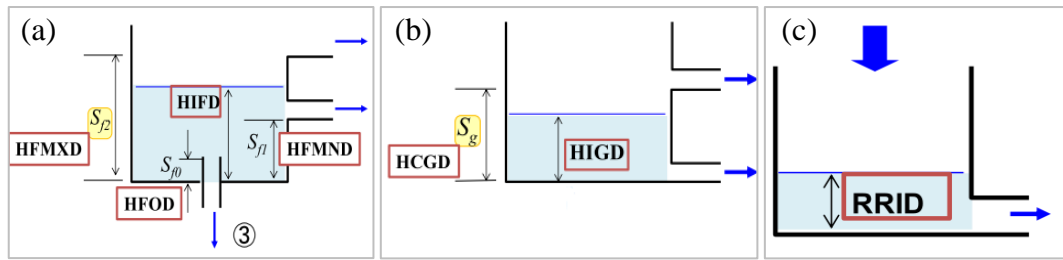


Figure 2-4 (a) Surface tank, (b) Groundwater tank, (c) River channel tank.

1) Surface tank model

The surface tank model contains three flow types (surface flow, sub-surface flow, and infiltration) necessary for estimating rainfall to runoff. The flows are calculated based on Manning's law, and Darcy's law as shown in Eq. (2-4) – Eq. (2-6), respectively.

$$\text{❖ Surface flow: } L \frac{1}{N} (h - S_{f_2})^{5/3} \sqrt{i} \quad (2-4)$$

$$\text{❖ Subsurface flow: } \alpha_n A f_0 \frac{h - S_{f_1}}{S_{f_2} - S_{f_1}} \quad (2-5)$$

$$\text{❖ Infiltration: } A f_0 \frac{h - S_{f_0}}{S_{f_2} - S_{f_0}} \quad (2-6)$$

where: f_0 is final infiltration capacity, S_{f_0} is height where the ground infiltration occurs, S_{f_1} is height from which rapid unsaturated subsurface flow occurs, S_{f_2} is height from which surface flow occurs, N is ground surface roughness coefficient, L is mesh length, i is slope with the adjacent cell, α_n is rapid unsaturated subsurface flow regulation coefficient, h is water height for the tank.

2) River tank model

The river course channel is the final tank. The flow from this tank is calculated based on Manning's equation as shown in Eq. (2-7).

$$\text{Manning equation: } B \frac{1}{n} h^{5/3} \sqrt{i} \quad (2-7)$$

where: B is breadth of river course, i is slope of river course, h is water height for the tank, n is roughness coefficient of river course.

3) Groundwater tank model

This tank has two outflows through orifices calculated based on the fraction unconfined (h^2) and confined (h) aquifers as shown in Eq. (2-8) and Eq. (2-9).

$$\text{❖ Unconfined groundwater flow: } A_u^2 \times h - S_g^2 \times A \quad (2-8)$$

$$\text{❖ Confined groundwater flow: } A_g \times h \times A \quad (2-9)$$

where: A_u is slow saturated subsurface flow coefficient, A_g is base flow coefficient, S_g is height where slow saturated subsurface flow occurs.

2.3.2. Model parameter sensitivity analysis

Model parameter sensitivity analysis is a process that evaluates the effect of model parameter values on the change of model outputs. The sensitivity analysis can help to estimate which parameter is influential in producing accurate results. Sensitive parameters are the parameters that has high contribution to the change in the model output (Sayasane et al., 2015). The level of sensitive of parameters depends on the amount or percentage of changes in model outputs.

2.3.3. Model parameter calibration and validation

The model parameter calibration is a process involving the modification of sensitive model parameters to simulate streamflow. A comparison of simulated output with observation data is performed until the defined objective is achieved (Hafiz et al., 2013). After all sensitive model parameters are identified, these parameter values will be used for calibration of IFAS model using IFAS Calibrator. The model parameters were automatically adjusted in the maximum and minimum range of parameter values in order to simulate streamflow to best match with the observation judging based on statistical performance indices (Mohd Sidek, 2014).

After the model produce sufficiently good results, the optimal parameter values are believed to be obtained. The optimal parameter values are used to validate streamflow prediction in other catchments which are not used during calibration. The hydrologic, physical, and climate characteristics in gauged catchment should be sufficiently similar to the catchment of interest (Hafiz et al., 2013). The objective of model validation aims to modified optimal parameter values to simulate streamflow in ungauged catchments without making any further adjustment of parameter values (Chiew et al., 2018).

2.3.4. Previous studies on streamflow simulation

To simulate streamflow in data limitation catchment, IFAS uses the theoretical tank model, Manning's law, Darcy's law, and kinematic wave methods. Parameters

can be estimated by using grid-based global data set on topography, soil classes, and land use. When the actual flood event is reproduced by storage function method. Flood reproducibility is not enough in medium/small size floods, because the storage function method is non-linear and one-layer tank. For numerical calculation, approximation function was used to solve time integral equation. Discharge calculated in the river channel tank is solved by kinematic wave equation (Rajabi et al., 2015). There are many researchers who studied the hydrologic model for streamflow simulations and future impact of climate change assessment on streamflow and their work are reviewed in following section.

Aziz and Tanaka (2011) applied Integrated Flood Analysis System (IFAS) to minimize the losses and damages to the lowest level due to flooding of the Upper-Middle Indus River, Pakistan. The satellite precipitation of GSMaP and 3B42RT were used as input data to develop the regional variable. The results presented that the flood duration and flood peak that calculated by the satellite GSMaP had the best fit with the observed data. The satellite 3B42TR, flood duration was good for most of the cases.

Kimura et al. (2014) applied IFAS model to simulate the flood peak in a local watershed using hyetograph created from extreme weather data of high-resolution MRI-AGCM3.2S. The modified ranking method was used to present flooding in near-future and far-future periods using the top 10 extreme rainfall events. The results illustrated that when the hydrograph was generated using modified ranking method, the flood peak simulated through the IFAS model was overestimated for lower peak of cumulative rainfall depth due to the sharpness of distribution of rainfall dimensionless. The effect of global climate change illustrated that the future flood peak can increase up to three times of present term peaks. This might lead to different flood control for the downstream of river reaches.

Sayasane et al. (2015) applied Soil and Water Analysis Tool (SWAT) to assess the impact of future climate and land use changes on streamflow in the Nam Song watershed. The future land use was predicted using the logistic regression method. The results showed that the streamflow could be decreased by 11.7-12.2% over the Nam Song watershed for the next 20 years, particularly in the middle part of watershed due to climate and land use changes. Water transferred to Nam Ngum 1 reservoir to increase hydropower production could be a reason.

Limlahapun and Fukui (2016) applied IFAS model to simulate streamflow for historical and future scenarios. The fifth phase of the Coupled Model Intercomparison Project (CMIP5) was used to derive precipitation scenarios. Hydrologic Engineering Center model was used to generate inundated areas. This research focused on data integration and approach that are manageable and flexible leading to an improved

modelling for flood monitoring. The result indicated that the flood map with real-time stream data can help the local communities to identify risk areas of flooding in advance.

Kimmany et al. (2016) applied IFAS to assess the effectiveness of hydrologic models for streamflow prediction in the Nam Song River basin which is a tributary of Nam Ngum River basin. The aim of the study was to assess the performance of rainfall-runoff models for streamflow predictions under the data scarcity. Three rainfall-runoff models, i.e., HEC-HMS, IFAS and SWAT, with different complexities were tested. The result suggested that IFAS outperformed than other rainfall-runoff models.



CHAPTER 3

STUDY AREA

This chapter focuses on the characteristics of the NNRB, which is the study area of this research. The background of the NNRB will be presented first to establish an understanding of the basin. The following parts of this chapter cover the geographical, hydrological, and meteorological conditions, hydropower development, and flood problem.

3.1. Background of the NNRB

The NNRB is one of the main streams of the Mekong River, starting from the northern mountainous area of the Xiengkhuang province, passing through the Vientiane Province, and joining with the Mekong River in the capital of Laos, the city of Vientiane. The NNRB is the fourth largest river in Laos based on the area size and was the pilot basin where the Integrated Water Resources Management (IWRM) was implemented in Laos (WREA, 2009). The total length of the river is approximately 415.5 km, and the area of the river basin is 16,931 km², making up 7.3% of the entire area of Laos and accommodating 9% of the total population in the country. The basin covers 5 provinces (Table 3-1), 19 districts, and 18 sub-basins. The basin can be divided into two parts. The upper part is hilly and mountainous, while the lower part is a flat area. As the NNRB has procured a sufficient reserve amount of water resources, as well as excellent geographical conditions, many reservoirs have been operated and planned to be constructed for hydropower generation within the river basins and their tributaries (WREA, 2008). The location of the hydropower plants development within the NNRB is shown in Figure 3-1.

Table 3-1 The area size of province within the NNRB

No	Province	Area size (km ²)	Area size within basin (km ²)	Area size within basin (%)
1	Vientiane Capital	3,920	1,928	11.4
2	Luangphabang	16,875	696	4.1
3	Xiengkhuang	14,751	2,858	16.9
4	Vientiane	15,610	6,957	41.1
5	Bolikhamxay	14,863	63	0.4
6	Xaysomboon	8,551	4,429	26.2
Total		74,570	16,931	100

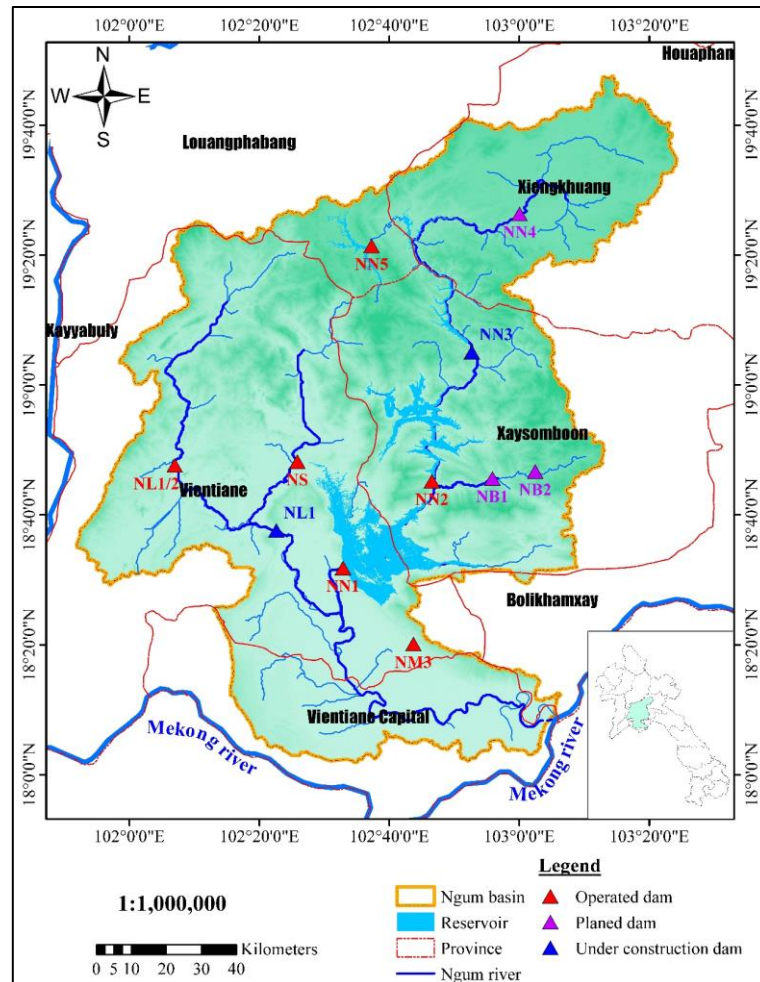


Figure 3-1 The Nam Ngum River Basin map.

3.2. Hydropower development

Hydropower development is important in supporting the short and long term of Lao economy. Presently, more than 95% of power production in the country is from hydropower stations and most hydropower production is exported to neighboring countries. It is predicted that the electricity demand from neighboring countries is higher than the hydropower production that Lao PDR can supply, thus the electric trade in the Asian region could be increased in the future. However, only 58% of the population in Lao PDR can access electricity, and the internal energy consumption is increasing with the GDP growth. Based on the increase of internal and external energy demand, the NNRB is a key of the energy sector in Lao PDR. According to the potential for effective utilization of rainfalls and outflow amount within the basin, the NNRB is set up with many hydropower plans for generating hydropower to meet those demands. Six hydropower plants are currently in operation in the NNRB. Two hydropower plants are under construction, and another three power plants are in the

planning stage (MOU signed) (WREA, 2008). The main features of each power plant in different stages of development are shown in Figure 3-2 and Table 3-2.

Among these hydropower projects, three main hydropower projects from both operated and under-construction dams including NN1, NN2, and NN3 are considered as the case study for this research. This is because three of them are the largest hydropower based on reservoir and power generation capacity in the NNRB and NN1 is located in central Laos, which is a very important hydropower for people in Vientiane as well as national economic growth. The key features of NN1, NN2, and NN3 are shown in Table 3-3. The details of each project are presented in the following sections.

The Nam Ngum 1 (NN1) HPP has started its power generation in 1971 with 30 MW installed capacity. Consequently, it was expanded up to 110 MW with additional 2 units of 40 MW in 1979. Then, in 1985, NN1 was expanded up to 150 MW, with an additional one unit of 40MW. Furthermore, Units No.1 and No.2 were rehabilitated from 2003 to 2004, hence the total installed capacity became 155 MW at present. NN1 was developed in the Nam Ngum River system with the largest reservoir in Laos with 7 billion m³ of storage capacity and 370 km² of reservoir area at full supply level (FSL). NN1 has mainly covered peak loads because it has high capability of flexible control of power output with its particularly large reservoir.

Nam Ngum 2 (NN2) HPP has operated by Nam Ngum 2 Power Company (NN2PC). It is located approximately 90 km north of Vientiane in the middle of Laos and approximately 35 km upstream from the existing NN1. NN2 dam is in the mainstream of the Nam Ngum River and is the Concrete Face Rockfill Dam (CFRD). The NN2 HPP was constructed with the total capacity of 615 MW for supplying energy to the electricity network of Thailand and all electricity production amount is sold to the EGAT of Thailand based on the Power Purchase Agreement (PPA). The catchment area of NN2 is 67% of NN1 and the effective reservoir volume is 2,994 MCM. The inflow into the NN1 reservoir after commencement of power generation of NN2 is closely regulated throughout the year.

The Nam Ngum 3 (NN3) HPP was planned further upstream of the NN2 project site, and the catchment area is 69% of NN2. Although the detailed design of the project has been completed, the timing of commencement of power generation is not yet fixed. This is because the PPA was not finalized between the developer and EGAT. The dam is located approximately 4.5 km upstream of the point of joining of the Nam Ngum River and the Nam Phay River and is approximately 150 km away from the point of joining of the Nam Ngum River and the Mekong River.

Currently, the NN3 HPP construction project is being constructed by Sinohydro Company (China). The construction has started since 2015 and was expected to take approximately five years to be completed in 2021. The NN3 reservoir has dead storage capacity of 439 MCM at dead water level of EL.670 m.

Table 3-2 Project features of hydropower plant in the NNRB

Status	Name of project	Installed capacity (MW)	Operation Year	Planned market
Operating	Nam Ngum 1 (NN1)	155	1971	Laos/Thailand
	Nam Ngum 2 (NN2)	615	2012	Thailand
	Nam Ngum 5 (NN5)	120	2012	Laos/Vietnam
	Nam Song (NS)	6	1996	Laos
	Nam Lik 1/2 (NL1/2)	100	2010	Laos
	Nam Mang 3 (NM3)	40	2004	Laos/Thailand
Under construction	Nam Ngum 3 (NN3)	480	-	Thailand
	Nam Lik 1 (NL1)	64.8	-	Laos
Planning stage	Nam Ngum 4 (NN4)	240	-	Laos
	Nam Bak 1 (NB1)	160	-	Thailand
	Nam Bak 2 (NB2)	85	-	Laos/Thailand

Table 3-3 Characteristic of NN1, NN2, and NN3 hydropower plants.

Characteristics	NN1 HPP	NN2 HPP	NN3 HPP	Unit
Operation date	1971	2011	-	year
Catchment area	8,460	5,640	3,913	km ²
Storage volume	7,030	4,890	979	MCM
Dam crest elevation	215	381	729.5	masl
Weir crest elevation	202.3	359	705	masl
Maximum flood level	213	378.5	-	masl
Full supply level (FSL)	212	375	723	masl
Minimum supply level (MSL)	196	345	670	masl
Maximum tailwater level	178	225	385	masl
Rated flow per turbine	117/57	149.4	160	m ³ /s
Installed capacity	155	615	480	MWh
Full operation tailwater	166	212	380	masl
Rate head	40	148	330	m
Turbine efficiency	95	96.5	97.5	%
Time generation	18	16	19	hr/day

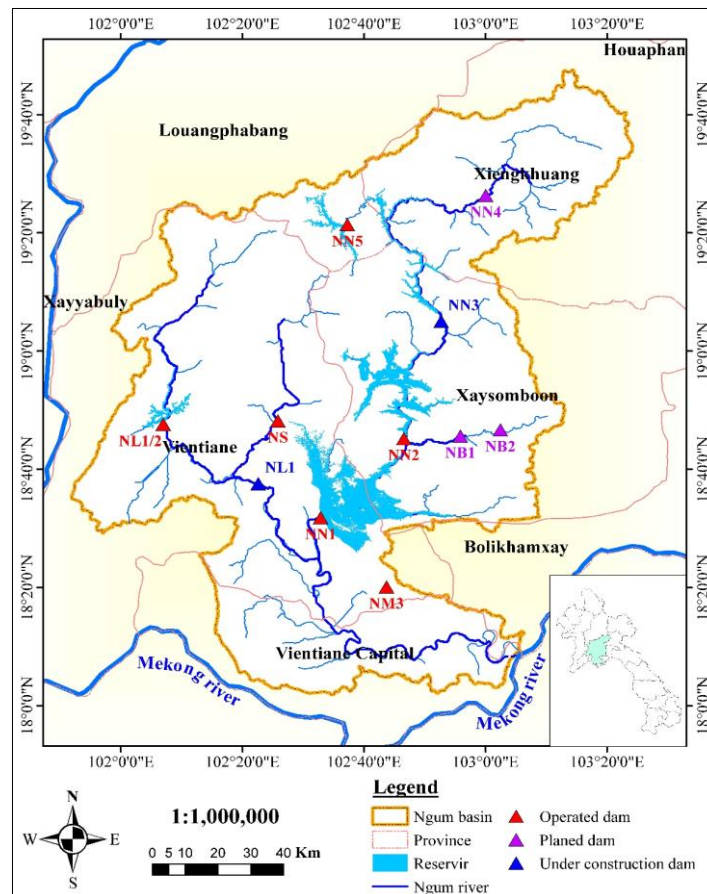


Figure 3-2 Location of hydropower plant in the NNRB

3.3. Existing reservoir operation

As mentioned in the previous section, there are six hydropower plants that are currently in operation in the NNRB. The Lao government has attempted to find the techniques to obtain maximum benefit from the hydropower production through the reservoir operation (WREA, 2009). There are few traditional reservoir operation techniques that have been used to operate the reservoir. These techniques include using the experience of operators, current reservoir level, water and electricity demands, and hydrological conditions. While there has been an attempt to obtain the optimal operating rule curves using some optimization techniques in the past (Sorachampa et al., 2020), until the present year, many hydropower plants in the NNRB have been operated using old operating rules or the experience of operators. This operation manner could not fully represent the hydropower development and obstruct the maximum efficiency of the operation. Specifically, the flood and water shortage still occurred in the rainy and dry seasons, respectively. Moreover, there remains a challenge in operations due to uncertainty in reservoir inflow caused by natural and climate changes as well as megaproject development within the river

basin. Because hydropower projects in the NNRB are managed by different agencies, the reservoirs are operated based on the different set of operating rule curves. In addition, most reservoirs in the NNRB are operated as stand-alone hydropower plants with no consideration to the impacts to the downstream ecosystem, population, and the other hydropower plants (Promwungkwa et al., 2019). Joint operation of multiple reservoirs could enhance the efficiency of hydropower production.

Some stakeholders at the district level blamed the reservoir operators for downstream flooding due to the NN1 reservoir release, health problems, and water quality in the NNRB Plan workshop. During the rainy season, the reservoir releases the large amount of water than needed and this could lead to floods. The stakeholders also reported that the main challenge of water management of lower the NNRB is the crop damages and the lack of proper warning systems (Bartlett et al., 2012).

3.4. Geographical features

The geographical features of the NNRB refer to the surface elevation level, the status of land use, and soil type classification. The detail of each feature is presented in the following sections.

3.4.1. Topography

The geographical feature of the NNRB is mostly hilly and mountainous in the upper and flat in the lower parts of the basin. The upper part of the NNRB is composed of the plateau area of the hilly sections higher than 500 meters above sea level (masl) accounting for approximately 71.8% of the total basin area. The lower part of the basin, which includes the floodplain where the Nam Ngum and Nam Lik rivers meet, is where the elevation is generally lower than 500 masl making up 28.2% of the total basin area as shown in Figure 3-3. Most of the basin area has a slope ranging from 5° to 25° approximately 63.6%. The basin area with a slope lower than 5° covers 16.3%, and the slope higher than 25° is 20.1% (WREA, 2008).

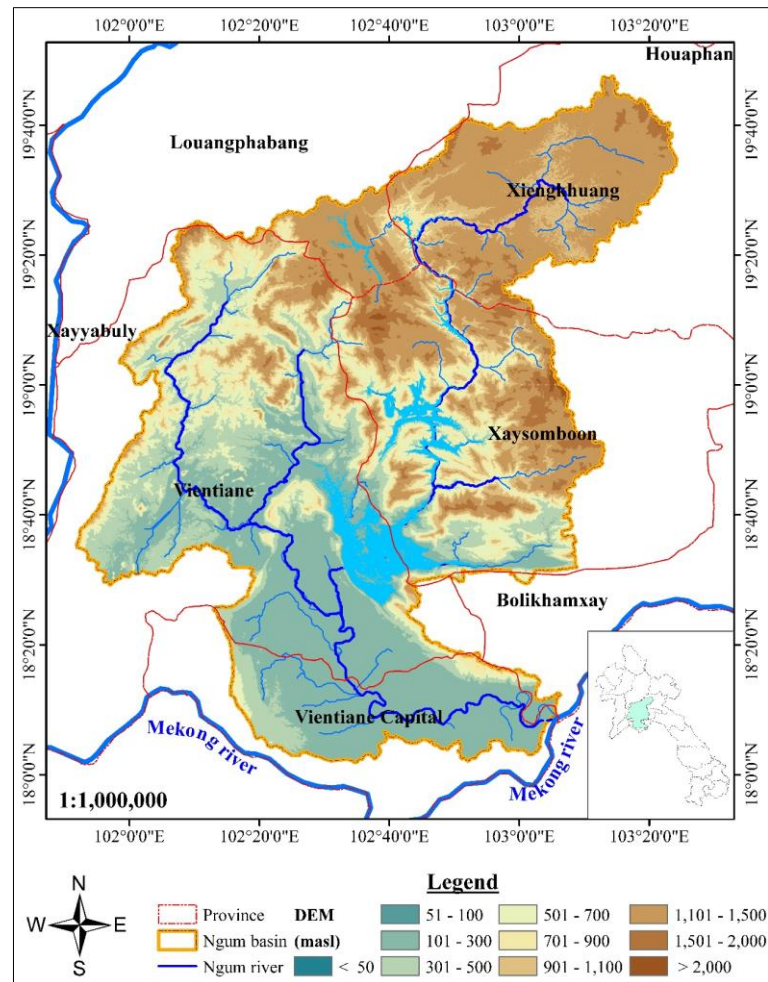


Figure 3-3 Distribution of surface elevation map.

3.4.2. Land use

According to the data from NAFRI, 2010, major land use in the NNRB is the forest which is approximately 81% of the entire river basin area. The agriculture area forming in the NNRB takes the second biggest portions about 8.0%. The urban area is at the lower part of the downstream of the NNRB. The priority of the land management of the Lao government is stopping the shifting cultivation. The traditional cultivation techniques are based on slash and burn agriculture. This largely affects the forest area. However, the fast growth of population within the NNRB induces the increase of urban and decrease of forest areas. Land use change in the basin is one of the causes of streamflow variability and water quality (Suhardiman et al., 2019). The land use distribution over the NNRB is shown in Table 3-4 and Figure 3-4.

Table 3-4 Land use distribution in the NNRB

No.	Land use	Area (km ²)	Area (%)
1	Forest	13,713.2	81.0
2	Agriculture	1,353.1	8.0
3	Water	585.5	3.5
4	Urban	23.8	0.1
5	Others	1,255.6	7.4
Total		16,931	100

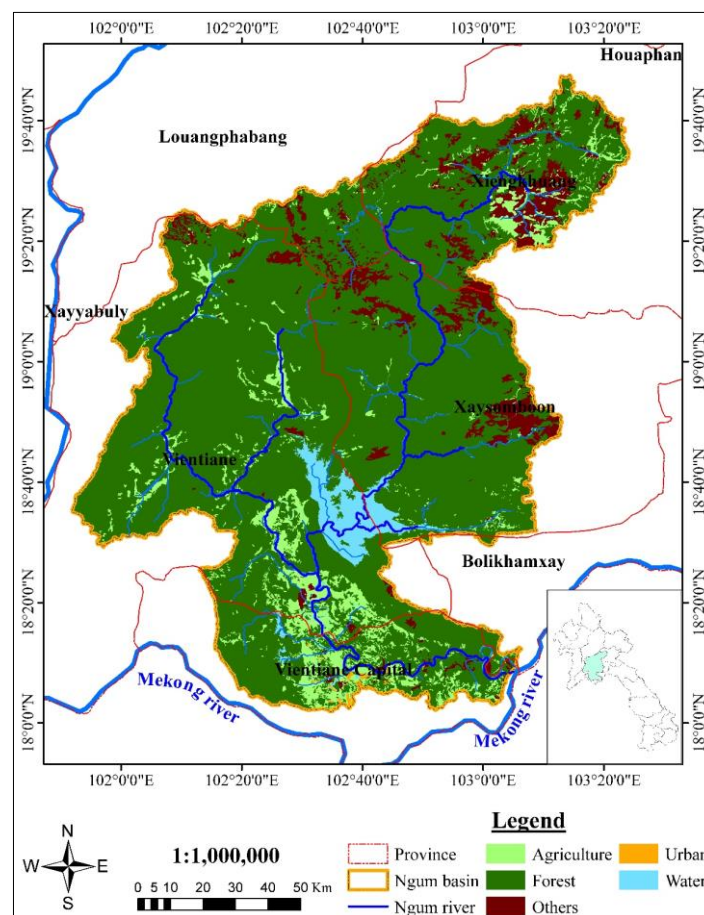


Figure 3-4 Land use distribution map of the NNRB

3.4.3. Soil type

The soil type of the NNRB is one of the factors affecting the amount of streamflow. According to the Soil classification report by Food and Agricultural Organization (FAO) in 2010, the major soil type in the basin is ferric acrisols (ACf) taking up to 41.8% of the total basin area. About 18.3% of the basin is covered by haplic acrisols (ACh), while 11.6% of the basin area is covered by Alf; other soil

types covered 28.3% of the total basin area. Acrisols (AC) is the soil type that contains higher clay and associated with the humid and tropical climate. It is soil with a low base-saturation degree and strongly acidic due to the weathering effect. The distribution of the soil type in the basin is shown in the Table 3-5 and Figure 3-5.

Table 3-5 Soil distribution in the NNRB

No	Soil Code	Area (km ²)	Area (%)
1	ACf	7,072.3	41.8
2	ACh	3,093.4	18.3
3	ALf	1,968.5	11.6
4	LXf	769.6	4.5
5	CMd	470.7	2.8
6	LVh	308.3	1.8
7	ALh	832.8	4.9
8	LVf	322.1	1.9
9	CMe	142.7	0.8
10	LXh	56.4	0.3
11	LPd	80.7	0.5
12	RGd	205.8	1.2
13	LVg	54.5	0.3
14	GLd	88.6	0.5
15	FLd	5.9	0.0
16	CMg	40.6	0.2
17	LXg	16.6	0.1
18	ALg	339.8	2.0
19	CMo	9.3	0.1
20	Reside	6.0	0.0
21	GLe	4.1	0.0
22	ACp	47.4	0.3
23	FLe	32.6	0.2
24	Swamp	852.9	5.0
25	GLu	17.5	0.1
26	GLm	5.1	0.0
27	LPe	86.9	0.5
Total		16,931	100

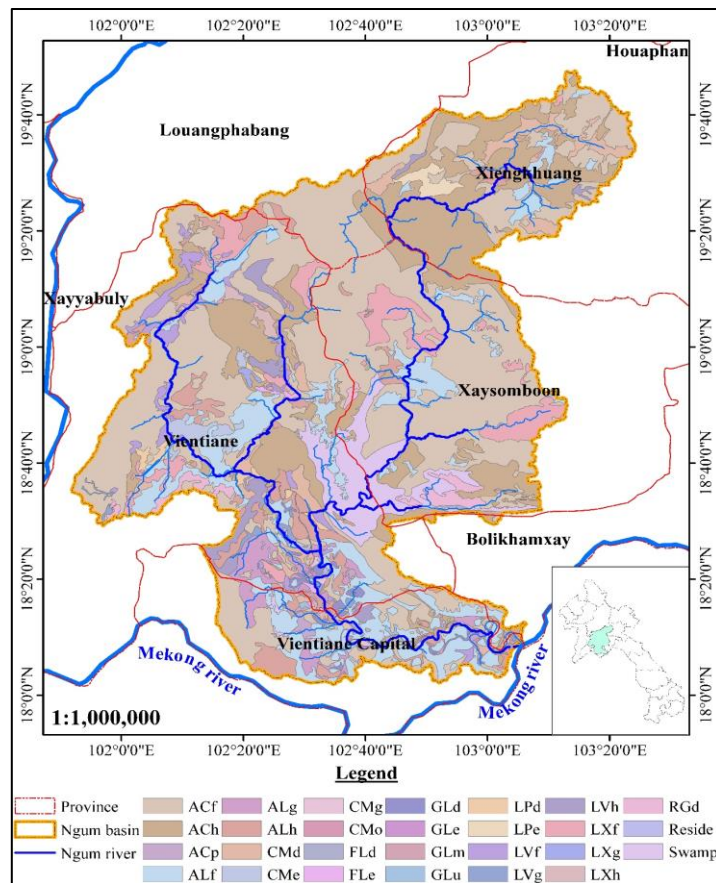


Figure 3-5 Soil distribution map of the NNRB

3.5. Meteorological and hydrological conditions

The NNRB is located in tropical zone and influenced by seasonal monsoon climate with two distinct seasons. The dry season starts from November to April and the rainy season from May to October. There are 11 rainfall, 6 weather, and 5 flow observed stations available within and nearby the NNRB. The data are obtained from the Department of Meteorology and Hydrology (DMH), Ministry of Natural Resources and Environment (MONRE), Lao PDR. Three meteorological stations with evaporation loss and rainfall records at different locations and altitudes were considered to be representative of the climate characteristics of the NNRB. Thonghaihin observed station represents the upstream area of the basin and is located in the mountainous section of elevation around 1,100 masl. Vangvieng observed station is in the middle area of the river basin. Phonehong observed station is located in the flat area of Vientiane at the downstream of Nam Ngum 1 (NN1) reservoir with elevation around 300 masl. The observed data in these three stations are recorded more than 30 years. The locations of the hydrological and meteorological observed stations and period of available data are presented in Table 3-6, Table 3-7 and Figure 3-6.

Table 3-6 Hydrological observed stations within the NNRB

No.	Station	Province	Coordinate		Available period
			Latitude	Longitude	
1	Hinheup	Vientiane	18.663	102.355	1990-2015
2	Vuenkham	Vientiane Capital	18.176	102.615	1990-2015
3	Pakkayoung	Vientiane Capital	18.431	102.538	1990-2015
4	Naluang	Vientiane	18.908	102.774	1990-2008
5	Kasy	Vientiane	19.234	102.253	1990-2015

Table 3-7 Meteorological observed stations within the NNRB

No.	Station	Province	Coordinate		Available period
			Latitude	Longitude	
1	Thonghaihin	Xieng Khuang	19.450	101.167	1990-2015
2	Naluang	Vientiane	18.913	103.067	2008-2013
3	Kasy	Vientiane	19.217	102.250	1990-2015
4	Phatang	Vientiane	19.100	102.250	1991-2013
5	Vangvieng	Vientiane	18.923	102.448	1990-2015
6	Hineheup	Vientiane	18.617	102.355	1990-2015
7	Nam Ngum 1	Vientiane	19.533	102.545	1990-2015
8	Phonehong	Vientiane	19.533	102.433	1980-2015
9	Napheng	Vientiane	18.317	102.667	1994-2015
10	Veunkham	Vientiane Capital	18.183	102.617	1990-2015
11	Vientiane	Vientiane Capital	17.928	102.620	1990-2015

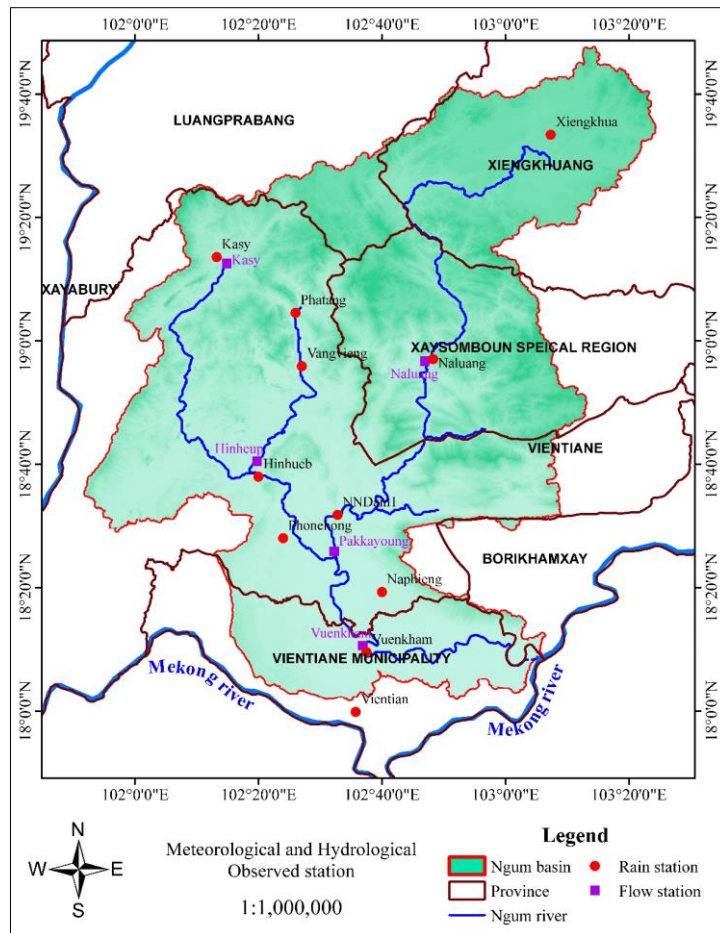


Figure 3-6 Locations of the meteorological and hydrological observed stations in the NNRB

3.5.1. Rainfall

The analysis of rainfall used in this study is based on historical data recorded in the period of 1990-2015. The NNRB is distinctively categorized into the rainy season (May-Oct) and dry season (Nov-Apr). High rainfall gradient is found in the basin with 975 mm in the northern part at Xiengkhuang Province and 4,678 mm in the middle of the basin at Vangvieng Town. The northern and southern parts of the basin are relatively drier compared to the middle part of the basin which receives rainfall of about 3,500 mm/year, while the middle part of the basin is humid (see Figure 3-7). For the monthly average rainfall, the maximum rainfall is from July to August in Vangvieng, Phonehong and Thonghaihin stations. The minimum rainfall records for all stations are in December. The monthly average and the annual rainfall pattern for each observed station within the NNRB are presented in Figure 3-8 and Figure 3-9, respectively. About 80% or more of the annual average amount of rainfall ranging from 1,911 to 2,925 mm is in the rainy season. The annual amount of rainfall over the NNRB is approximately 2,322 mm.

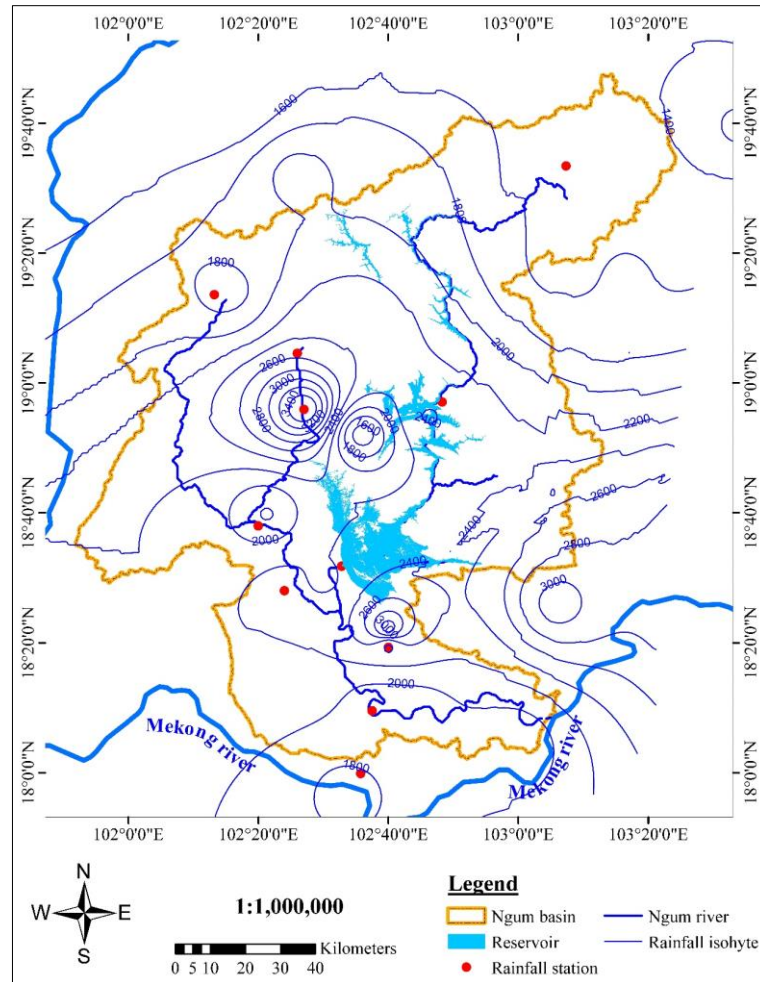


Figure 3-7 Isohyetal annual rainfall over the NNRB in period of 1990-2015

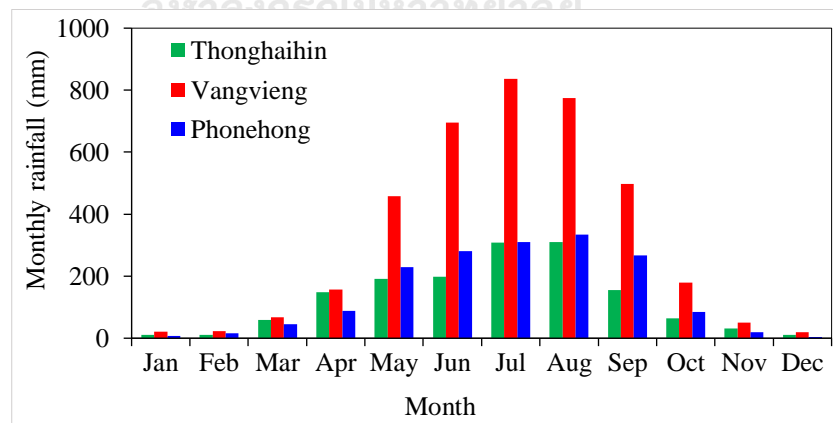


Figure 3-8 Monthly average rainfall over the NNRB in period of 1990-2015

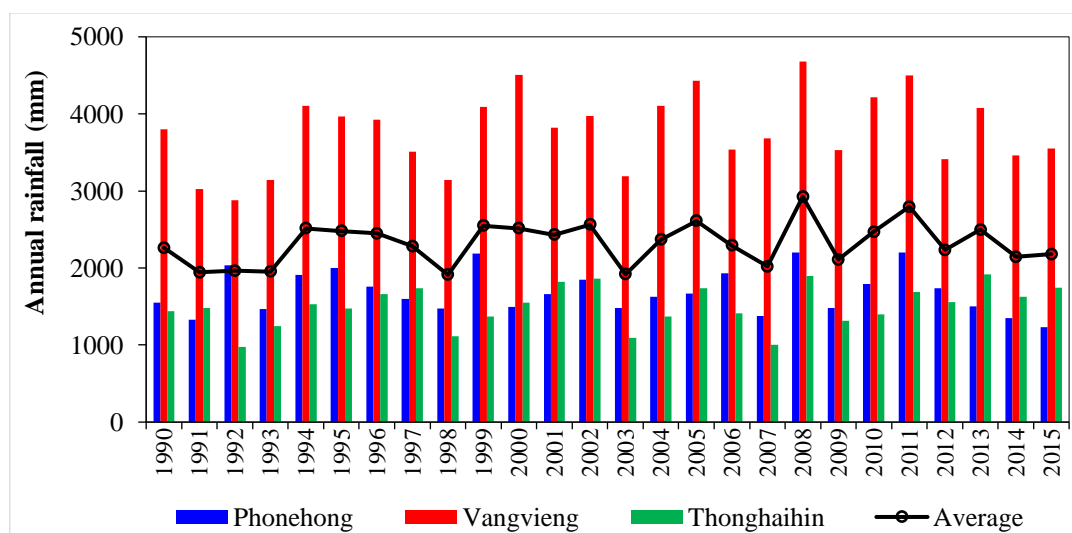


Figure 3-9 Annual rainfall pattern over the NNRB in period of 1990-2015

3.5.2. Evaporation

The analysis of evaporation in this study is based on three available observed stations recorded in the period of 2007-2015. The evaporation loss is generally high during the dry season and low during the rainy season. Figure 3-10 shows that high evaporation loss is in the Vientiane town area. This may be caused by urbanization. The maximum evaporation loss is 122 mm recorded in March and the minimum evaporation loss is 51.6 mm recorded in August. The monthly evaporation loss over the NNRB is 79.9 mm. The annual mean evaporation loss of approximately 60.8 % is generated in the dry season. The annual mean evaporation loss over the NNRB is 961.3 mm.

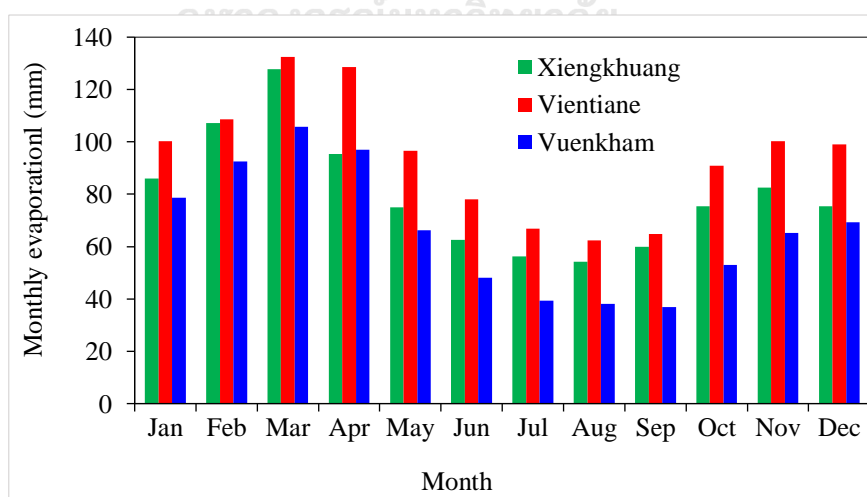


Figure 3-10 Monthly average evaporation loss over the NNRB in period of 2007-2015

3.5.3. Streamflow

There are five hydrological stations with available streamflow records as shown in Figure 3-6. Pakkayoung station, which is located the downstream of NN1 reservoir before joining with the Mekong River, is considered to be a representative streamflow station. The annual mean streamflow of the Nam Ngum River during the period of 1990-2015 is approximately 18,242 MCM. The lowest flow is 12,353 MCM recorded in 1998, while the highest flow is 294,006 m³/s recorded in 2005. Figure 3-11 presents that streamflow fluctuation has decreased since 2012 after the NN2 reservoir started to operate. The analysis of streamflow data provides evidence that NN2 can reduce the inflow fluctuation before flowing into NN1. The average monthly streamflow ranges from 775 MCM recorded in February to 3,159 MCM recorded in August as shown in Figure 3-12.

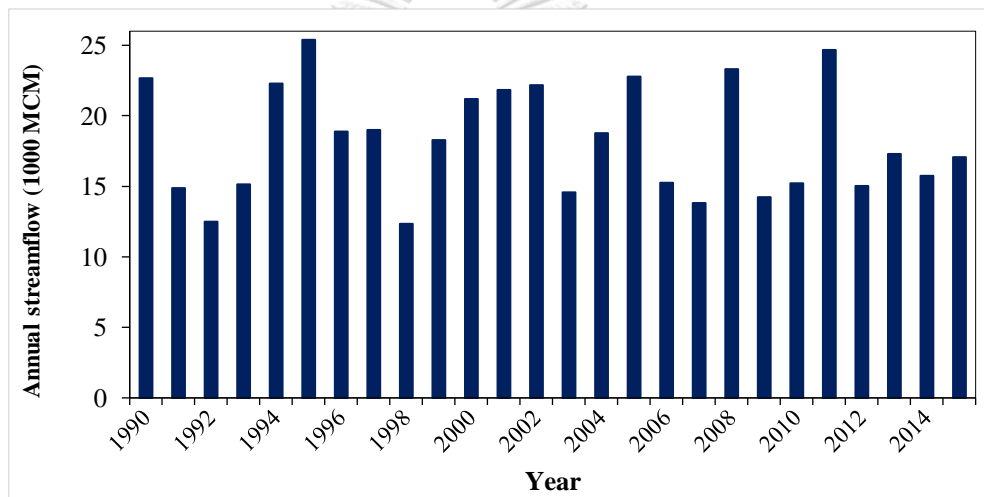


Figure 3-11 Annual streamflow pattern at Pakkayoung station in period of 1990-2015

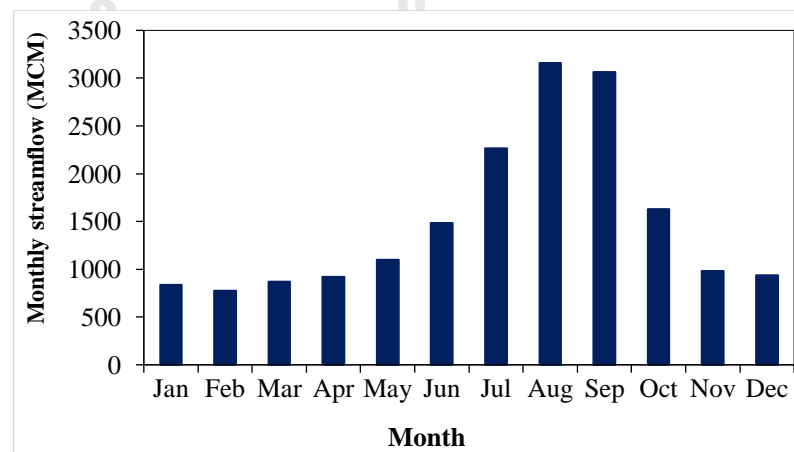


Figure 3-12 Monthly mean streamflow at Pakkayoung station in period of 1990-2015

3.6. Population status

According to the Results of Population and Housing Census reported by Lao Statistical Information Service (LAOSIS, 2019), the population of six provinces increased about 14.8% during 2005-2015. The population within the NNRB is estimated based on the population and population density in the provinces. Table 3-8 shows the estimated population within the province and NNRB region 2019 based on 2015. The population density in the NNRB is higher than the average of Laos (see Figure 3-13). The most population increases in NNRB are found in Vientiane Capital with the rise up to 58.1 %. The projected population in the NNRB is calculated to increase by approximately 1.42 % per year. The continuous population growth might have a large effect on future water resources in the NNRB with the increase in the amount of water demand and increase in damage from disasters related to water.

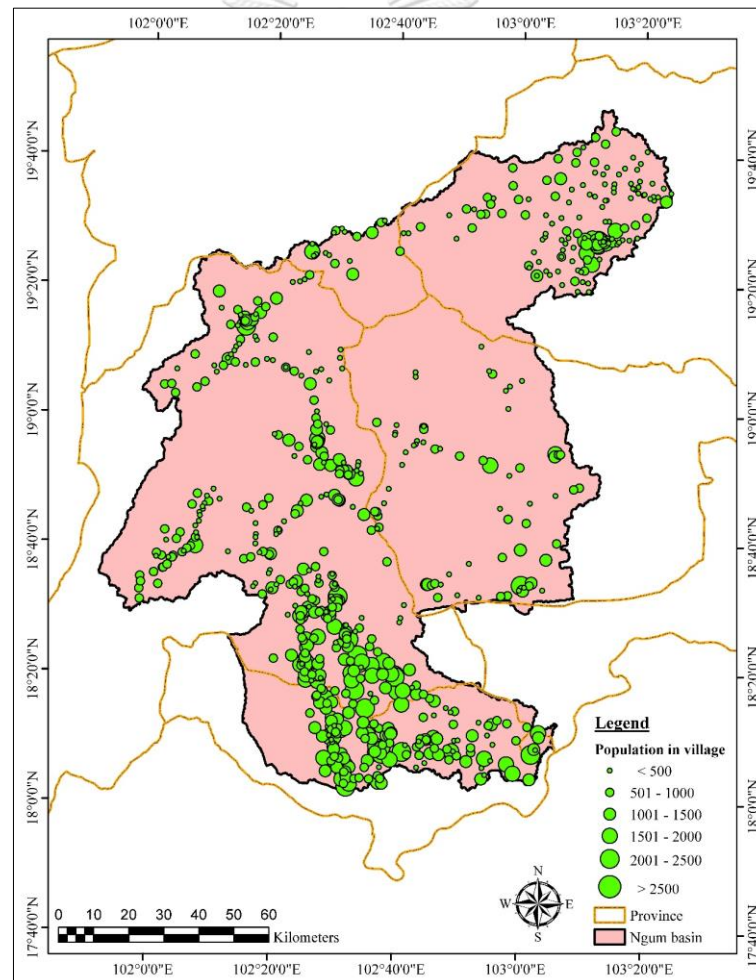


Figure 3-13 Distribution of population in village in the NNRB

Table 3-8 Population distribution within the NNRB region 2019

Nam of province	Population within the province (persons)	Population within the basin (persons)	Population ratio in the basin (%)
Vientiane Capital	927,617	456,294	58.1
Vientiane	455,981	203,238	25.9
Xaisomboun	105,222	54,464	6.9
Xiengkhuang	264,765	51,287	6.5
Luangphabang	462,997	19,082	2.4
Bolikhamsay	308,734	1,354	0.2
Total	2,525,316	785,718	100

3.7. Water use

Many sectors use water from the NNRB, but some of them are small users. This study focuses on the main water usage including domestic water usage and irrigation water usage. The total mean annual streamflow of Nam Ngum River is approximately 21 km³. The mean annual water usage for domestic and irrigation is about 0.063 km³ and 0.0273 km³, respectively. Current water usage is estimated at 1% of the total mean annual flow in the basin. It is predicted that water usage will increase up to 3-6% in the future due to irrigation development, fast population growth, and other water users.

3.7.1. Domestic water usage

According to the Nam Ngum River Basin Profile reported by Asia Development Bank (ADB, 2013), the average water usage for domestic is estimated to be 230 liter/person/day. There are approximately 785,718 people live in the NNRB region in 2019, the total water use can be estimated at about 5,421,453 m³/month. While the annual report on Vientiane Capital Water Supply State Enterprise (2019) identified that the downstream of NN1 reservoir region used amount of water for domestic about 5,456,000 m³/month (WREA, 2008). This does not include the water consumption in the upper part of the basin because most people in the upper part collect raw water from their own well or mountain spring. The estimated monthly amount of water usage within the NNRB region is presented in Table 3-9.

Table 3-9 The estimated monthly amount of water usage within the NNRB region

Name of province	Population within the basin (person)	Monthly water use within the basin (m ³)
Vientiane Capital	456,294	3,148,429
Luangprabang	19,082	131,663
Xiengkhuang	51,287	353,879
Vientiane	203,238	1,402,345
Bolikhamxay	1,354	9,340
Xaisomboun	54,464	375,798
Total	785,718	5,421,454

3.7.2. Irrigation water usage

Lao PDR is a landlocked country in Southeast Asia lying in the Mekong River basin. The irrigation development project or agriculture sector has been considered as a priority by the Lao government policy to support rice production. Many reservoirs ranging from small to large scale were constructed for multiple purposes. The data from the Department of Irrigation, Ministry of Agriculture and Forest showing existing irrigation areas in the NNRB region (see Figure 3-14) reveal that most irrigation areas in Laos are concentrated in Vientiane (47.4%) and Vientiane Capital (39.9%). In general, irrigation area is classified into two categories including rained and dry irrigation areas. Most irrigation area in the dry season is distributed in Vientiane Plain located downstream of NN1 hydropower. The amount of water in the NN1 reservoir is expected to be sufficient for the ecosystem of the lower NN1 reservoir and the rest of the flow can be supplied for irrigation in Vientiane Plain. Based on the report on the Irrigation Database in Lao PDR issued by the Department of Irrigation, Laos, water use for irrigation areas within the NNRB is estimated to be 1,425.6 m³/ha/month (Lacombe et al., 2014). The irrigation areas and water use in each province over the NNRB are presented in Table 3-10.

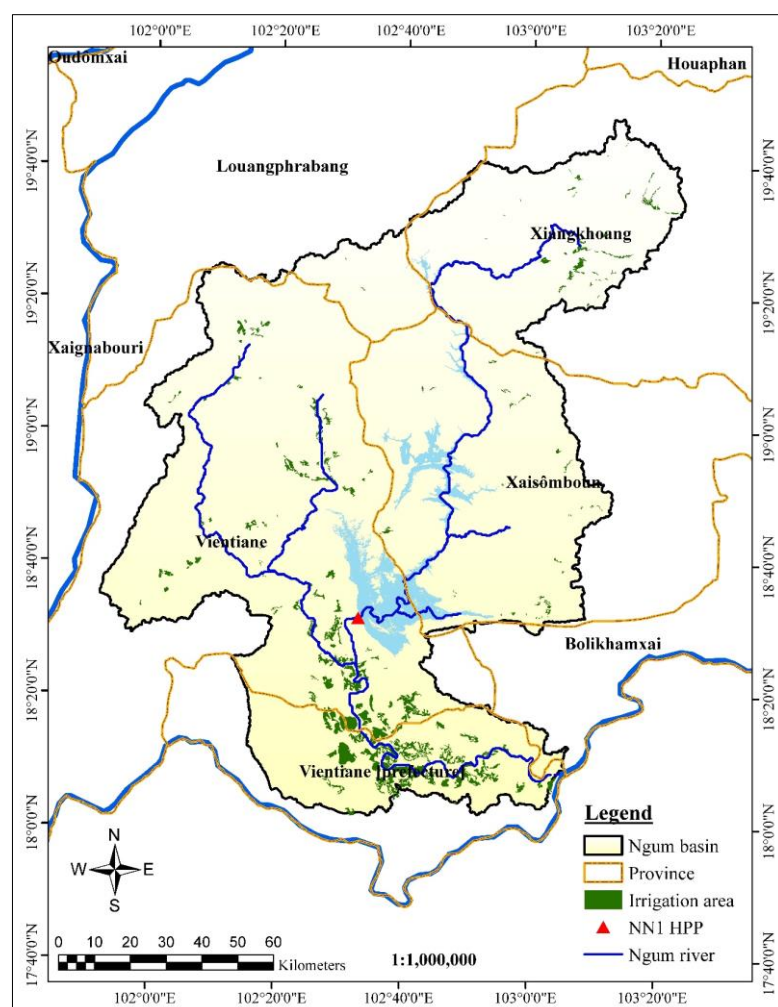


Figure 3-14 Existing irrigation areas in the NNRB region 2015

Table 3-10 The irrigation areas and water use in the NNRB

No.	Name of province	Irrigation area (ha)	Irrigation area (%)	Water use (million m ³ /month)
1	Luangprabang	6	0.01	0.01
2	Xaisomboun	1,002	1.2	1.4
3	Xiengkhuang	10,063	11.5	14.4
4	Vientiane	41,338	47.4	58.9
5	Vientiane Capital	34,772	39.9	49.6
Total		87,181	100.00	124.3

3.8. Flood problem

The effect of climate change and human activities such as deforestation and reservoir operations are major causes of floods and droughts. From the past to the present many flood events occurring in Laos. Most large floods occur in the central part of Laos as well as in the NNRB region (Keophila et al., 2018). While many reservoirs were constructed in the NNRB for hydropower generation and flood protection, flood and drought are still repeating problems downstream of the NNRB due to difficulty in planning and operating high variation of reservoir inflow. Climate change is another factor exacerbating flood and drought in the NNRB. It is predicted that the extreme rainfalls in the NNRB could increase up to 5-10% in the worst-case (Promwungkwa et al., 2019). The flood and large flood events occurring in Laos are listed in Table 3-11.

Table 3-11 Flood and flood damage in Laos (1966-2011)

No.	Year	Type of flood	Damage cost (USD)	Region
1	1966	Large flood	13,800,000	Central
2	1968	Flood	2,830,000	Central and Southern
4	1971	Large flood	3,573,000	Central
7	1976	Flood	9,000,000	Central
8	1978	Large flood	5,700,000	Central and Southern
9	1980	Flood	3,000,000	Central
10	1981	Flood	682,000	Central
11	1984	Flood	3,430,000	Central and Southern
12	1986	Flood	2,000,000	Central and Southern
13	1991	Flood	3,650,000	Central
14	1992	Large flood,	302,151,200	Central and Northern
15	1993	Flood	21,827,930	Central and Northern
16	1994	Flood	21,150,000	Central and Northern
17	1995	Large flood	15,000,000	Central
18	1996	Flood	10,500,000	Central
19	1999	Flood	7,450,000	Central
20	2000	Flood	6,684,230	Central and Southern
21	2001	Flood	808,500	Central and Southern
22	2002	Large flood	14,170,000	Northern, Central and Southern
23	2005	Flash flood	1,316,580	Central and Southern
24	2006	Flood	3,636,000	Central and Southern
25	2007	Flood	8,056,000	Northern, Central and Southern
26	2008	Large flood	4,384,400	Central and Northern
27	2011	Large flood	220,000,000	Central and Northern

CHAPTER 4

METHODOLOGY

The proposed research methodology addresses the objectives of this study. This section is divided as follows: First, data collection and preliminary analysis are conducted, followed by the RCM data processing and RCM bias correction. Then, the process of reservoir inflow forecasting is presented, followed by the streamflow simulation. Finally, the optimal reservoir operation procedure for maximizing hydropower production with and without flood conditions is performed. Each step is explained in detail below (Figure 4-1).

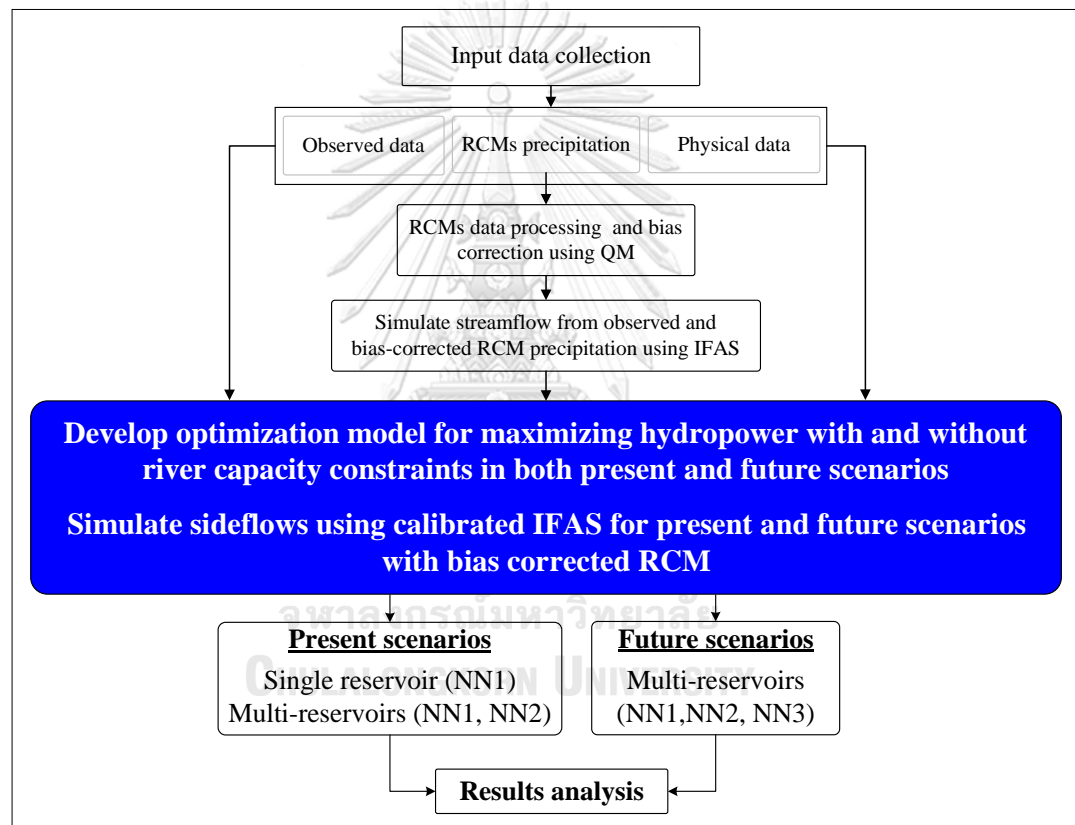


Figure 4-1 Overall research methodology flowchart

4.1. Data collection and preliminary analysis

Bias correction, time series, rainfall-runoff, and optimization models are used in this research. The data requirements, periods, and time scales for each model are different depending on the model and analysis. Each model and analysis are discussed as follows:

4.1.1. Observed data

1) Meteorological and hydrological data

The meteorological data, including 11 observed rainfall stations and six evaporation stations over the NNRB region and nearby areas, are from the Meteorology and Hydrology Department (DMH), Ministry of Natural Resources and Environment (MONRE), Lao PDR. The hydrological data, including five observed streamflow stations within the region, are also from the DMH. The reservoir inflows, release, and water spillway data of the NN1, NN2, and NN3 HPPs are from the Ministry of Energy and Mines, Lao PDR. The statistics of available meteorological and hydrological data are recorded in 26 years (1990–2015). The coordinates of rainfall, evaporation, and streamflow stations are presented in Figure 3-6, and the station names and available periods are shown in Table 3-6, Table 3-7. However, due to the limitation of streamflow data in Nam Ngum tributaries, the Integrated Flood Analysis System (IFAS), will be used for the streamflow prediction. The simulated scenarios are based on the observed rainfall and precipitation from the RCM data to represent the present and future scenarios.

2) Hydropower production

The observed hydropower production data for the NN1 and NN2 HPPs are from the Ministry of Energy and Mines (MEM), Lao PDR, and cover 26 years (1990–2015) and four years (2012–2015), respectively.

3) Water usage data

The main water usage data considered in this study are focused on domestic and irrigation water usage. The irrigation areas and water use for irrigation data are based on the irrigation database report in Lao PDR issued by the Department of Irrigation, Ministry of Agriculture and Forestry, Lao PDR. The irrigation areas and water use in each province over NNRB are presented in Table 3-10 and Figure 3-14. The water usage for domestic data are estimated using the Nam Ngum River Basin Profile reported by the Asia Development Bank in 2008.

4.1.2. RCMs data

Three RCMs, namely, ICHEC, IPSL, and MPI data, can be officially accessed in RU-CORE with a high-resolution of 25×25 km. Another RCM considered in this study is the NHRCM developed by the JMA/MRI, Japan, with a high-resolution of 5×5 km. These RCM data are selected on the basis of the resolution of model criteria and whether the data can be officially accessed. The RCPs refer to the levels of the greenhouse gas emissions pathways. The RCP4.5 scenario is corresponded to the stabilizing of the greenhouse gas emissions over long-term period up to the year 2100.

While RCP8.5 scenario corresponds to the highest greenhouse gas emissions compares to the other RCPs. The RCP8.5 also refers to baseline scenario without policy-driven mitigation (San José et al., 2016). RCM precipitation data from the original database over the NNRB region are processed to create time-series data using MATLAB software under RCP 4.5 and RCP8.5 scenarios. The RCM data processing, including the RCM selection procedure, is conducted to obtain the suitable RCM for the NNRB region. Then, the bias correction procedure of RCM precipitation is performed to correct bias adjustment based on the Quantile Mapping (QM) and ratio techniques. The future change in precipitation analysis procedure is also considered in this study. The different climate models used in this study are presented in Table 2-2.

4.1.3. Spatial data

The spatial data used in this study are diverse. The surface elevation level, land use, and soil type classification over the NNRB region are considered. The digital elevation model (DEM) data with a resolution of 30×30 m are from the Shuttle Radar Topography Mission (SRTM), NASA. The land use data are collected from the National Agriculture and Forestry Research Institute (NAFRI, 2010). The soil type classification data follow the soil classification report by the Food and Agricultural Organization in 2010. The details of DEM, land use, and soil type data are presented in Figure 3-3 to Figure 3-5, respectively.

4.1.4. Physical reservoir characteristic data

NN1, NN2, and NN3 HPPs physical characteristics are from the Nam Ngum River Basin Profile reported by the Asia Development Bank in 2008. They are the catchment area, storage volume, dam crest elevation, weir crest dam elevation, maximum flood level, full supply level, minimum supply level, maximum tailwater level, full operation tailwater, rated flow per turbine, installed power capacity, different head, turbine efficiency, and time generation data. The details of these data are presented in Table 4-1.

4.2. Optimization model development

This research aims to join the operation between NN1, NN2, and NN3 HPPs by formulating the optimization model to carry out the optimal hydropower production. In this study, the general algebraic modeling system (GAMS) is applied as the optimization model to maximize hydropower production. Few compositions, such as the input data, objective function, decision variables, constraints, and model processing, would be considered in the optimization model development. The involved process in the optimization model development for single and multiple reservoirs is illustrated in Figure 4-2.

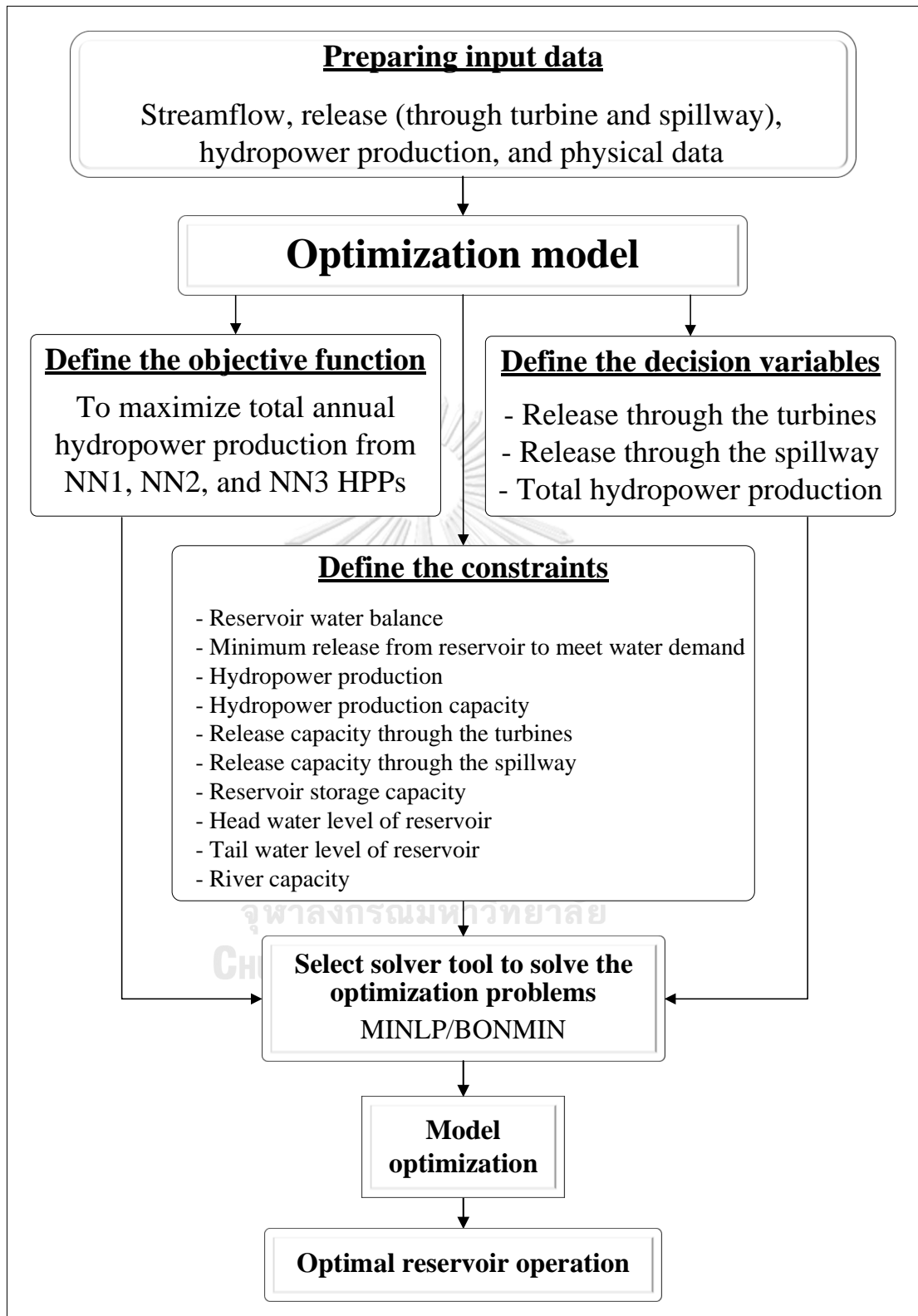


Figure 4-2 Schematic of the optimal reservoir operations

4.2.1. Input data requirement

Considerable data and information are required to develop the optimization model for maximizing hydropower production. The data used in the optimization model can be divided into physical and time-series data. The details of these data are presented in Table 4-1 and Table 4-2, respectively.

Table 4-1 Physical data requirement for optimization model

Characteristics	Considered reservoirs			Unit
	NN1	NN2	NN3	
Storage volume at:				
Maximum flood level	8,260.0	5,675.1	1,670.3	MCM
Full supply level	7,090.6	4,980.4	1,536.5	MCM
Minimum supply level	3,244.7	2,340.9	522.1	MCM
Maximum release	1,307.6	1,161.7	466.6	MCM
Minimum release	492.5	324.0	155.5	MCM
River capacity at downstream of NN1	3000	-	-	m ³ /s
Maximum headwater level	212.3	375.0	723.0	masl
Minimum headwater level	196.0	345.0	670.0	masl
Maximum tailwater level	178.0	225.0	385.0	masl
Minimum tailwater level	166.0	216.5	380.0	masl
Turbine efficiency	95.3	96.7	96.5	%
Time generation	18.0	16.0	19.0	hr/day
Reservoir surface area	Function of volume and elevation			km ²
Storage - Surface area - Elevation Curves				

Table 4-2 Time series data requirement for optimization model

Characteristics	Frequency	Available period			Unit
		NN1	NN2	NN3(future)	
Inflow	Daily	1990-2015	2012-2015	2020-2039	MCM
Sidelflow	Daily	1990-2015	2012-2015	2020-2039	MCM
Water release	Daily	1990-2015	2012-2015	2020-2039	MCM
Water spillway	Daily	1990-2015	2012-2015	2020-2039	MCM
Observed hydropower production	Daily	1990-2015	2012-2015	-	kW/h
Surface evaporation	Daily	1990-2015	2012-2015	2020-2039	mm
Headwater level	-	-	-	-	m
Tailwater level	-	-	-	-	m

4.2.2. Objective function

As mentioned earlier, this research aims to maximize hydropower production with and without flood conditions. According to the calculation, the minimum flow at downstream of NN1 is approximately of 508.9 MCM, while the total water demand for domestic and irrigation is approximately of 129.7 MCM. This calculation found that the minimum flow at downstream of NN1 is enough for the total water demand for domestic and irrigation. Therefore, the total annual hydropower production capacity from all considered hydropower plants is treated as the single objective function for this research. The water demand for domestic use, environmental flow, and irrigation is treated as constraints. For flood consideration, the river channel capacity of the NN1 HHP downstream is also set as a constraint. The variable considering whether a flow exists through the spillway is binary and set as integers of 0 (no spillway) and 1. Therefore, the proposed optimization model is mixed-integer nonlinear programming (MINLP) and is solved using GAMS. The objective function is given by.

$$\text{Maximize: } HP_{Total} = \sum_{t=1}^n (HP_{t,NN1} + HP_{t,NN2} + HP_{t,NN3}), \quad (4-1)$$

where HP_{Total} is total hydropower production from all considered hydropower plants, $HP_{t,NN1}$, $HP_{t,NN2}$ and $HP_{t,NN3}$ are hydropower production from NN1, NN2 and NN3 HPPs as expressed in kWh, at time t .

4.2.3. Constraints

The constraints considered in the optimization model include the reservoir water balance, water use downstream, channel capacity, turbine capacity, hydropower generation capacity, reservoir storage capacity, and water released through the spillway.

Hydropower production is a function of the water release through turbines, the time of hydropower generation, the effectiveness of the storage head, and the installed capacity of HPPs as shown in Eq. 4-2.

$$HP_t = \eta \times \gamma \times R_t \times H_t \times T, \quad (4-2)$$

where, HP_t is the hydropower generated from HPPs at time t , η is the efficiency of turbine, γ is specific weight of water ($\gamma \approx 9.81 \text{ KN} / \text{m}^3$), R_t is the release water through the turbine at time t , H_t is the differences in water between the head and tailwater levels as expressed in meters (m) at time t , and T is the time for generating hydropower as expressed in hours (hr). The components of hydropower plant are present in Figure 4-3 and Figure 4-4.



Figure 4-3 Num Ngum 1 hydropower project

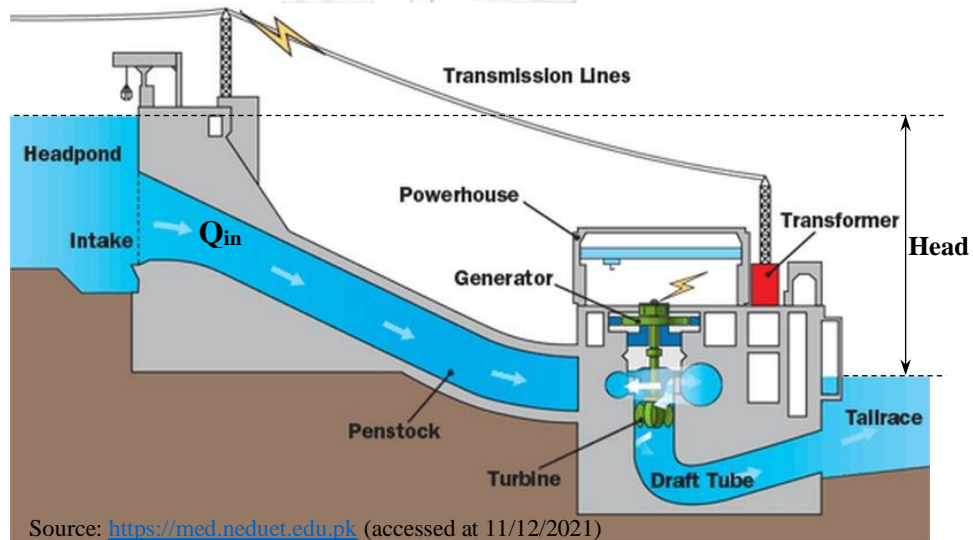


Figure 4-4 Components of a hydropower plant

The water balance equation is applied to define the reservoir water balance. The seepage is assumed to be negligible. Following the cascade reservoir system, the water balance is expressed as.

$$S_{t+1} = S_t + In_t - E_t - R_t - Sp_t, \quad (4-3)$$

where, S_{t+1} is the final storage capacity at time $t+1$, S_t is the initial storage capacity at time t , R_t is the total release through turbines at time t , In_t is the reservoir inflow at time t , E_t is monthly evaporation from the reservoir at time t , and Sp_t is the release through the spillway at time t as expressed in MCM.

The release from the reservoirs (included turbine and spillway) must be greater than or equal to the summation of domestic water use, environmental flow requirement, and irrigation water use at downstream as shown in Eq. 4-4.

$$R_{Total,t} \geq \sum_{t=1}^n ID_t + DD_t + ENVI_t \quad (4-4)$$

where, $R_{Total,t}$ is total release from the reservoirs at time t , ID_t is irrigation water demand at time t , DD_t is domestic water demand at time t , and $ENVI_t$ is environmental flow requirement at time t .

For flood consideration, the maximum river capacity is included as a constraint as shown in Eq. 4-5. The total release through turbines and overflow through spillway should not exceed the channel capacity to response flood at downstream area.

$$R_{Total,t} + Sp_t \leq RC_{max,t} \quad (4-5)$$

where, $R_{Total,t}$ is total release from the reservoirs at time t , Sp_t is water over spillway at time t , and $RC_{max,t}$ is maximum channel capacity at time t .

The water released through turbines should be less than the turbine capacity as shown in Eq. 4-6.

$$R_t \leq R_{max} \quad (4-6)$$

where, R_t is the total water release through turbines at time t , R_{max} is turbine capacity at any time as expressed in MCM.

The hydropower production at time t should not exceed or be equal to the maximum generating capacity of HPPs.

$$HP_{n,t} \leq HP_{max,n,t} \quad (4-7)$$

where, $HP_{n,t}$ is the hydropower produced by HPP n at time t , whereas $HP_{max,n,t}$ is the maximum hydropower production capacity of HPPs n at time t as expressed in kWh.

The storage in a reservoir at time t should not exceed the maximum storage capacity or normal pool level and should not be less than the dead storage or minimum pool level at time t .

$$S_{min} \leq S_t \leq S_{max} \quad (4-8)$$

where, S_t is the storage capacity at time t , whereas S_{min} and S_{max} are the minimum and maximum storage capacities at time t as expressed in MCM.

During flooding periods, when the water release is higher than the normal pool level, the excess water will be released through spillway. The overflow can be defined as the difference between the final and maximum storages at any time t .

$$Sp_t = S_{t+1} - S_{max} \quad (4-9)$$

where, Sp_t is the water released through the spillway at time t , whereas S_{t+1} is the final storage at time t . In the absence of overflow, the final storage can serve as the initial storage for the next time step $t+1$, but in the present of overflow, the maximum storage (S_{max}) can serve as the initial storage.

4.2.4. Solver tool

The problems of optimization for reservoir operation is complex combining binary and nonlinear variables. The Mixed Integer Nonlinear Programming (MINLP) is adopted for this study because it can be used to solve both binary and nonlinearity problems in the objective function and constraints in order to reach optimal solution. MINLP uses branch-and-bound (B&B) and outer approximation (OA) algorithms in BONMIN to search the optimal solutions in feasible regions.

4.3. Optimization model under flood condition

The multi-reservoir operation is also considered to optimize the hydropower production under the flood conditions at the NN1 reservoir downstream. The optimization model, GAMS, is also used to solve this problem. The optimization model development procedure is set similarly to the case of optimization without flood constraint. Thus, the NL river and checkpoint (flood control point) are added to the system, as shown in Figure 4-5. The maximum river capacity of 3,000 m³/s at the checkpoint is set as the flood constraint. The flood years of 1995, 2002, 2005, 2008, and 2011 are selected to assess the historical hydropower production under flood conditions. For future hydropower production under flood conditions, the future wet years of the 6th, 7th, 11th, and 16th are selected. The total outflow from NN1 HPP and streamflow from NL river will be checked at the checkpoint. The number of days with a total flow of more than 3,000 m³/s will be recorded as the flooding days. The river capacity constraint can be changed to optimize maximum hydropower production and flood reduction at the NN1 reservoir downstream.

4.4. The indicative reservoir operating curves development

The reservoir operating curves are used as the guideline of the monthly operational policies to maximize hydropower plant production. The upper and lower operating curves, including single and multiple operating curves, are developed. The storage level results from the optimization model with and without flood conditions are used as the basis. The upper and lower operation curves are estimated from the maximum and minimum reservoir water levels, respectively. These reservoir storage levels are simulated by the optimization model, which achieves the maximum and minimum hydropower production in all months. Because the operating curves are developed from the storage level resulting from the maximizing hydropower, therefore the operating curves for this study are consider as the indicative reservoir

operating curves. The historical single and multiple reservoir operating curves of NN1 and NN2 without flood conditions are developed from 2012 to 2015. Future multiple reservoir operation curves of NN1, NN2, and NN3 are developed from 20 years of future period. The historical single reservoir operating curves with flood conditions of NN1 are developed in the flood years of 1995, 2002, 2005, 2008, and 2011. Future multiple reservoir operation curves of NN1, NN2, and NN3 are developed through the wet years of the 6th, 7th, 11th, and 16th years.

4.5. Optimization model development procedure

To complete the optimization model for optimal multi-reservoir operation, the model development can be followed some steps bellow.

1) Collect the input data as shown in Table 4-1 and Table 4-2. The input data can setup in three ways including lists, tables, and direct assignments.

2) The optimization and simulation time periods for optimizing the hydropower production and predicting the streamflow for this study are set as:

- ❖ For the optimal reservoir operations without flood condition, the single and multiple reservoir operations for the NN1 and NN2 are optimized in time period of 2012-2015 for the present scenario. For the future scenario, multiple reservoir operations for NN1, NN2 and NN3 is optimized through the 20 years of future time period.
- ❖ For the optimal reservoir operations with flood condition, the single reservoir operations for NN1 are optimized in wet years of 1995, 2002, 2005, 2008, and 2011 for the present scenario. For the future scenario, multiple reservoir operations for the NN1, NN2 and NN3 are optimized through the 6th, 7th, 11th, and 16th years. The historical wet years are selected based on the year occurring the large flood in the past, while the future wet years are selected based on the probability of annual rainfall with more than or equal of 80%.

3) Defined and declare the decision variable and positive variables statement. The water release from all hydropower plants is defined as the decision variable.

4) Defined and declare the objective function. The objective function of this study is defined as the maximize hydropower production.

5) Defined and declare the model constraints. There many constraints are define for this study; the details of constraints are present in section 4.2.3.

6) The equations must be defined and declared in separate statements. This study is defined many equations including reservoir surface area, evaporation from surface area, water through spillway, head and tail water elevations, and hydropower production.

7) Select the model solver tool, there are some available solvers tools in GAMS. The MINLP solver is selected to solve the problems for this study.

8) The optimal output of optimization model is automatically reformed, and the related variables and equations are grouped together. The results will be compared with the observation.

9) The model optimization is performed based on the reservoir inflow. The whole time series data set of reservoir inflow are inputted into the optimization model. This means that the optimization model has already known the future streamflow while in actual operations, a long time series of reservoir inflow data is not readily available, and the reservoir operators only have the inflow data for the previous month.

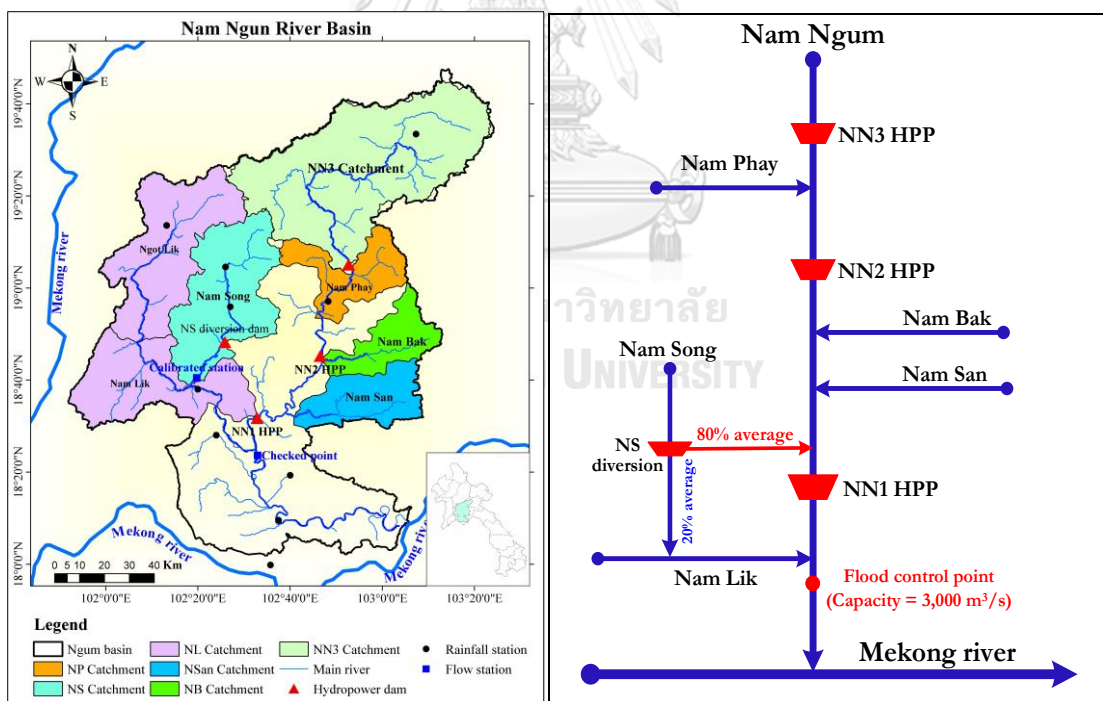


Figure 4-5 Schematic of sideflow system and sub-basin in the NNRB

CHAPTER 5

RESULTS AND DISCUSSION

This chapter presents the results and provides discussions about the study. The first section shows the results of the optimal single reservoir operation followed by the optimal multi-reservoir operations. The third and fourth sections present the optimal reservoir operations under future climate change and flood conditions, respectively. The final section discusses the recommended reservoir operating curves. The discussion of the results is provided throughout the chapter accompanied with relevant results.

5.1. Optimal single reservoir operations

5.1.1. Monthly hydropower production

The optimal average monthly power production under the observed inflow scenarios (Opt_power (Obs_inflow)) compared with the actual hydropower production (Obs_power) is shown in Figure 5-1. The average monthly hydropower production ranges from 90 GW to 111.1 GW. In the wet month periods, the optimal hydropower production under the observed inflow scenario was greater than the actual hydropower production. This phenomenon may occur because the water level of the reservoir during the wet months was at its maximum most of the time, thereby increasing the high head for hydropower production. For dry months, the average monthly hydropower production under the observed inflow scenario was slightly higher than the actual hydropower production. This situation may be due to the reservoir inflows from 2012–2015 being quite low when compared with other years. The optimization model attempted to maximize hydropower in wet months rather than in the dry months. This finding suggests that the optimization model could improve power production for a single reservoir.

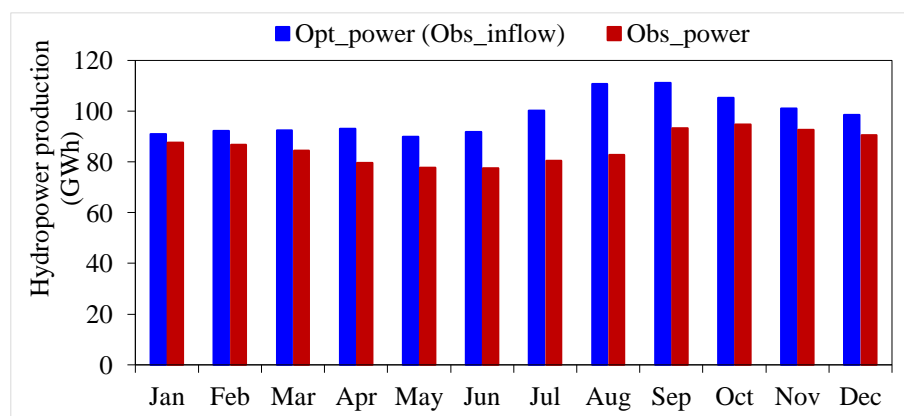


Figure 5-1 Comparison of average monthly hydropower production of NN1 between the optimization and observation.

5.1.2. Annual hydropower production

The optimal annual hydropower production results under the different inflow scenarios are shown in Table 5-1 and Figure 5-2. The optimized result shows that the annual hydropower production higher than the observed hydropower. The increase of 12.2% in power obtained from optimization model suggests that the application of the optimization model proposed here can contribute to control of better release. However, this increase may be because all the monthly inflow was inputted into the optimization model, whereas in the observed (actual) operation case, the operator has the inflow records only up to a previous month.

Table 5-1 Annual hydropower production

Year	Observed power (GW)	Optimized power (GW)	Difference (%)
2012	1,041	1,231	18.3
2013	1,180	1,312	11.6
2014	1,142	1,325	16.0
2015	1,210	1,231	3.0
Average increase (%)			12.2

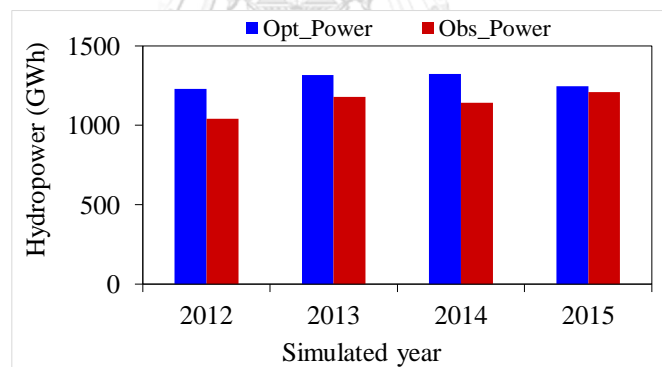


Figure 5-2 Comparison of annual hydropower production of NN1 between the optimization model and the observation.

5.2. Optimal multi-reservoir operation for present

5.2.1. Monthly hydropower production

The optimization model is formulated to assess the potential of the joint operation of NN1 and NN2. From the optimization model, the average hydropower production of NN1 and NN2 during 2012 to 2015 resented in Figure 5-3 and Figure 5-4, respectively. The average hydropower yield of NN1 is high when considered over a period of 12 months. Many dry months, especially Dec, show higher improvement over the Obs_Power and even higher than those of the wet months. This phenomenon is possibly because the actual operation was based on electricity demand, while the

optimization model attempted to be optimized on the basis of inflow to the reservoir. The electricity demand in dry months might be lower than the capacity of turbines in hydropower production, whereas the optimization model attempted to simulate the maximum hydropower capacity. The optimization model can adapt the release based on various reservoir inflows in each month to maximize hydropower production. Furthermore, the water that discharges through the spillway gates of two reservoirs can be reduced, thereby possibly increasing all hydropower production. In addition, the increasing of hydropower of NN1 may result from the increasing of release of NN2 which is inflow of NN1.

However, while the monthly time series data for reservoir inflow are inputted into the optimization model, in actual operations, a long time series of inflow data is not readily available, and reservoir operators only have the inflow data for the previous month. Therefore, this may be another reason that causes the hydropower production from the optimization model to be higher than the actual operation. The average monthly hydropower production of NN1 and NN2 from the optimization model during 2012 to 2015 is shown in Figure 5-5. The maximum hydropower of 461.3 GWh is recorded in September, whereas the minimum hydropower of 252.5 GWh is recorded in December.

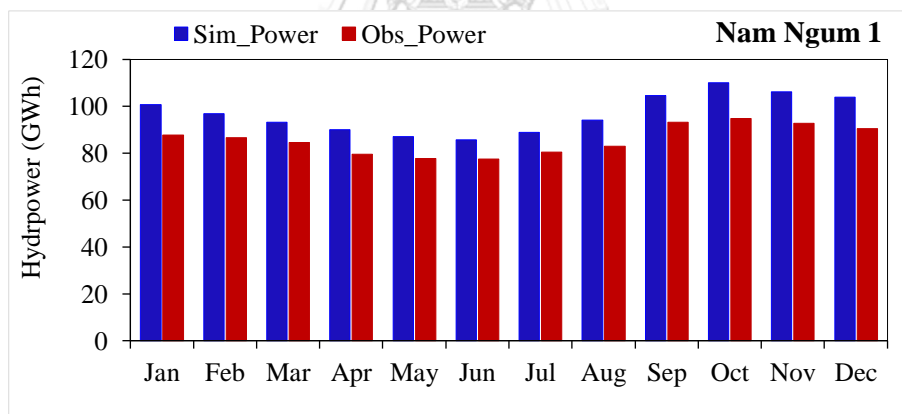


Figure 5-3 Comparison of average monthly hydropower production of NN1 from the multi-reservoir optimization and the observation.

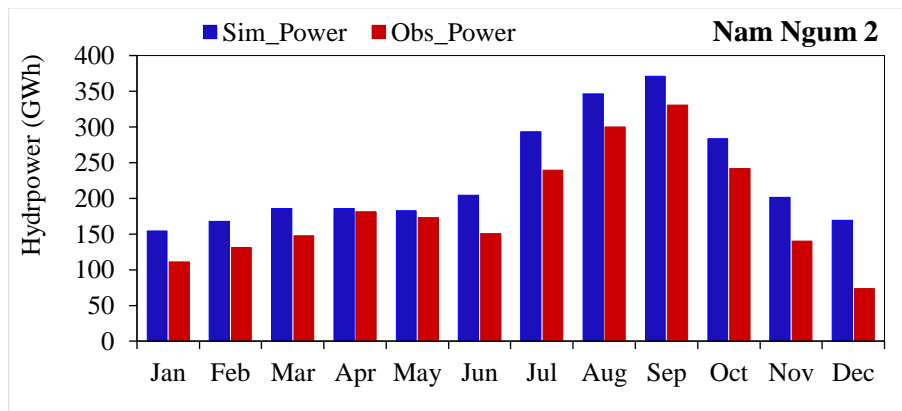


Figure 5-4 Comparison of average monthly hydropower production of NN2 from the multi-reservoir optimization and the observation.

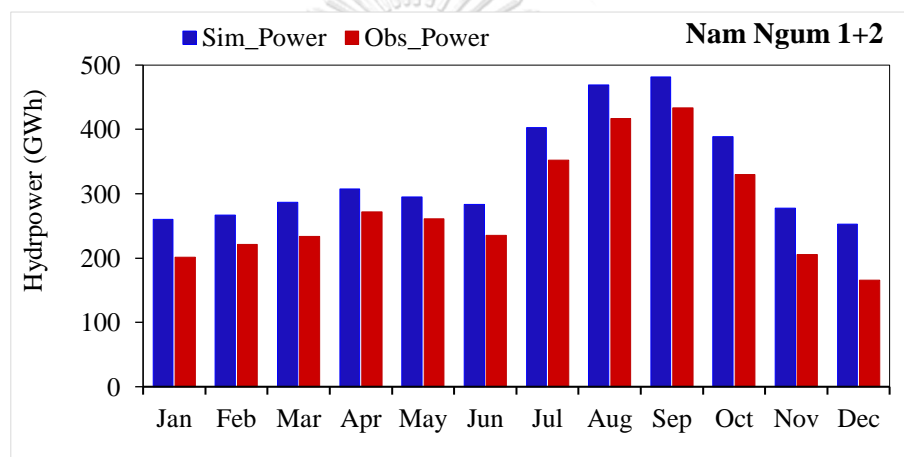


Figure 5-5 Comparison of average monthly hydropower production of NN1 and NN2 from the multi-reservoir optimization and the observation.

5.2.2. Annual hydropower production

The optimal annual hydropower production is higher than the observed hydropower (Figure 5-6). The optimization model can increase hydropower production by 20.2% (6.0% from NN1 and 14.2% from NN2) on average compared with the observed hydropower production. The optimization model of joint operation increases the release of water to maximize the hydropower production of HPPs. In comparison with the observation, the individual analysis of hydropower production results suggest that the hydropower production for NN1 and NN2 increases by 16.7% and 19.8% on average, respectively. In addition, the results show that the annual average hydropower production of NN1 from multi-reservoir optimization is higher than the single reservoir optimization. The possible reason maybe because the optimization model could control the release better for maximizing hydropower production in multi-reservoir system operation. The increasing might be due to the rising NN1 inflow, which increases the hydropower production in multi-reservoir

system operation. However, the reservoir inflow of NN1 increased to only approximately 7.9%, while hydropower production increased by 16.7% in average. Therefore, the increasing of hydropower production could be caused by the model efficiency and increasing of the reservoir inflow.

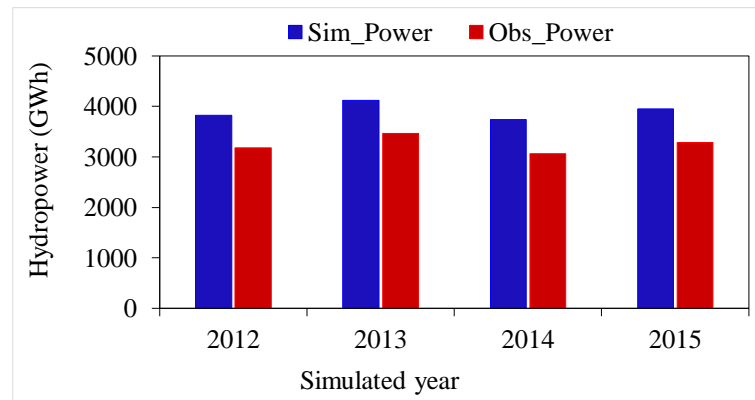


Figure 5-6 Annual hydropower from the optimization model compared to the observation of NN1 and NN2.

5.3. Optimal reservoir operation under future climate change scenarios

The previous section considered NN1 and NN2 HPPs under the period of 2011–2015. To access the impact of climate change on reservoir operation under different climate conditions, this section considered NN1, NN2, and NN3 HPPs as multi-reservoir systems. The future hydropower production under climate condition is optimized using an optimization model for near future of 20 years. The optimization model is optimized for the reservoir inflows from future RCM precipitation scenarios under RCP4.5 and RCP8.5 scenarios. The results of the impact of climate change on reservoir operation are presented as follows.

5.3.1. Monthly hydropower production under climate change scenarios

Generally, the results show that the optimization model can obtain higher monthly hydropower on average under both RCPs when compared with the observation. The optimal total monthly hydropower production from different hydropower plants for RCP4.5 and RCP8.5 scenarios are shown in Figure 5-7 to Figure 5-12.

Figure 5-7 shows the near future monthly hydropower production of NN1 from the optimization model under RCP4.5 and RCP8.5 scenarios. NN1 HPP yield maximum hydropower production by 117.7 GWh and 121.6 GWh under RCP4.5 and RCP8.5 scenarios, respectively. The minimum hydropower production of 80.8 GWh and 82.0 GWh under RCP4.5 and RCP8.5 scenarios, respectively. Figure 5-8 revealed that the average hydropower production yield of NN1 HPP is high when considered over a period of 12 months under both scenarios. In addition, the increase in the

hydropower of NN1 may result in the rising of the releases from NN2, which is the inflow of NN1. Figure 5-9 and Figure 5-10 show the future monthly and average hydropower production of NN2 HPP under RCP4.5 and RCP8.5. The maximum hydropower production of 456.7 and 470.9 GWh under RCP4.5 and RCP8.5 scenarios, respectively; whereas the minimum hydropower of 114.0 and 124.7 GWh under RCP4.5 and RCP8.5 scenarios, respectively (Figure 5-9).

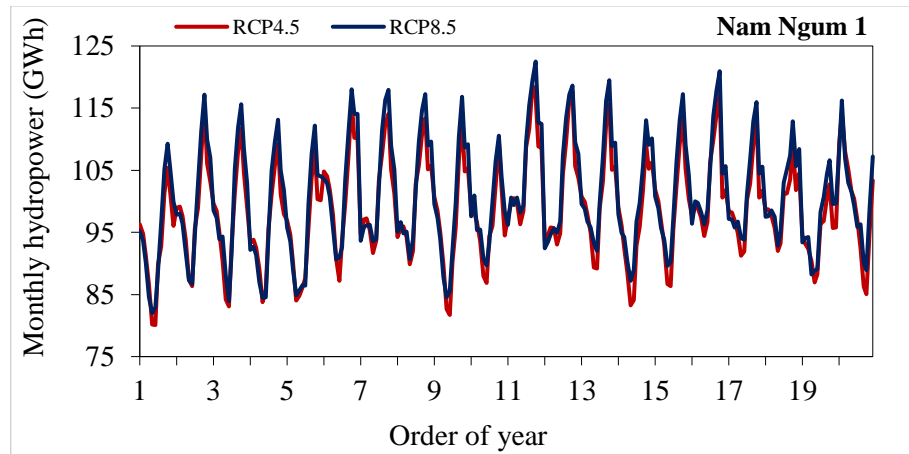


Figure 5-7 Future monthly hydropower production of NN1 HPP under RCP4.5 and RCP8.5 inflow scenarios.

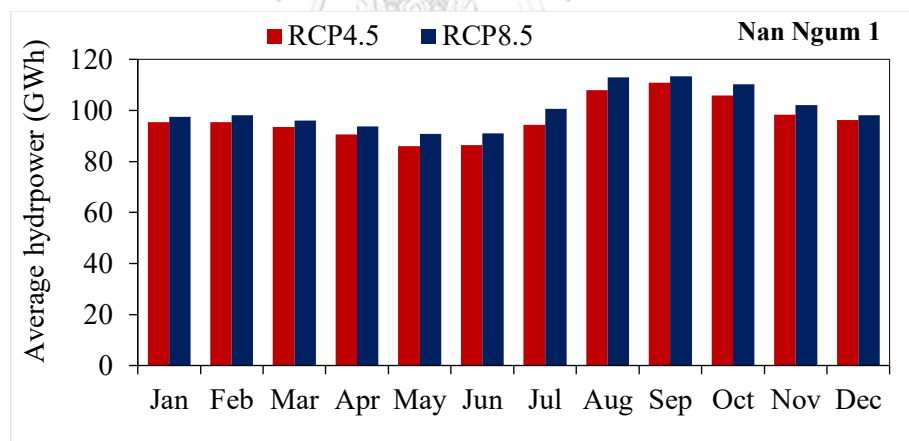


Figure 5-8 Comparison of future average monthly hydropower production of NN1 HPP under RCP4.5 and RCP8.5 inflow scenarios.

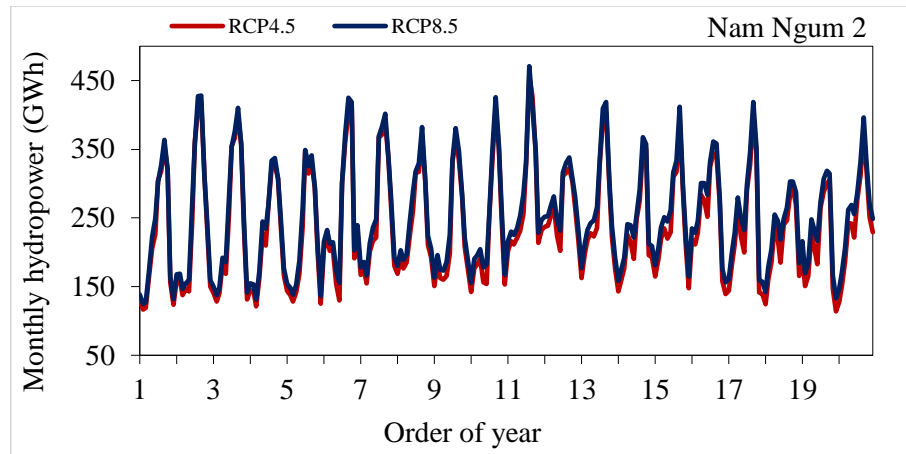


Figure 5-9 Future monthly hydropower production of NN2 HPP under RCP4.5 and RCP8.5 inflow scenarios.

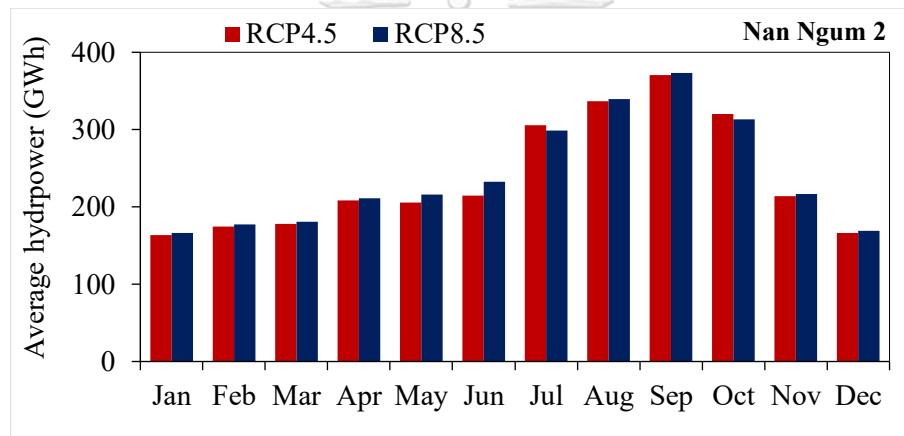


Figure 5-10 Comparison of future average monthly hydropower production of NN2 HPP under RCP4.5 and RCP8.5 inflow scenarios.

The results of future monthly and average hydropower production from NN3 HPP is presented in Figure 5-11 and Figure 5-12, respectively. Both figures show the future monthly and average hydropower production in similar trend with NN2 HPP. Figure 5-11 shows that the future maximum hydropower production could be 314.5 and 332.1 GWh under RCP4.5 and RCP8.5 scenarios, respectively; whereas the minimum hydropower could be 185.9 and 199 GWh under RCP4.5 and RCP8.5 scenarios, respectively.

Figure 5-11 also shows that in the future, the monthly hydropower production tends to increase by 3.49% and 4.63% on average under RCP4.5 and RCP8.5 scenarios, respectively. Furthermore, the monthly hydropower production from NN3 HPP has slightly higher variation than other HPPs. This may cause the NN3 HPP located at the upstream because of the variation of inflow due to climate change. Moreover, Figure 5-12 revealed that the average hydropower production under both

RCP scenarios is maximum in August, whereas the minimum hydropower is in December.

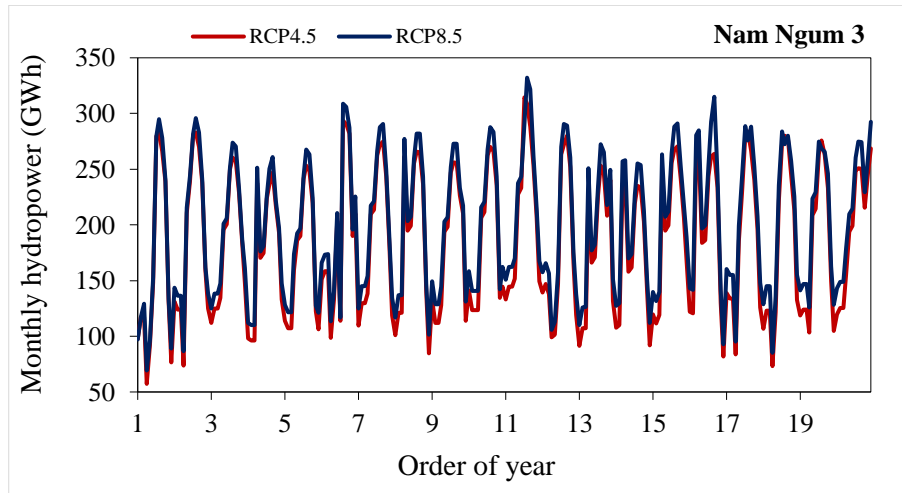


Figure 5-11 Future monthly hydropower production of NN3 HPP under RCP4.5 and RCP8.5 inflow scenarios.

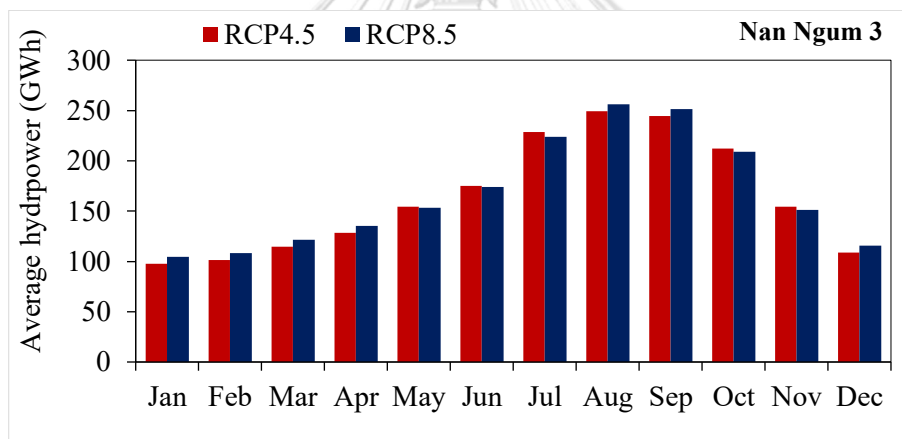


Figure 5-12 Comparison of future average monthly hydropower production of NN3 HPP under RCP4.5 and RCP8.5 inflow scenarios.

5.3.2. Annual hydropower production under climate change scenarios

The result of annual hydropower production from multi-reservoir optimization under different future inflow scenarios are presented. Figure 5-13 shows the future annual hydropower production under the inflow from RCP4.5 and RCP8.5, respectively. Figure 5-13 presented that the inflow from RCP4.5 has produced a maximum of 1,265, 2,554, and 3,338 GWh hydropower for NN1, NN2, and NN3 HPPs, respectively.

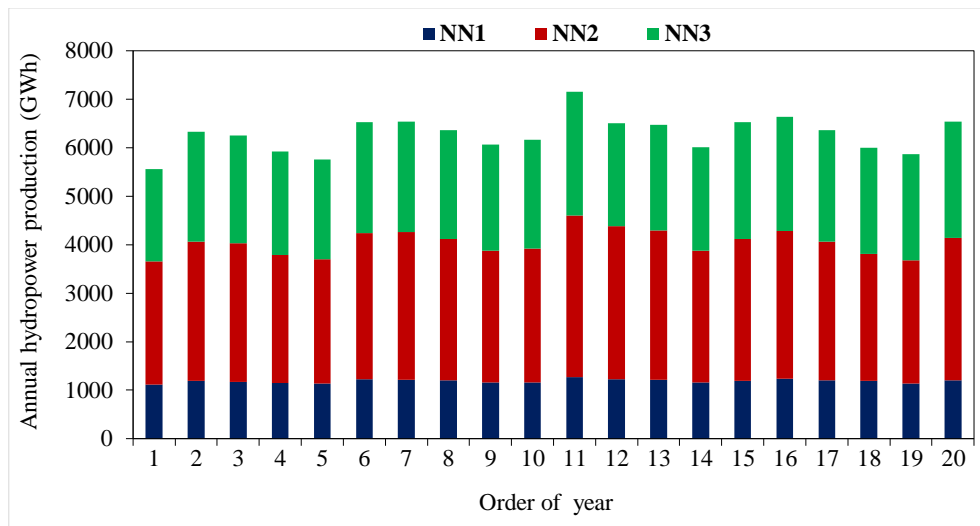


Figure 5-13 Annual hydropower production from NN1, 2, and 3 HPPs under climate change of RCP4.5 scenario.

The Figure 5-14 shows the future annual hydropower production under the inflow from RCP8.5 scenario. The result under this scenario found that the model produced a maximum of 1,286, 2,714, and 3,481 GWh hydropower for NN1, NN2, and NN3 HPPs, respectively. In addition, the increase pattern of NN3 HPP is higher than other HPPs, whereas the trend of NN1 HPP is slightly constant in RCP 4.5 and RCP8.5 scenarios. This finding may be because the NN3 reservoir has affected higher variation in the amount of future rainfall than NN1 and NN2. The total hydropower production from all HPPs is also analyzed in the Figure 5-15. The hydropower production increases in almost the same trend for NN2 and NN3 HPPs. The total hydropower production could be the lowest by 5,561 GWh and 5,753 GWh and the highest by 6,326 GWh and 6,560 GWh for RCP4.5 and RCP8.5 scenarios, respectively. The annual hydropower production could increase by 12.1% and 17.1% for RCP4.5 and RCP8.5 scenarios, respectively when compares to the observation. All the increases in hydropower may be due to neglecting the flood constraint at downstream of NN1 reservoir. This finding shows that the optimization model attempted to release more water to achieve the maximum hydropower production in all scenarios. When compared the average annual hydropower production of the present and future scenarios with the observation considering NN1+NN2. The average annual hydropower production is reduced when compared to the present scenario. This might be due to the impact of climate change, variation of reservoir inflow, and the effect of reservoir operation of NN3. According to the results presented above, the model could optimize the hydropower production under climate change conditions. Therefore, this optimization model is expected to be adopted for optimizing hydropower production under future climate change conditions.

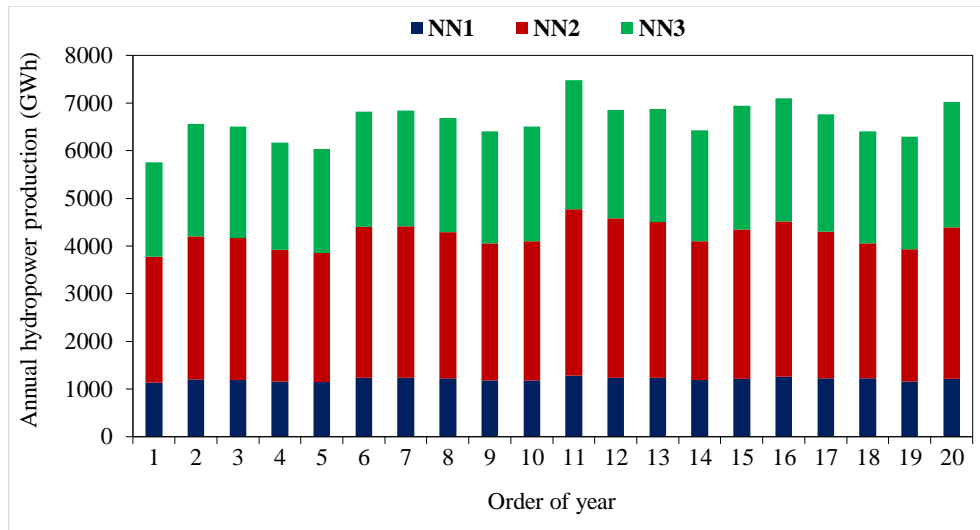


Figure 5-14 Annual hydropower production from NN1, 2, and 3 HPPs under climate change of RCP8.5 scenario.

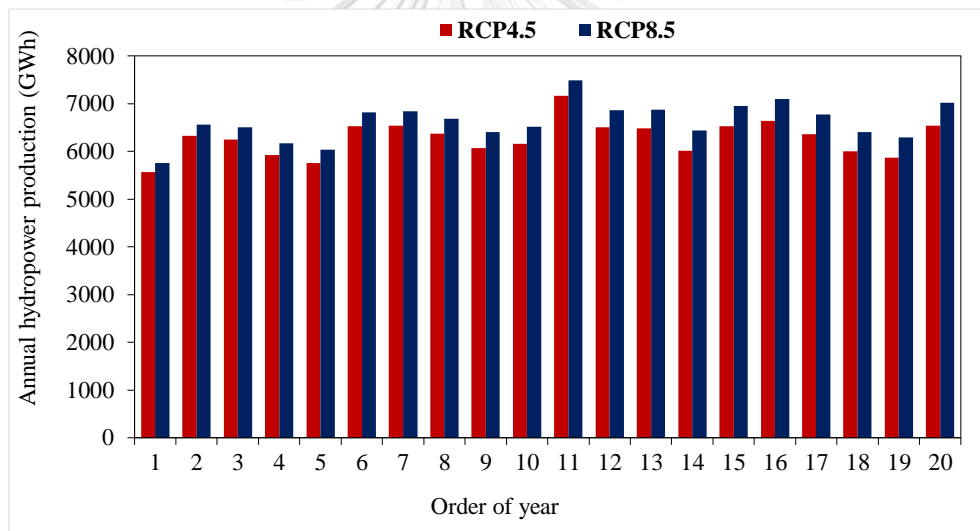


Figure 5-15 Total annual hydropower production from NN1, 2, and 3 HPPs under RCP4.5 and RCP8.5 inflow scenarios.

5.4. Optimal reservoir operation with and without flood conditions

Considering the reservoir operation, this research considered two operation cases, namely, single reservoir operation model (NN1) for historical scenarios and cascade operation model (NN1, NN2, and NN3) for future scenario. The flood years of 1995, 2002, 2005, 2008, and 2011 are selected for historical scenario. For the near future scenario, the 6th, 7th, 11th, and 16th years are selected and the NN2 and NN3 will be added to system. The number of days with a total flow of more than 3,000 m³/s will be recorded as the flooding days or flood period.

5.4.1. Optimal reservoir operation without river capacity constraint

The optimization results show that the case of historical condition is optimized, and the objective function is followed as illustrated in reducing flooding day, flow amount over spillway, and increasing in hydropower production when compared with the observation data. The historical optimization results of monthly hydropower production compared with the observation data are presented in Figure 5-16, and the annual hydropower production are summarized in Table 5-2. As shown in Figure 5-16, when compared with the observation data, the monthly hydropower optimized by the optimization model increases significantly in the wet months but are slightly below the observation data in some months, especially in the dry months. In Figure 5-57, the optimization hydropower keeps a pattern similar to the observation data. Table 5-2 summarizes the benefits from the optimization model compared with the observation for the NN1 reservoir in representative wet years. The average annual hydropower output was 1,188.7 GWh. With the optimal reservoir operation, the hydropower production ranges from a minimum of 1,061.1 in 1995 to a maximum of 1,236.5 GWh in 2011. However, the largest increase in hydropower production can be found in 1995, which is equal to approximately 9.6% when compared with the observation data.

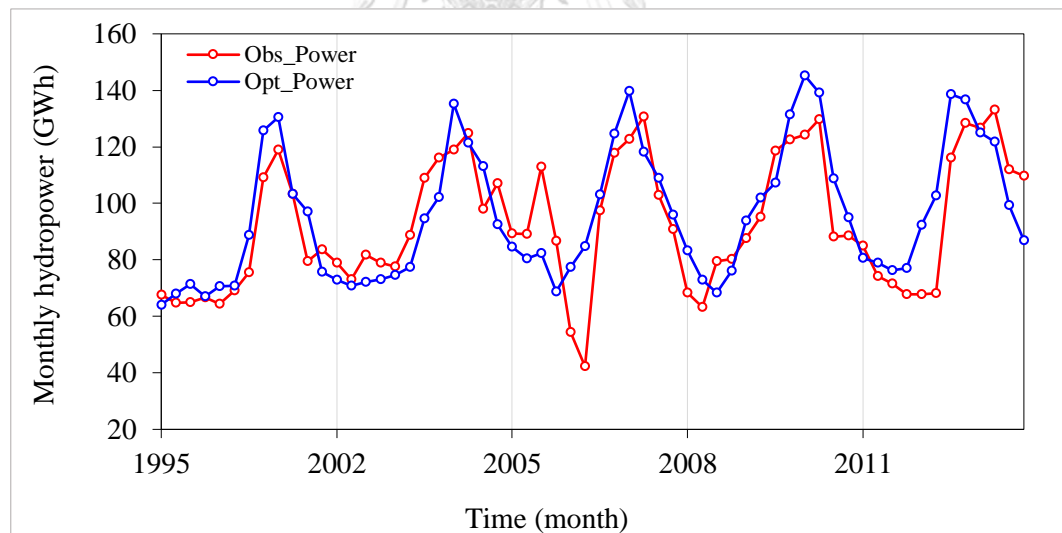


Figure 5-16 The monthly hydropower production from optimization and observation without river capacity constraint.

Table 5-2 Summary of annual hydropower production from optimization and observation without river capacity constraint.

Year	Observation	Optimization	Difference	
	GWh	GWh	GWh	%
1995	967.9	1,061.1	93.2	9.6
2002	1,153.0	1,213.4	60.4	5.2
2005	1,137.0	1,203.1	66.1	5.8
2008	1,145.8	1,229.5	83.8	7.3
2011	1,160.7	1,236.5	75.8	6.5
Average	1,112.8	1,188.7	75.8	6.9

Figure 5-17 and Figure 5-18 present the actual and the optimization result of daily outflow (discharge through turbine and spillway) from NN1 at the flood control point, respectively. The actual daily outflow shows that the largest flood occurred in September of 1995 with a maximum flood peak of 4,040 m³/s. Meanwhile, in 2008, the flood event came earlier than in others year with a maximum flood peak of 3,513 m³/s. The optimization results in Figure 5-18 illustrated that the outflow variation decreases when compared with the observation in Figure 5-17. The largest flood still occurred in 1995, and the optimization model can also reduce the maximum flood peak to 3,716 and 3,433 m³/s in 1995 and 2008, respectively. In addition, Table 5-3 presents the amount of annual outflow volume, flow through spillway, and flood period from the actual operation and optimization model. The optimization result found that the amount of outflow volume reduced from 20,693 to 19,483 MCM, flow through spillway declined from 1,453 to 1,371 MCM, and flood period shortened from 24 to 20 days in 1995.

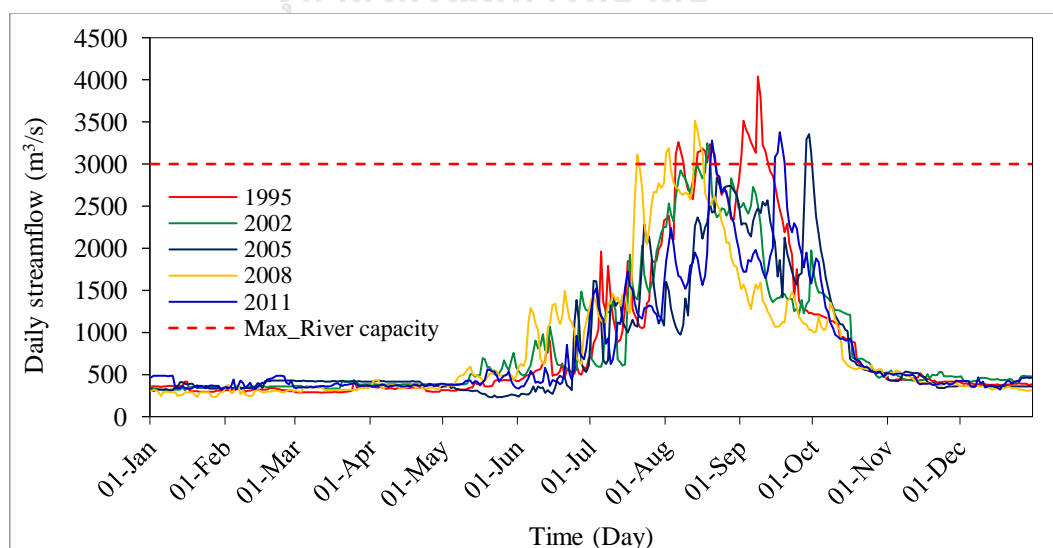


Figure 5-17 Observed daily outflow from NN1 reservoir at flood control point.

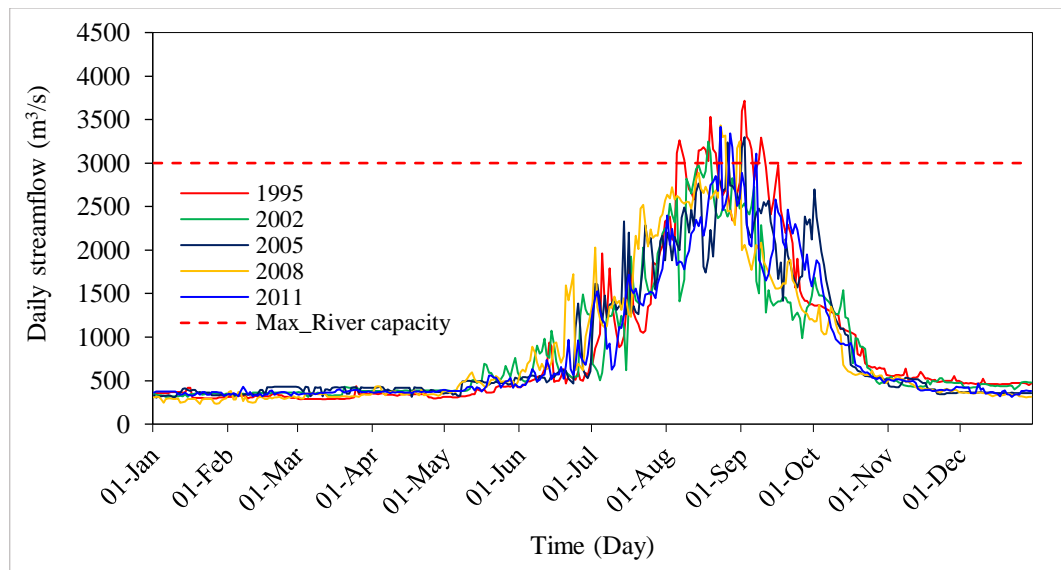


Figure 5-18 Optimized daily outflow without river capacity constraint scenario at flood control point.

Table 5-3 Summary of annual outflow volume, flow through spillway, and flood period without river capacity constraint.

Year	Observation			Optimization		
	Outflow	Spillway	Flood period	Outflow	Spillway	Flood period
	MCM	MCM	Day	MCM	MCM	Day
1995	20,693	1,453	24	19,483	1,371	20
2002	15,738	2,050	2	15,201	1,928	2
2005	17,819	2,547	3	16,693	2,493	3
2008	17,602	2,551	7	16,621	2,497	5
2011	18,672	2,595	7	18,315	2,530	4

For the near future scenario, NN2 and NN3 HPPs are added to the system. The results show that the optimization model can optimize the hydropower production under flood condition in both scenarios significantly. The maximum peak flow from RCP4.5 scenario is approximately lower than the actual single reservoir operation on average. Meanwhile, the maximum peak flow from RCP8.5 scenario is approximately higher than the optimal and actual single reservoir operations on average. These phenomena may be due to the high precipitation of future scenarios.

The optimization results also found that the average hydropower, total outflow, and water through spillway could be higher than observation data by 9.9%, 18.7%, and 12.2%, respectively for RCP4.5 scenario. While the average hydropower,

total outflow, and water through spillway of RCP8.5 scenario could be higher than observation data by 15.6%, 25.7%, and 19.4%, respectively. This finding may be due to the limitation of hydropower production of the turbines, which led to the high release through the spillway. Due to the large inflow, large flood events will probably occur in the near future and may last longer than those in the past as presented in Figure 5-19 and Figure 5-20 for RCP4.5 and RCP8.5, respectively.

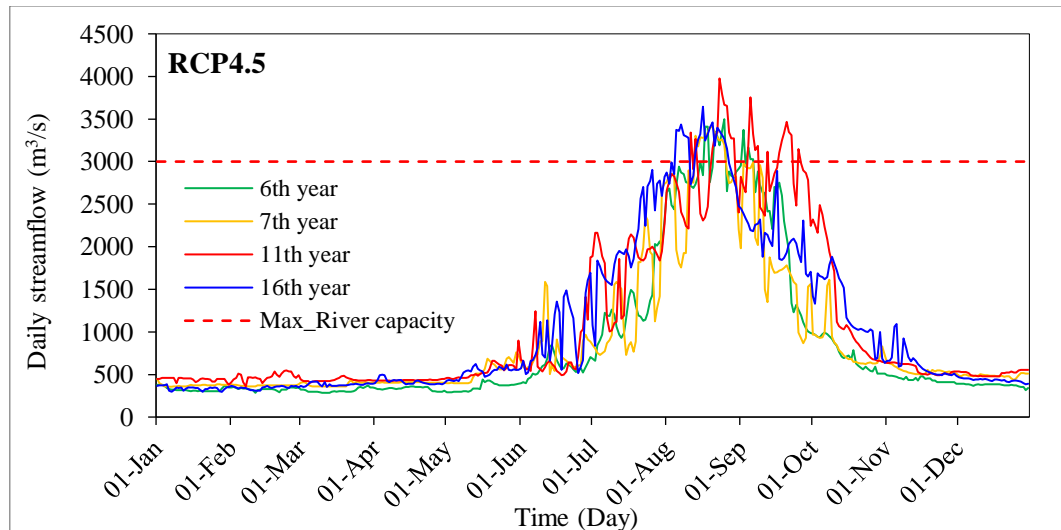


Figure 5-19 Future daily outflow without river capacity constraint at flood control point under RCP4.5 scenario.

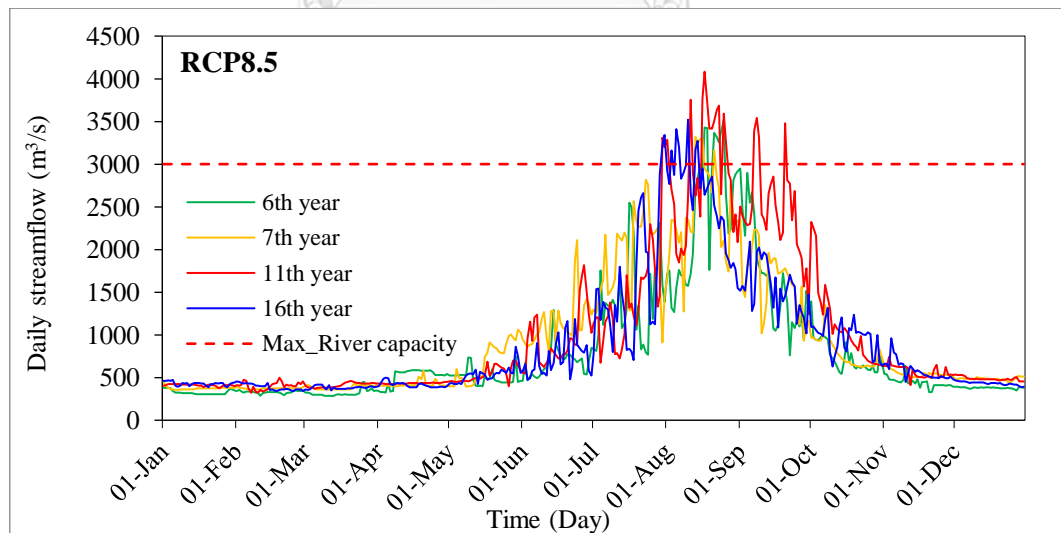


Figure 5-20 Future daily outflow without river capacity constraint at flood control point under RCP8.5 scenario.

5.4.2. Optimal reservoir operation with river capacity constraint

The optimal single reservoir operation (NN1) is also considered to assess the optimal hydropower production with river capacity constraint. The flood years of 1995, 2002, 2005, 2008, and 2011 are selected for historical scenario. The optimization results of monthly hydropower production compared with the observation are presented in Figure 5-21, and the annual hydropower productions are summarized in Table 5-4. The results show that the hydropower production is optimized, the objective function is followed, and similar patterns with the observation are kept. The monthly hydropower production is higher than the observation in the period of dry months, while hydropower production in some of wet months are lower than the observation. The results in Table 5-4 also illustrated that the annual hydropower production has slightly increased and ranges from a minimum of 1,009 in 1995 to a maximum of 1,178 GWh in 2011. However, the largest increase in hydropower production can be found in 1995, which is equal to approximately 4.3% when compared with the observation data.

The optimization results in Figure 5-22 illustrate that the outflow variation decreases, especially in wet months, when compared with the observation in Figure 5-17. Considering that the limitation of the maximum river capacity is set as the constraint, flooding does not occur at the downstream of NN1. Table 5-5 presents the amount of annual outflow volume and flow through spillway from the actual operation and optimization model. The optimization result found that the amount of outflow volume and flow through spillway do not vary greatly, the amount of outflow volume reduced to approximately 4.01%, and flow through spillway decreased to approximately 11.5%. These phenomena may cause the limitation of the maximum river capacity. Hence, the model attempts to start releasing more water than the observation to have more space of reservoir in dry months before the start of the rainy season. Moreover, model tries to store the water in the reservoir to reduce the outflow from reservoir for flood protection at the downstream of reservoir. However, even though this case can protect flood at downstream of reservoir, it increases the release in dry months, which may lead to water shortage at the downstream of reservoir. In addition, the profit from hydropower production also declines when compared with the other cases.

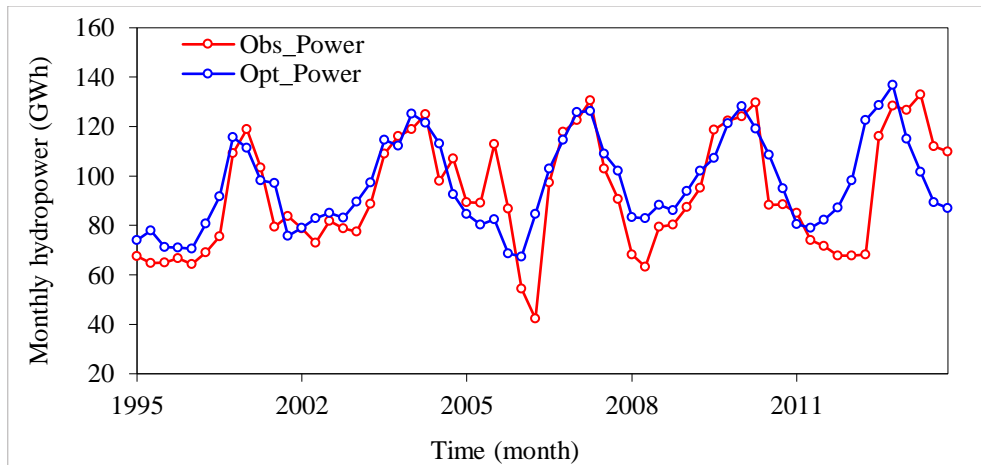


Figure 5-21 The monthly hydropower production from optimization and observation with river capacity constraint.

Table 5-4 Summary of annual hydropower production from optimization and observation with river capacity constraint.

Year	Observation	Optimization	Difference
	GWh	GWh	%
1995	968	1,009	4.30
2002	1,153	1,161	0.67
2005	1,137	1,142	0.42
2008	1,146	1,166	1.80
2011	1,161	1,178	1.50
Average	1,113	1,131	1.74

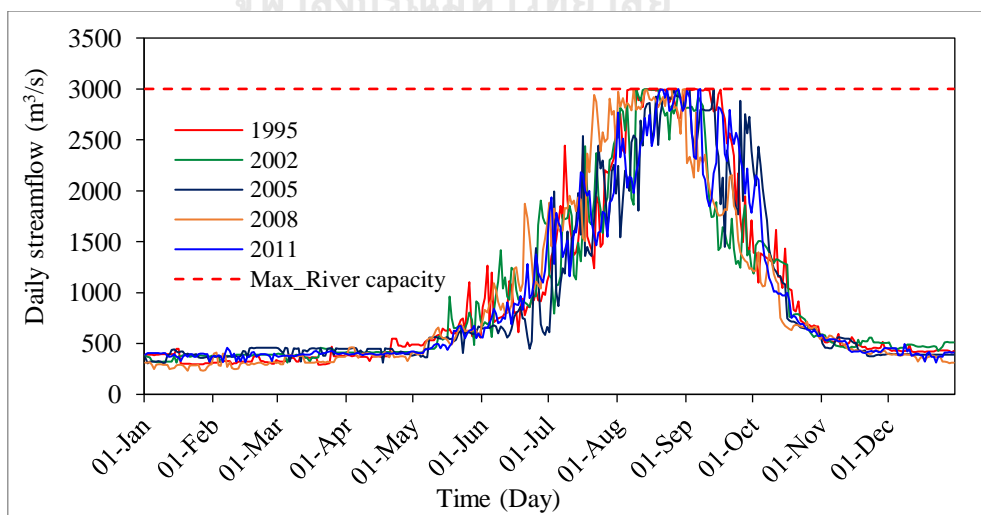


Figure 5-22 Optimized daily outflow with river capacity constraint scenario at flood control point.

Table 5-5 Summary of annual outflow volume and flow through spillway with river capacity constraint.

Year	Observation		Optimization	
	Outflow	Spillway	Outflow	Spillway
	MCM	MCM	MCM	MCM
1995	20,693	1,453	18,443	1,177
2002	15,738	2,050	15,281	1,750
2005	17,819	2,547	16,921	2,307
2008	17,602	2,551	17,108	2,319
2011	18,672	2,595	17,138	2,352

5.5. Indicative reservoir operating curves

5.5.1. Indicative reservoir operating curves for present

The reservoir operating curves are also used to formulate monthly operational policies that can maximize the hydropower generation of NN1 and NN2. The upper and lower operating curves (UOC and LOC, respectively) of NN1 and NN2 are obtained from the results of the optimization model. These curves can be developed on the basis of the storage water level recorded at each period (i.e., each month in this study). UOC and LOC are estimated from the maximum and minimum reservoir water levels, respectively, for each month from 2012 to 2015. These water levels are simulated using the optimization model, which achieves the maximum and minimum hydropower production for every month. The reservoir water level is simulated by the optimization model on the basis of the area-storage-water level curve. The optimal operation curves for NN1 and NN2 are shown in Figure 5-23 and Figure 5-24, respectively.

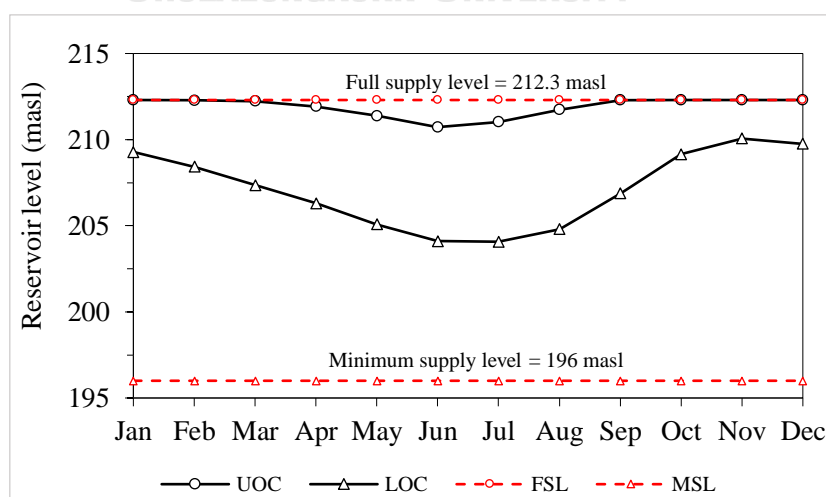


Figure 5-23 Indicative optimal reservoir operating curves for NN1 reservoir

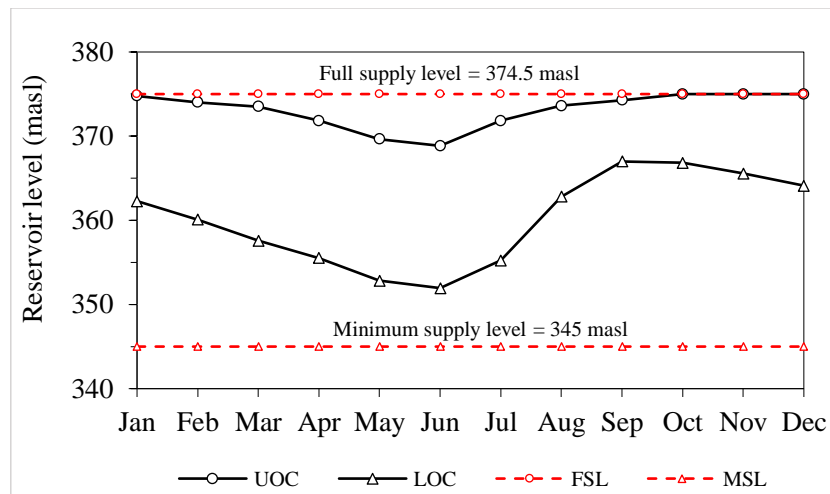


Figure 5-24 Indicative optimal reservoir operating curves for NN2 reservoir

Figure 5-23 shows that the range between UOC and LOC is generally small. The UOC is almost constant with full supply level, whereas the LOC dropped in the dry season during the mid-year. These phenomena may be due to the large storage capacity of NN1 reservoir, thereby storing enough amount of water from wet season to dry season. The characteristic rule curves of NN2 (Figure 5-24) illustrate that the UOC is similar to the NN1, but the range between UOC and LOC is higher than the NN1, especially in the wet season. This phenomenon may be due to the small storage capacity of NN2 reservoir, and the water in wet season cannot be kept until the full operation in dry season. Thus, the amount of water has to be released through the turbine in wet season, thereby increasing the hydropower production in wet season. Increased amount of hydropower generated based on the proposed rule curves for NN1 and NN2 suggests that the proposed rule curves could offer more efficient operation than the existing rule curves.

The impact on water use for other downstream activities was also assessed. The monthly average domestic and irrigation water use at the downstream area of NN1 is 4.3MCM and 65MCM, respectively, which is negligible in comparison with the monthly minimum release from NN1 of 825.2MCM. The monthly maximum release of 1,092.2 MCM from NN1 is less than 7,889.4MCM, which is the river capacity at the downstream area of NN1. As a result, the recommended rule curves proposed do not pose increasing risk of water shortage or flooding in the downstream area. However, these curves are established on the basis of the optimal release of water for maximizing the hydropower production of NN1 and NN2 within the study period and may change along with the variations in reservoir inflow. The new rule curves of NN1 and NN2 may change the water release in each month to make the balance of water use and maximize hydropower production.

5.5.2. Indicative reservoir operating curves under climate change scenarios

The following figures show the future reservoir operating curves of NN1, 2, and 3 HPPs developed through the optimal multi-reservoir operation with optimization model under future inflow from RCP4.5 and RCP8.5 scenarios. The future operation curves are developed on the basis of near future inflow over 20 years. These operation curves are suggested as the final reservoir operating curves when the optimized operating areas are distributed between the highest and lowest reservoir levels.

Figure 5-25 presented the future reservoir operating curves for NN1 HPP under climate change scenarios. The operation curves ensure that the reservoir operates to lower operation curve during the dry season to increase hydropower production at the normal inflow, and it recovers the reservoir level up to the full supply level at the end of the rainy season. Figure 5-25 also shows that the operation curve patterns are very close to the historical operation curves generated by the optimization model in the period of 2012–2015. The future lower operation curve is shifted down to approximately of 0.42 m for RCP4.5 scenario when compared with the historical lower operation curve because of the high variation of inflow caused by climate change. In other words, the future lower operation curve is shifted up from the historical lower operation curve by approximately 0.25 m for the RCP8.5 scenario.

The future reservoir operating curves for NN2 HPP under climate change scenarios presented in Figure 5-26 show that they operated at higher levels than the historical reservoir operating curves in RCP4.5 and RCP8.5 scenarios. With regard to the results of hydropower production in the previous section, the NN2 HPP can maximize its hydropower production by adhering to the upper and lower reservoir operation curves. In addition, the future lower operation curve is lower than the historical lower operation curve by approximately 1.37 m.

For the NN3 HPP, which is under construction and located at the upstream of NN2, the optimization model attempted to optimize the reservoir operation with the future inflow under climate scenarios. The future reservoir operating curves under climate change scenarios for NN3 HPP (Figure 5-27) was developed on the basis of various storage levels from the optimization output. According to the results of inflow predictions, the NN3 reservoir has higher variation of the inflow than NN1 and NN2. Higher variation of the inflow can lead to higher variation in the maximum and minimum of the storage level from reservoir operation. This phenomenon might lead to the upper operating curve of RCP8.5 to become higher than that of the RCP4.5, while the lower operating curve of RCP8.5 becomes lower than that of the RCP4.5.

However, the reservoir operating curves for all HPPs should be compared with the actual rule curves to clarify the impact of climate change on reservoir operation. In addition, these future reservoir operating curves have been developed generally on the basis of a maximum and minimum storage level of optimization model only. This finding demonstrated that these reservoir operating curves can generate flood at the downstream of NN1 HPP. Although the impact of climate change on reservoir operation for the near future is not large, but the hydropower development in main river and tributaries upper NN1 HPP might affect to the operating of NN1 reservoir. Therefore, the existing rule curves of NN1 reservoir are needed to revise.

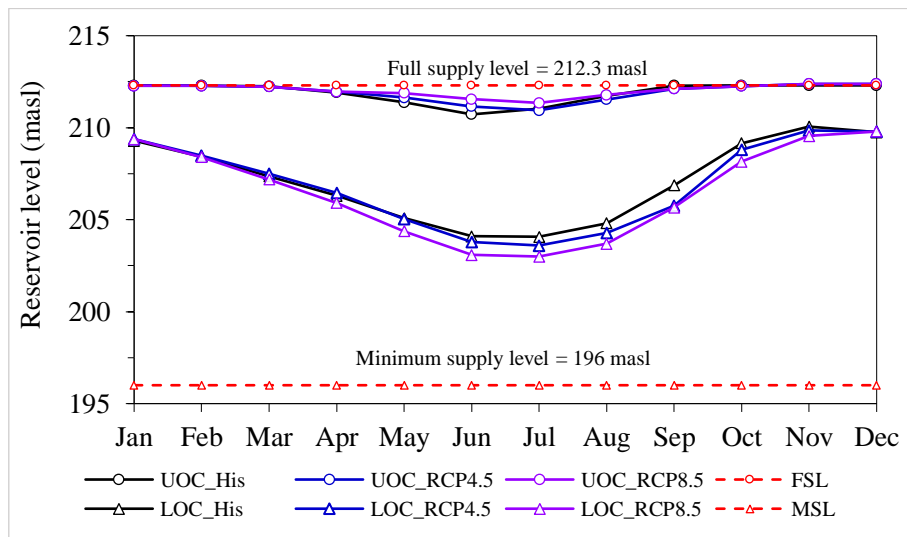


Figure 5-25 Indicative the future reservoir operating curves for NN1 HPP under climate change scenarios.

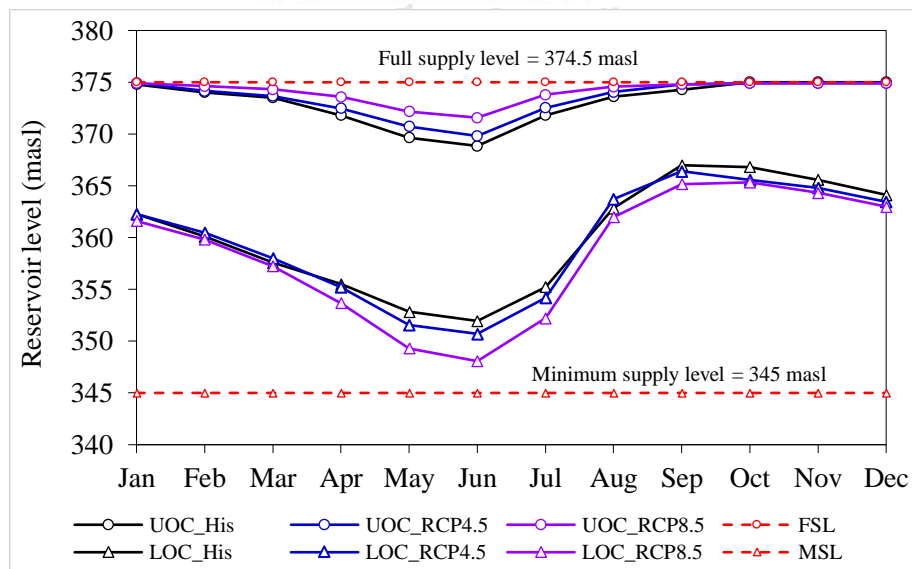


Figure 5-26 Indicative the future reservoir operating curves for NN2 HPP under climate change scenarios.

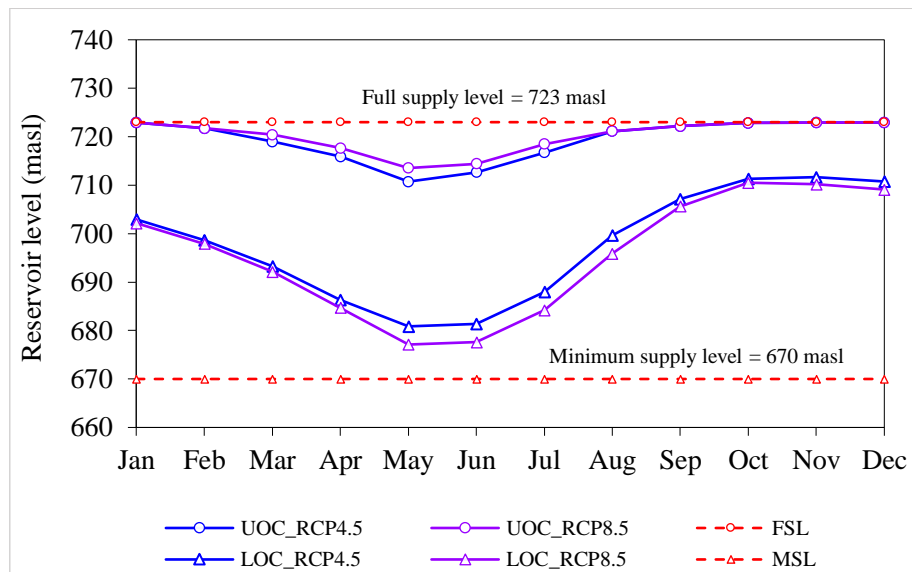


Figure 5-27 Indicative the future reservoir operating curves for NN3 HPP under climate change scenarios.

5.6. Summary

This research aims to join the operation among NN1, NN2, and NN3 HPPs to carry out the optimal hydropower production. The GAMS is applied as the optimization model to maximize hydropower production. Single and multiple reservoir systems were tested as present scenario, whereas future scenarios were tested in multiple reservoir systems. Moreover, the single and multiple reservoir system operations were optimized with and without flood conditions under present and future scenarios. The IFAS model was used to predict historical and future streamflow in NNRB.

The present scenario results show that the single reservoir operation was optimized higher than the observed hydropower production by increasing 12.2%. For the multi-reservoir operations, the optimization model can increase hydropower production by 20.2% (6.0% from NN1 and 14.2% from NN2) on average compared with the observed hydropower production. The optimization model suggests that the application of the proposed optimization model can contribute to control release better. However, the results also show that the annual average hydropower production of NN1 from multi-reservoir optimization is lower than the single reservoir optimization. Moreover, the optimization model could reduce the flooding days and the amount of water through spillway.

Future scenarios were optimized under future climate conditions over a period of 20 years (2020–2039), and the NN3 HPP was added to the multi-reservoir system.

The future scenarios found that the optimization model produced minimum hydropower in 2020 and tends to increase to maximum in 2030. Meanwhile, the trend of NN1 HPP is slightly constant in RCP 4.5 and RCP8.5 scenarios. The hydropower production optimized under RCP8.5 is higher than the hydropower production under RCP4.5 over a future period. This might cause from the future streamflow under RCP8.5 scenario predicted by IFAS are mostly higher than the future streamflow under RCP4.5 scenario, especially in wet months. The increase in hydropower production under climate change conditions could evidently show that the optimization model could optimize hydropower under high variation of reservoir inflow. The results also found that the large flood events probably occurred in the near future, especially in 2030, and lasted longer than those in the past.

The indicative reservoir operating curves proposed do not pose increasing risk of water shortage but might risk to flooding at the downstream area. However, these curves are established on the basis of the optimal release of water for maximizing the hydropower production of NN1 and NN2 within the study period and may change along with the variations in reservoir inflow. The new rule curves of NN1 and NN2 may change the water release in each month to make the balance of water use and maximize hydropower. The future reservoir operating curves for NN1 HPP are very close to the historical operating curves generated by the optimization model in the period of 2012–2015. Higher variation of the inflow can lead to higher variation in the maximum and minimum of the storage level from reservoir operation. This phenomenon might lead to the upper operating curve of RCP8.5 to become higher than that of the RCP4.5, while the lower operating curve of RCP8.5 becomes lower than that of the RCP4.5. However, the reservoir operating curves for all HPPs should be compared with the actual rule curves to clarify the impact of climate change on reservoir operation. In addition, these future reservoir operating curves have been developed generally on the basis of a maximum and minimum output of optimization model only. This finding demonstrated that these reservoir operating curves can generate flood at the downstream of NN1 HPP.

CHAPTER 6

CONCLUSIONS AND RECOMMENDATIONS

6.1. Conclusions

The main objective of this research is to develop the optimization model for maximizing hydropower production in the NNRB through optimal reservoir operation with and without flood conditions under the impact of climate change. Four RCMs including MPI, IPSL, ICHEC, and NHRCM were analyzed and compared to the observed data to obtain a relatively more suitable RCM. Both ratio and QM bias correction methods were tested in seasonal and monthly time scales. The bias correction performance was evaluated using statistical parameters including maximum, mean precipitation, R^2 , RMSE, NSE, and SD. The IFAS model was used to predict the present and future streamflow in NNRB. The NN1 and NN2 HPPs are considered in the present scenario, NN3 was added to the system when modelling the future scenario. The general algebraic modeling system (GAMS) was applied as the optimization model to maximize hydropower production in NNRB. Both single and multiple reservoir systems were tested in the present scenario, while future scenarios were tested in multiple reservoirs system. Moreover, the single and multiple reservoirs systems operations were optimized with and without flood conditions under present and future scenarios. The indicative present and future reservoir operating curves were developed generally based on the maximum and minimum storage level of the optimization model. Key findings obtained from each step conducted in the research are summarized in the following sections.

6.1.1. RCM analysis

1) RCM selection

The monthly precipitation from the IPSL and NHRCM are generally underestimated while other products are generally overestimated when compared to the observation. The largest error is evident in the ICHEC product, while the MPI has approximately the smallest error. However, all RCMs can well capture at low monthly precipitation (<45 mm/month) when compared to the observation. The spatial variation of the NNRB is probably a factor influencing the performance of the RCMs. A relatively coarse gridded dataset of the RCMs model might not adequately represent highly variable precipitation in this area. The analysis suggested that the MPI model outperforms all other models with the highest R^2 and NSE, lowest RMSE, and error in the mean. Therefore, the MPI model is considered to be a representative RCM model to be used further for the analysis of future climate modeling in this research.

2) RCM bias correction

In this study, the ratio and QM methods were adopted to correct the biases of precipitation from RCM over the NNRB. Both methods were tested in seasonal and monthly time scales to select a suitable bias correction method for future climate change impact assessment. The results suggested that both methods significantly improved monthly RCM precipitation over the NNRB. The SR and MR methods could reduce the biases in the dry season rather than the wet season. The bias correction by MR with different values of scaling factor for each month can improve the biased precipitation over the NNRB better than the SR and SQM methods. However, the RCM precipitation still tends to overestimate monthly precipitation. This error might be caused by the limited ability of the ratio method using a too simple scaling factor for wet and dry seasons to capture the bias in a highly variable climate regime. Despite the complexity of spatial distribution of seasonal precipitation, the MQM method reasonably outperformed other methods because it yielded the highest R^2 and NSE values and lowest RMSE and SD values.

3) The future change of precipitation

The annual precipitation of both RCPs has approximately a five-year cycle changing. The annual precipitation over the NNRB could increase in both RCP4.5 and RCP8.5 scenarios by approximately 8.2% and 17.4% on average, respectively. The average monthly precipitation was higher than the observation in almost all months under both scenarios except January and December. The monthly precipitation changes from -12.2 to 19.2% for RCP4.5 and for RCP8.5 scenario, it changes from -15.6 to 25.0%.

6.1.2. Streamflow prediction

1) Parameter sensitivity analysis

There are 7 sensitive parameters influencing the total and peak flows in the NNRB. The most sensitive parameters for streamflow prediction were SKF, RNS, and SNF. AGD, HFMXD, and HCGD were considered moderately sensitive. FALFX was least sensitive parameter. The HFMND and HFOD were found almost insensitive.

2) Model calibration and validation

Both calibration and validation results demonstrated that the model successfully simulates daily and monthly streamflow with good and reasonable accuracy. The daily streamflow in wet years shows a good match with the observed daily streamflow at the basin outlet, especially in high streamflow. The daily streamflow has slightly overestimated the streamflow, especially low flow. While the

monthly streamflow seems to be better with improvement when simulates low flow but slightly failed to capture the peak flow in few years during the calibration period.

3) The future change of streamflow

The future streamflow prediction results illustrated that both future daily and monthly streamflow under the RCP8.5 scenario are mostly higher than those of the RCP4.5 scenario, especially in the high streamflow period. The daily streamflow in the future period was increased continuously and reduced after reaching the maximum streamflow under both scenarios. It seems to be clear that the future streamflow during wet years resulted in the similar trend of precipitation under both scenarios. Higher monthly streamflow is generally simulated over the period for RCP8.5 compared to RCP4.5 scenario for all rivers. Exceptions are found for low streamflow period in some years when monthly streamflow from RCP8.5 is slightly lower than that of RCP4.5. A higher variation of daily and monthly streamflow is found in the RCP8.5 compared to the RCP4.5 scenario.

6.1.3. Optimal reservoir operation

1) Present scenario

The single reservoir operation using optimization model could increase the annual hydropower production by 12.2% compared to the observation data. Increase in the hydropower production was due mainly to improved operations in wet months. During dry months the hydropower production was slightly higher than the observed hydropower production.

For the multi-reservoir operations, the optimization model can increase the annual hydropower production by 20.2% (6.0% from NN1 and 14.2% from NN2) on average compared to the observed hydropower production. When considering the contribution from NN1 and NN2 to the increase in the multi-reservoir hydropower production, it was found that 16.7% and 19.8% on average were from for NN1 and NN2, respectively. The annual average hydropower production of NN1 from multi-reservoir optimization is higher than the single reservoir optimization. The increase in hydropower production was contributed by improvement in the operation in dry months especially in December. However, it is noted that the increase in hydropower production could be partly resulted from increasing reservoir inflow. The pattern of average monthly hydropower production of NN1 and NN2 from the optimization model is similar to that of the observed hydropower production. The results suggest that the application of the optimization model could potentially contribute to better control of the release. Moreover, the optimization model could also reduce the flooding days and the amount of water lost through spillway.

2) Future scenarios

For future scenarios, it was found that the optimization model yielded higher monthly hydropower on average under both RCPs when compared to observed hydropower. The hydropower production increases in almost the same trend for NN2 and NN3 HPPs. The increasing pattern of NN3 HPP is higher than NN2 and NN1 HPPs. The hydropower of NN1 HPP varied in a small range with no significant increasing trend for both RCP 4.5 and RCP8.5 scenarios. The hydropower production optimized under RCP8.5 is higher than hydropower production under RCP4.5 over the future period. The variation of monthly hydropower production from NN3 HPP is slightly higher than that of others HPPs. The average hydropower production under both RCP scenarios is at its maximum value in August, whereas the minimum hydropower is recorded in December. The large flood events probably occur in the near future and last longer than what occurred in the past. The increase of hydropower production under climate change conditions suggests that the optimization model could support decision making in reservoir operations and hydropower production under the impact of climate change and high variation of reservoir inflow. It was expected that this optimization model could be adopted for optimizing hydropower production in the NNRB under future climate change conditions.

6.1.4. The optimal reservoir operation with and without river capacity constraints

In the case of the present condition, the model could optimize and follow the objective function as illustrated in reducing flooding day, flow amount over the spillway, and increasing in hydropower production when compared to the observation data. The monthly hydropower optimized by the optimization model increases significantly in the wet months, but some dry months are slightly below the observation data. The largest increase in hydropower production was found in 1995, which is equal to about 9.6% compared to that of the observation data. The optimization model could reduce the flood peak, the amount of outflow volume, flow-through spillway by approximately 4.8, 3.6, and 4.7%, respectively on average. The model could reduce the flood period from 24 to 20 days instead of 1995.

For the future scenario, the optimization model much contributed to the increase in hydropower production under flood conditions in both scenarios. The peak flow and variation of both scenarios are slightly increased. The peak flow from the RCP4.5 scenario is higher than that of the optimal single reservoir operation but still lower than that of the observation. The peak flood from the RCP8.5 scenario is higher than both optimal and actual single reservoir operations. Due to the large inflow, the large flood events probably last longer than what occurred in the past.

The river capacity was added as additional constraint to optimize the hydropower while considering flooding condition, The hydropower production is optimized and followed the objective function. The monthly hydropower production obtained from optimization is higher than the observation in dry months and lower than the observation in some wet months. The outflow variation decreases, especially in wet months when compared to that of the observation. The amount of outflow volume and flow through spillway were reduced approximately 4.01 and 11.5%, respectively. While the releases suggested by the model could help prevent flooding downstream, it could also lead to water shortage due to higher release in dry months.

6.1.5. Indicative reservoir operating curves

Regarding the indicative present operating curves, the range between UOC and LOC of NN1 is generally small. The UOC is almost constant with a full supply level, whereas the LOC dropped in the dry season during the mid-year. The UOC of NN2 is similar to that of the NN1, but the range between UOC and LOC is larger, especially in wet months. The higher amount of water has to be released through the turbine in the wet season led to the increasing hydropower production in wet months. The recommended operating curves proposed do not pose an increasing risk of water shortage or flooding in the downstream area over the study period. The proposed rule curves could offer a more efficient operation than the existing rule curves.

For the future indicative operating curves of NN1 the LOC is shifted down approximately 0.25 and 0.42 m on average for RCP4.5 and RCP8.5 scenarios, respectively when compared to the present LOC. The UOC is similar to the present UOC for both scenarios. For the NN2, the LOC is shifted down approximately 1.43 and 3.52 m on average for RCP4.5 and RCP8.5 scenarios, respectively when compares to the present LOC. The future UOC is shifted up from the present LOC approximately 0.91 and 1.73 m on average for RCP4.5 and RCP8.5 scenarios, respectively.

For the future indicative operating curves of NN3, the reservoir has a higher variation of the inflow than NN1 and NN2. Higher variation of the inflow could lead to a higher variation of the maximum and minimum of the storage level from reservoir operation. This is probably the cause that the LOC of both RCPs is at very low levels at the beginning of wet months and possibly lead to drought in some dry months.

It is noted that the indicative UOC and LOC curves suggested in this study are developed based on the optimal release of water for maximizing the hydropower production within the study periods and may change along with the variations in

reservoir inflow. The new operating curves may change the water release each month in order to make the balance of water use and maximize hydropower production.

6.2. Recommendations

In order to improve a study on the impact of climate change in near future on streamflow and reservoir operation and carry out the trend/pattern of precipitation in the NNRB, more updated versions and more RCMs products should be assessed to quantify uncertainties from RCMs. The other high-resolution RCMs data are recommended for future assessment of the impact of climate change on streamflow and reservoir operation in the NNRB with the longer time period. Moreover, the bias correction techniques used in this research is corrected by averaging at basin scale; the higher resolution of bias correcting at grid scale and other bias correction techniques should be investigated.

For further research of the streamflow prediction, the rain gauge stations in the upper part of the basin are required to obtain higher reliability and improvement in streamflow prediction in NNRB. More updated land use data set and land use change issue should be considered for the streamflow prediction. Moreover, due to the limitation of the meteorological data, satellite precipitation data should be considered.

The solver tool in the optimization model used in this research is only for local optimization, the global optimization solver tool should be considered for further study. The optimization of reservoir operations involves nonlinear problems which are non-convex and are likely to have multiple locally optimal solutions. These problems are difficult to solve but possibly achievable using some non-linear solvers with a very high number of runs to increase the chance to obtain the solution that converges to a global optimal solution.

According to the result analysis when the river capacity constraint was set, the optimization model could reduce flood at downstream of NN1 HPP at the expense of decreasing hydropower production. For further research, the economic benefit from saving flood and economic loss from decreasing of hydropower production should be estimated and compared. This research assessed only flood duration at downstream of NN1 HPP, flood model should be considered to assess the flood area and flood inundation maps, then the flood damage cost should be estimated.

Because of the indicative reservoir operating curves have been developed generally on the basis of maximum and minimum storage level of optimization model for maximizing hydropower production only. This finding demonstrated that these indicative reservoir operating curves could generate flood at the downstream of NN1 HPP. Therefore, these indicative reservoir operating curves might not be suitable for wet years. In addition, the indicative reservoir operating curves for all HPPs should be

compared with the existing rule curves to make a clearer picture on the impact of climate change on reservoir operation. Although the impact of climate change on reservoir operation for the near future is not large, but the hydropower development in main river and tributaries upper NN1 HPP might affect the operating of NN1 reservoir. Therefore, the existing rule curves of NN1 reservoir should be revised.

Uncertainties from climate change scenarios and socio-economic development scenarios should be considered in future work. Chance constrained optimization could be developed to quantify and compare impacts from climate change and socio-economic development.



REFERENCES

- Abiodun, B. J., and Adedoyin, A., (2016). A modelling perspective of future climate change. In T. M. Letcher (Ed.), *Climate Change (Second Edition)*, Boston: Elsevier, pp. 355-371.
- Ahmad, A., and El-Shafie, A., (2014). Reservoir Optimization in Water Resources: a Review. *Water Resources Management*, 28, 15
- Ahmadi, M., Bozorg-Haddad, O., and Loaiciga, H., (2014). Adaptive Reservoir Operation Rules Under Climatic Change (Vol. 29).
- Akhter, M., (2017). Selection of Suitable General Circulation Model and Future Climate Assessment of Kashmir Valley. *Engineering, Technology and Applied Science Research*, 5, 196-202
- Akter, T., Quevauviller, P., Eisenreich, S. J., and Vaes, G., (2018). Impacts of climate and land use changes on flood risk management for the Schijn River, Belgium. *Environmental Science & Policy*, 89, 163-175
- Aldrian, E., Dümenil-Gates, L., Jacob, D., Podzun, R., and Gunawan, D., (2004). Long-term simulation of Indonesian rainfall with the MPI regional model. *Climate Dynamics*, 22(8), 795-814
- Amsal, F., Harsa, H., Sopaheluwakan, A., Linarka, U., Pradana, R., and Satyaningsih, R., (2019). Bias correction of daily precipitation from downscaled CMIP5 climate projections over the Indonesian region. *IOP Conference Series: Earth and Environmental Science*, 303, 012046
- Androulakis, I. P., (2009). MINLP: branch and bound global optimization algorithm. *MINLP: Branch and Bound Global Optimization Algorithm*. In C. A. Floudas & P. M. Pardalos (Eds.), *Encyclopedia of Optimization*, Boston, MA: Springer US, pp. 2132-2138.
- Anwar Tinumbang Aulia, F., Yorozu, K., Tachikawa, Y., Tanaka, T., Kim, S., and Ichikawa, Y., (2018). Evaluation of River Discharge Simulated by a Distributed Hydrologic Model Utilizing NHRCM 5km Data. *Proceeding of Annual Conference*, 31, 96
- Argueso, D., Evans, J., and Fita, L., (2013). Precipitation bias correction of very high resolution regional climate models (Vol. 17).
- Arunkumar, R., and Jothiprakash, V., (2012). Optimal Reservoir Operation for Hydropower Generation Using Non-Linear Programming Model (Vol. 93).
- Ayvaz, T., (2013). A linked simulation–optimization model for simultaneously estimating the Manning’s surface roughness values and their parameter structures in shallow water flows. *Journal of Hydrology*, 500, 183-199
- Aziz, A., and Tanaka, S., (2011). Regional Parameterization and Applicability of Integrated Flood Analysis System (IFAS) for Flood Forecasting of Upper-Middle Indus River. *Pakistan J. Meteor.*, 8, 21-38
- Bangsulin, N., Promwungkwa, A., and Ngamsanroaj, K., (2017). Multi-reservoir operational management for optimal electricity production of Namkhan 2 and 3 hydropower plants. *International Journal of Mechanical And Production Engineering*, 5(2), 56-61

- Bartlett, R., Baker, J., Lacombe, G., Douangsavanh, S., and Jeuland, M., (2012). Analyzing Economic Tradeoffs of Water Use in the Nam Ngum River Basin, Lao PDR.
- Belotti, P., Kirches, C., Leyffer, S., Linderoth, J., Luedtke, J., and Mahajan, A., (2013). Mixed-integer nonlinear optimization. *Acta Numerica*, 22, 1-131
- Berg, P., Feldmann, H., and Panitz, H. J., (2012). Bias correction of high resolution regional climate model data. *Journal of Hydrology*, 448-449, 80-92
- Birhanu, K., Alamirew, T., Olumana Dinka, M., Ayalew, S., and Aklog, D., (2014). Optimizing Reservoir Operation Policy Using Chance Constraint Nonlinear Programming for Koga Irrigation Dam, Ethiopia. *Water Resources Management*, 28(14), 4957-4970
- Bonami, P., Biegler, L. T., Conn, A. R., Cornuéjols, G., Grossmann, I. E., Laird, C. D., Lee, J., Lodi, A., Margot, F., Sawaya, N., and Wächter, A., (2008). An algorithmic framework for convex mixed integer nonlinear programs. *Discrete Optimization*, 5(2), 186-204
- Bonami, P., and Lee, J., (2011). BONMIN Users' Manual. In.
- Cannon, A., Sobie, S., and Murdock, T., (2015). Bias Correction of GCM Precipitation by Quantile Mapping: How Well Do Methods Preserve Changes in Quantiles and Extremes? *Journal of Climate*, 28, 6938–6959
- Chang, J., Wang, Y., and Huang, Q., (2005). Reservoir Systems Operation Model Using Simulation and Neural Network. In, Boston, MA: Springer US, pp. 519-526.
- Chiew, F., Zheng, H., and Potter, N., (2018). Rainfall-Runoff Modelling Considerations to Predict Streamflow Characteristics in Ungauged Catchments and under Climate Change. *10(10)*, 1319
- Chokkavarapu, N., and Mandla, V. R., (2019). Comparative study of GCMs, RCMs, downscaling and hydrological models: a review toward future climate change impact estimation. *SN Applied Sciences*, 1(12), 1698
- Cruz, F. T., and Sasaki, H., (2017). Simulation of Present Climate over Southeast Asia Using the Non-Hydrostatic Regional Climate Model. *SOLA*, 13, 13-18
- Eden, J. M., Widmann, M., Maraun, D., and Vrac, M., (2014). Comparison of GCM- and RCM-simulated precipitation following stochastic postprocessing. *119(19)*, 11,040-011,053
- Enayati, M., Bozorg-Haddad, O., Bazrafshan, J., Hejabi, S., and Chu, X., (2020). Bias correction capabilities of quantile mapping methods for rainfall and temperature variables. *Journal of Water and Climate Change*, 2040-2244
- Fu, C., Wang, S., Xiong, Z., Gutowski, W., Lee, D.-K., McGregor, J., Sato, Y., Kato, H., Kim, J.-W., and Suh, M.-S., (2005). Regional Climate Model Intercomparison project for Asia. *Bulletin of the American Meteorological Society*, 86, 102-125
- Fukami, K., Sugiura, T., Magome, J., and Kawakami, T., (2009). Integrated Flood Analysis Systems IFAS Version 1.2 User's manual. In Vol. 14, pp. 227.
- G. Flato, J. Marotzke, B. Abiodun, P. Braconnot, S.C. Chou, W. Collins, P. Cox, F. Driouech, S. Emori, Eyring, V., C. Forest, P. Gleckler, E. Guilyardi, C. Jakob, V. Kattsov, Reason, C., and Rummukainen, M., (2013). Evaluation of Climate Models. In A. Pitman, S. Planton, & Z. C. Zhao (Eds.), *Climate Change 2013: The Physical*

- Science Basis. The Fifth Assessment Report of the Intergovernmental Panel on Climate Change, Cambridge University Press: Cambridge, United Kingdom and New York, NY, USA., pp. 741-866.
- Ganopolski, A., (2019). Climate Change Models. In B. Fath (Ed.), *Encyclopedia of Ecology* (Second Edition), Oxford: Elsevier, pp. 48-57.
- Ginting, B. M., Harlan, D., Taufik, A., and Ginting, H., (2017). Optimization of reservoir operation using linear program, case study of Riam Jerawi Reservoir, Indonesia. *International Journal of River Basin Management*, 15(2), 187-198
- Hafiz, I., Nor, N., Mohd Sidek, L., Basri, H., Hanapi, M. N., and L, L., (2013). Application of Integrated Flood Analysis System (IFAS) for Dungun River Basin (Vol. 16).
- Hay, L. E., and Clark, M. P., (2003). Use of statistically and dynamically downscaled atmospheric model output for hydrologic simulations in three mountainous basins in the western United States. *Journal of Hydrology*, 282(1), 56-75
- Heo, J.-H., Ahn, H., Shin, J.-y., Kjeldsen, T., and Jeong, C., (2019). Probability Distributions for a Quantile Mapping Technique for a Bias Correction of Precipitation Data: A Case Study to Precipitation Data Under Climate Change. *Water*, 11
- Hosseini, H., Ghorbani, M. A., and Bavani, A. R., (2014). Impacts of Climate Change on Streamflow and Reservoir Operation.
- Ines, A., and Hansen, J., (2006). Bias Correction of Daily GCM Rainfall for Crop Simulation Studies. *Agricultural and Forest Meteorology*, 138, 44-53
- IPCC. (2013). *Climate Change 2013: The Physical Science Basis. Contribution of Working Group I to the Fifth Assessment Report of the Intergovernmental Panel on Climate Change.*
- Jayasekera, D., Kaluarachchi, J., and Hoanh, C., (2016a). Climate change adaptation strategies for the Nam Ngum River Basin (Vol. 12).
- Jayasekera, D., Kaluarachchi, J., and Hoanh, C., (2016b). Climate change adaptation strategies for the Nam Ngum River basin, Laos.
- Jothiprakash, V., and Arunkumar, R., (2014). Multi-reservoir optimization for hydropower production using NLP technique. *KSCE Journal of Civil Engineering*, 18(1), 344-354
- Karamouz, M., Khodatalab, N., Araghy Nejad, S., and Kerachian, R., (2002). Multipurpose Reservoir Operation Optimization: Application of Genetic Algorithm.
- Keophila, V., Promwungkwa, A., and Ngamsanroj, K., (2018). Effectiveness of Cascades Reservoir for Flood Control Operation and Electricity Production in Nam Ngum River. *International Journal of Mechanical and Production Engineering (IJMPE)*, 6(1), 7-13
- Kerkhoff, C., Künsch, H., and Schär, C., (2012). Relations between RCMs and GCMs in the ensembles simulations. 1873
- Kimmany, B., Sriariyawat, A., and Visessri.S. (2016). Effectiveness of hydrologic models for streamflow prediction in the Nam Song River basin. (Master). Chulalongkorn University. (52292)

- Kimura, N., Tai, A., Chiang, S., Wei, H.-P., Su, Y.-F., Cheng, C.-T., and Kitoh, A., (2014). Hydrological Flood Simulation Using a Design Hyetograph Created from Extreme Weather Data of a High-Resolution Atmospheric General Circulation Model. *Journal of Water*, 6
- Lacombe, G., Douangsavanh, S., Baker, J., Hoanh, Bartlett, R., Jeuland, M., and Phongpachith. (2014). Are hydropower and irrigation development complements or substitutes? The example of the Nam Ngum River in the Mekong Basin. *Water International*, 39
- Liang, X.-Z., Kunkel, K. E., Meehl, G. A., Jones, R. G., and Wang, J. X. L., (2008). Regional climate models downscaling analysis of general circulation models present climate biases propagation into future change projections. 35(8)
- Limlahapun, P., and Fukui, H., (2016). Database assessment of CMIP5 and hydrological models to determine flood risk areas. *Earth and Environmental Science*, 46(6)
- Luo, M., Liu, T., Meng, F., Duan, Y., Frankl, A., Bao, A., and De Maeyer, P., (2018). Comparing Bias Correction Methods Used in Downscaling Precipitation and Temperature from Regional Climate Models: A Case Study from the Kaidu River Basin in Western China. 10(8), 1046
- Lutz, A., ter Maat, H., Biemans, H., Shrestha, A., Wester, P., and Immerzeel, W. W., (2016). Selecting representative climate models for climate change impact studies: An advanced envelope-based selection approach. *International Journal of Climatology*, 36, 3988-4005
- Mechoso, C. R., and Arakawa, A., (2015). Numerical model in General Circulation Models. In, Oxford: Academic Press, pp. 153-160.
- Merli, A., and Capatti. (2016). Different Measuring Methods for Estimating the Hydraulic Conductivity on the Shallow Aquifer Along a Stretch of the Rimini Coast. *Procedia Engineering*, 158, 434-439
- Milad Jajarmizadeh, S. H., Mohsen Salarpour. (2012). A Review on Theoretical Consideration and Types of Models in Hydrology. *Journal of Environmental Science and Technology*(5), 249-261
- Ministry of Energy and Mines, L. P., (2018a). Lao PDR Energy Statistics 2018. National Library of Indonesia Cataloguing-in-Publication Data: Economic Research Institute for ASEAN and East Asia.
- Ministry of Energy and Mines, L. P., (2018b). Summary of hydropower project in Laos 2018.
- Mohd Sidek, L., (2014). Integrated Flood Analysis System (IFAS) for Kelantan River Basin.
- Ngai, S. T., Sasaki, H., Murata, A., Nosaka, M., Chung, J. X., Juneng, L., Supari, S., Salimun, E., and Tangang, F., (2020). Extreme Rainfall Projections for Malaysia at the end of 21st Century using the high resolution Non-Hydrostatic Regional Climate Model (NHRCM). *SOLA*, 38-55
- Ngai, S. T., Tangang, F., and Juneng, L., (2017). Bias correction of global and regional simulated daily precipitation and surface mean temperature over Southeast Asia using quantile mapping method. *Global and Planetary Change*, 149, 79-90
- Ngo-Duc, T., Tangang, F., Santisirisomboon, J., Cruz, F., Trinh, L., Xuan, T., Phan-

- Van, T., Juneng, L., Narisma, G., Singhruck, P., Gunawan, D., and Aldrian, E., (2016). Performance evaluation of RegCM4 in simulating extreme rainfall and temperature indices over the CORDEX-Southeast Asia region. *International Journal of Climatology*, 10, 10
- Nguyen, H., Mehrotra, R., and Sharma, A., (2016). Correcting for systematic biases in GCM simulations in the frequency domain. *Journal of Hydrology*, 538, 117-126
- Oeurng, C., Cochrane, T., Chung, S., Kondolf, g. m., Piman, T., and Arias, M., (2019). Assessing Climate Change Impacts on River Flows in the Tonle Sap Lake Basin, Cambodia. *Water*, 11, 618
- Piman, T., Cochrane, T. A., Arias, M. E., Dat, N. D., and Vonnarart, O., (2015). Managing Hydropower Under Climate Change Uncertainty in the Mekong Tributaries: Examples from Asia, Europe, Latin America, and Australia. In S. Shrestha, A. K. Anal, P. A. Salam, & M. van der Valk (Eds.): Springer International Publishing, pp. 223-248.
- Promwungkwa, A., Keophila, V., and Ngamsanroj, K., (2019). Multi-objective optimization for flood control operation and electricity production of Nam Ngum 1 and 2 hydropower plants. *Interdisciplinary Research Review*, 13(5), 1-9
- Rajabi, J., Sayama, T., and Takara, K., (2015). Application of Integrated Flood Analysis System (IFAS) for Flood Forecasting at Upstream of the Kabul River Basin. *Water Science and Engineering*, 8(1)
- Ranatunga, T., Tong, S., and Yang, J., (2017). An approach to measure parameter sensitivity in watershed hydrological modelling. *Hydrological Sciences Journal*, 62(1), 76-92
- Räty, O., Räisänen, J., and Ylhäisi, J. S., (2014). Evaluation of delta change and bias correction methods for future daily precipitation: intermodel cross-validation using ensembles simulations. *Climate Dynamics*, 42(9), 2287-2303
- Razavi, T., and Coulibaly, P., (2016). Improving Streamflow Estimation in Ungauged Basins using Multi-Modelling Approach. *Hydrological Sciences Journal*, 61
- Ringard, J., Seyler, F., and Linguet, L., (2017). A Quantile Mapping Bias Correction Method Based on Hydroclimatic Classification of the Guiana Shield. *Sensors (Basel, Switzerland)*, 17(6), 1413
- Rittima, A., (2009). Hedging Policy for Reservoir System Operation: A Case Study of Mun Bon and Lam Chae Reservoirs. *Nat. Sci*, 43, 833 - 842
- Rohde, F. G., and Naparaxawong, K., (1981). Modified standard operation rules for reservoirs. *Journal of Hydrology*, 51(1), 169-177
- Rosenthal, R., (2008). GAMS - A User's Guide. In W. GAMS Development Corporation, DC, USA (Ed.), Internal Documents.
- Ruane, A., and McDermid, S., (2017). Selection of a representative subset of global climate models that captures the profile of regional changes for integrated climate impacts assessment. *Earth Perspectives*, 4
- Samadi, S., Gummeneni, S., and Tajiki, M., (2010). Comparison of General Circulation Models: methodology for selecting the best GCM in Kermanshah Synoptic Station, Iran. *Int. J. of Global Warming*, 2, 347-365
- San José, R., Pérez, J. L., González, R. M., Pecci, J., Garzón, A., and Palacios, M.,

- (2016). Impacts of the 4.5 and 8.5 RCP global climate scenarios on urban meteorology and air quality: Application to Madrid, Antwerp, Milan, Helsinki and London. *Journal of Computational and Applied Mathematics*, 293, 192-207
- Sayasane, R., Kawasaki, A., Shrestha, S., and Takamatsu, M., (2015). Assessment of potential impacts of climate and land use changes on stream flow: a case study of the Nam Xong Watershed in Lao PDR. *Journal of Water and Climate Change*, 7, 184-197
- Schl, M., Jose A. Egea, and Banga, J. R., (2008). Extended Ant Colony Optimization for non-convex Mixed Integer Nonlinear Programming. *Computers & Operations Research*, 36(7), 2217-2229
- Seree Chanyotha, C. s., (2013). *Basic Hydraulic of Open channel Flow*. Chulalongkorn University Press.
- Sharma, D., Das Gupta, A., and Babel, M. S., (2007). Spatial disaggregation of bias-corrected GCM precipitation for improved hydrologic simulation: Ping River Basin, Thailand. *Hydrol. Earth Syst. Sci.*, 11(4), 1373-1390
- Smith, J. B., and Hulme, M., (1998). *Climate Change Scenarios*.
- Soltani, M. A., (2008). Stochastic Multi-Purpose Reservoir Operation Planning by Scenario Optimization and Differential Evolutionary Algorithm. *Journal of Applied Sciences*, 22(8), 4186-4191
- Sorachampa, P., Tippayawong, N., and Ngamsanroj, K., (2020). Optimizing multiple reservoir system operation for maximum hydroelectric power generation. *Energy Reports*, 6, 67-75
- Souverijns, N., (2019). Precipitation and clouds over Antarctica from an observational and modelling perspective. (12), 79-92
- Suhardiman, D., Keovilignavong, O., and Kenney-Lazar, M., (2019). The territorial politics of land use planning in Laos. *Land Use Policy*, 83, 346-356
- Switanek, M. B., Troch, P. A., Castro, C. L., Leuprecht, A., Chang, H. I., Mukherjee, R., and Demaria, E. M. C., (2017). Scaled distribution mapping: a bias correction method that preserves raw climate model projected changes. *Hydrol. Earth Syst. Sci.*, 21(6), 2649-2666
- Taesoon, K., Heo, J. H., Bae, D. H., and Kim, J. H., (2008). Single-reservoir operating rules for a year using multiobjective genetic algorithm (Vol. 10). IWA.
- Tangang, F., Santisirisomboon, J., Juneng, L., Salimun, E., Chung, J., Supari, S., Cruz, F., Ngai, S. T., Ngo-Duc, T., Singhruck, P., Narisma, G., Santisirisomboon, J., Wongsaree, W., Promjirapawat, K., Sukamongkol, Y., Srisawadwong, R., Setsirichok, D., Phan-Van, T., Aldrian, E., Gunawan, D., Nikulin, G., and Yang, H., (2019). Projected future changes in mean precipitation over Thailand based on multi-model regional climate simulations of CORDEX Southeast Asia. 39(14), 5413-5436
- Tangang, F., Supari, S., Chung, J. X., Cruz, F., Salimun, E., Ngai, S. T., Juneng, L., Santisirisomboon, J., Santisirisomboon, J., Ngo-Duc, T., and Phan-Van, T., (2018). Future changes in annual precipitation extremes over Southeast Asia under global warming of 2°C. *APN Science Bulletin*, 8(10), 436
- Trenberth, K., (2011). Changes in Precipitation with Climate Change. *Climate Change*

- Research. *Climate Research*, 47, 123-138
- Trinh, L., Matsumoto, J., Tangang, F., Juneng, L., Cruz, F., Narisma, G., Santisirisomboon, J., Phan-Van, T., Gunawan, D., Aldrian, E., and Ngo-Duc, T., (2019). Application of Quantile Mapping Bias Correction for Mid-future Precipitation Projections over Vietnam.
- Tuyet, N., Thanh, N., and Phan-Van, T., (2019). Performance of SEACLID/CORDEX-SEA multi-model experiments in simulating temperature and rainfall in Vietnam. *VIETNAM JOURNAL OF EARTH SCIENCES*, 41, 374-387
- Ullah, K., and Shrestha, S., (2012). A Decision Support Tool for Selection of Suitable General Circulation Model and Future Climate Assessment. *Journal of Earth Science & Climatic Change*, 03
- Vasiliades, L., (2014). Streamflow simulation methods for ungauged and poorly gauged watersheds. *Natural hazards and earth system sciences*, 2, 32-41
- Villa, R., Rodríguez, M., and Bienvenido, J., (2016). Multiobjective Optimization Modeling Approach for Multipurpose Single Reservoir Operation. *Water*, 10(10), 3390
- Wilby, R. L., and Wigley, T. M. L., (1997). Downscaling general circulation model output: a review of methods and limitations. 21(4), 530-548
- WREA. (2008). Nam Ngum River Basin Profile.
- WREA. (2009). Nam Ngum River Basin Integrated water resources management Plan.
- Xizhi, L., Zuo, Z., Ni, Y., Sun, J., and Wang, H., (2019). The effects of climate and catchment characteristic change on streamflow in a typical tributary of the Yellow River. *Scientific Reports*, 9(1), 14535
- Xu, H., Zhu. (2016). Studies on hydraulic conductivity and compressibility of backfills for soil-bentonite cutoff walls. *Applied Clay Science*, 132-133, 326-335
- Yukimoto, S., Adachi, Y., Hosaka, M., Sakami, T., Yoshimura, H., Hirabara, M., and Tanaka, T. Y., (2012). A New Global Climate Model of the Meteorological Research Institute: MRI-CGCM3: Model Description and Basic Performance. *Journal of the Meteorological Society of Japan*, 9A, 42
- Zhang, S., H., (2005). Rainfall-runoff modelling in a catchment with a complex groundwater flow system: application of the Representative Elementary Watershed (REW) approach. *Hydrol. Earth Syst. Sci.*, 9(3), 243-261



APPENDIX

จุฬาลงกรณ์มหาวิทยาลัย
CHULALONGKORN UNIVERSITY

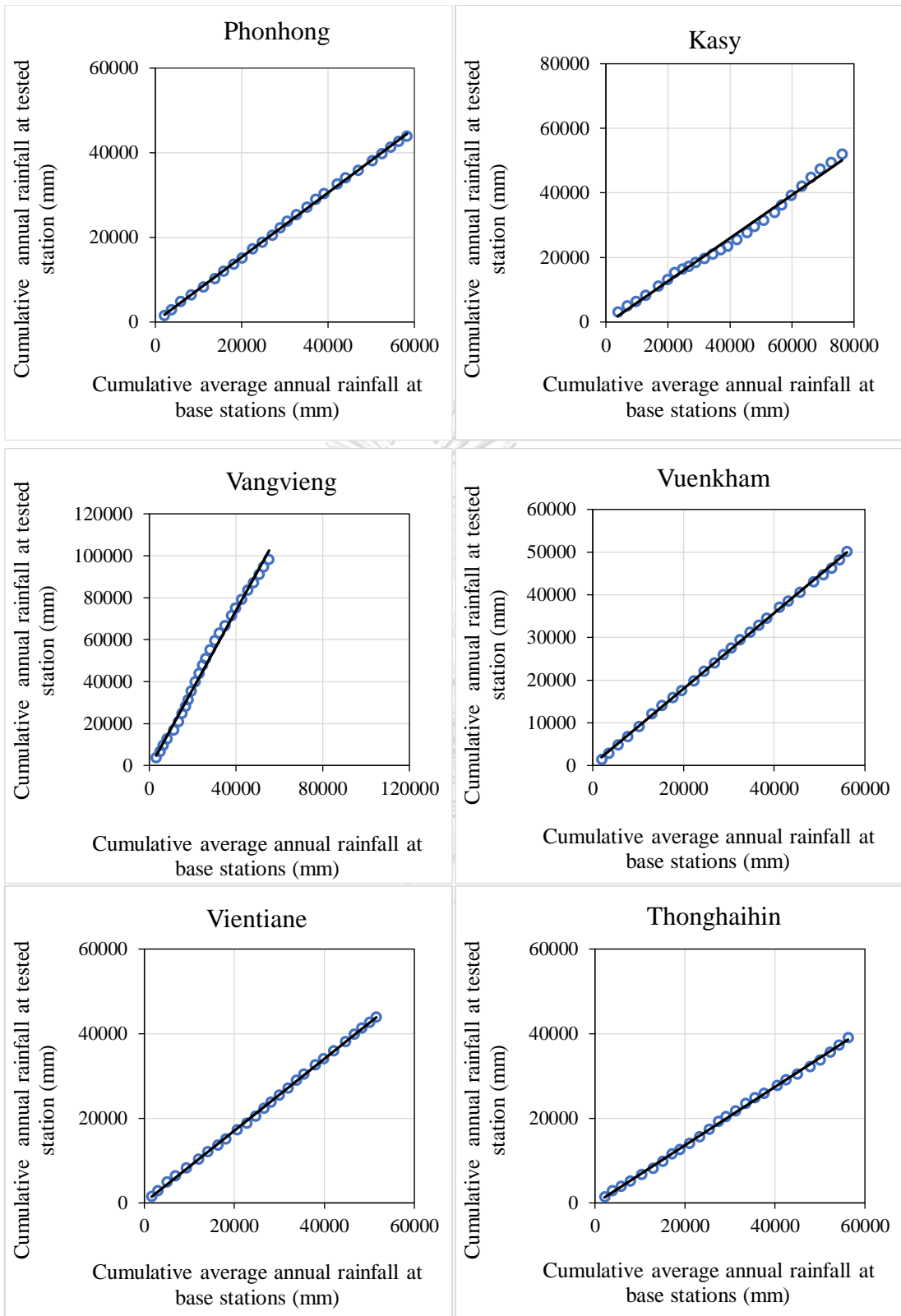
Appendix A

Consistency of the observed rainfall data

The consistency analysis of the observed rainfall data is to assess the initial data quality and to ensure that the rainfall data are reliable before using this data set for this study. The 11 rainfall stations are compared to other stations in terms to carry out the trend of annual rainfall in each station. The double-mass curve method is applied as a tool to check the rainfall data consistency for this study.

Table A-1 Observed rainfall stations within NNRB

No.	Station	Province	Coordinate		Available period
			Latitude	Longitude	
1	Thonghaihin	Xieng Khuang	19.450	101.167	1990-2015
2	Naluang	Vientiane	18.913	103.067	2008-2013
3	Kasy	Vientiane	19.217	102.250	1990-2015
4	Phatang	Vientiane	19.100	102.250	1991-2013
5	Vangvieng	Vientiane	18.923	102.448	1990-2015
6	Hineheup	Vientiane	18.617	102.355	1990-2015
7	Nam Ngum 1	Vientiane	19.533	102.545	1990-2015
8	Phonehong	Vientiane	19.533	102.433	1980-2015
9	Napheng	Vientiane	18.317	102.667	1994-2015
10	Veunkham	Vientiane Capital	18.183	102.617	1990-2015
11	Vientiane	Vientiane Capital	17.928	102.620	1990-2015



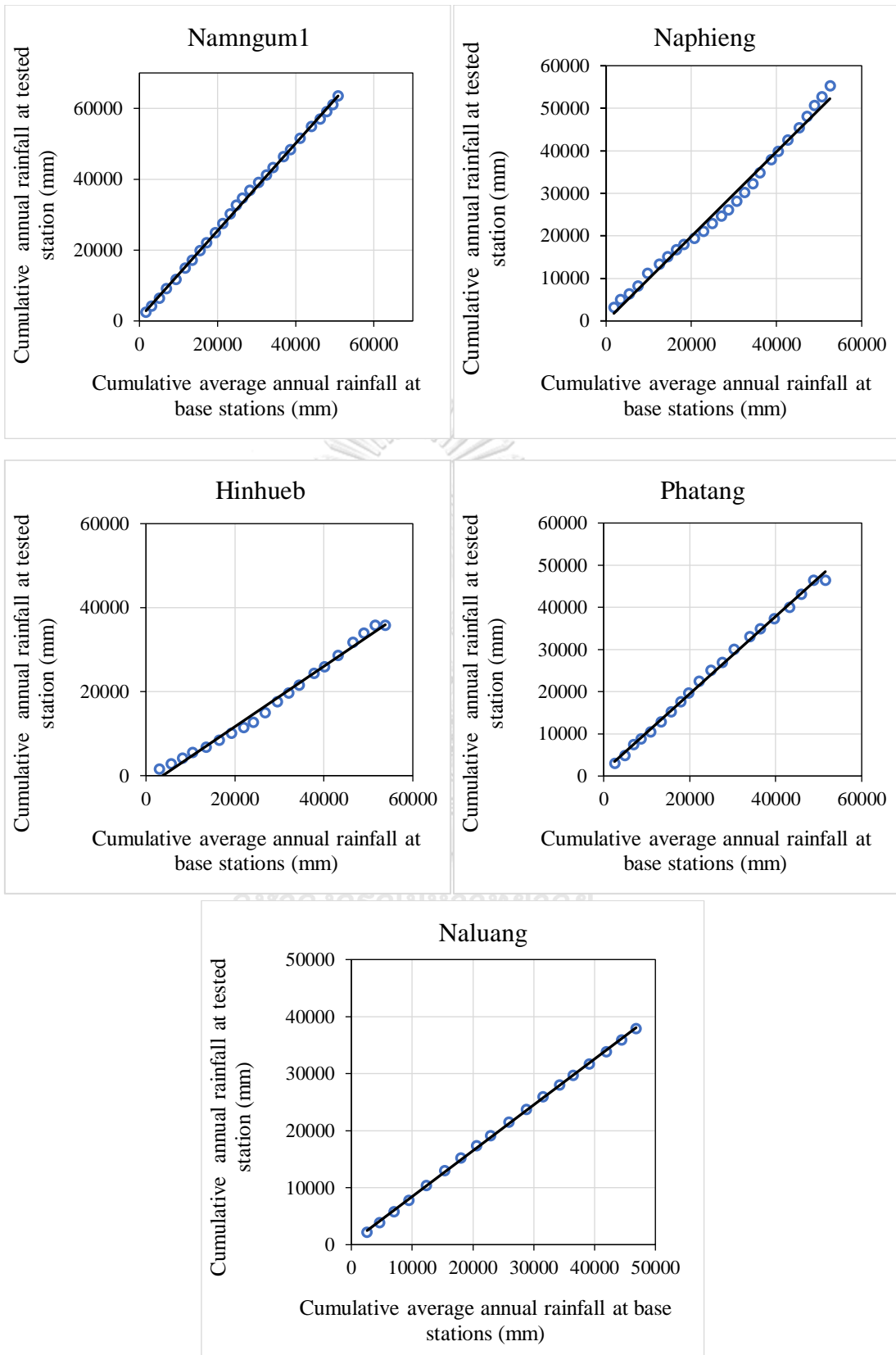


Figure A-1 Consistency of rainfall data within NNRB

Appendix B

Impact of climate change scenarios

B.1. RCM selection

In this study, precipitation from four RCMs, including MPI, IPSL, ICHEC, and NHRCM, were analyzed to determine the model that capture historical patterns of precipitation in the study area. The NHRCM has been developed by MRI, Japan. MPI, IPSL, and ICHEC were developed by the SEACLID/CORDEX-SEA. Table B-1 presents the RCM characteristics. A total of 11 observed rainfall stations over basin were selected to compare with the precipitation from RCMs. The performance of the RCMs was analyzed using statistical parameters including coefficient of determination (R^2), root mean square error (RMSE), Nash–Sutcliffe efficiency (NSE), and standard deviation (SD).

The monthly precipitation presented in Figure B-1 show that the IPSL and NHRCM are generally underestimated while other products are generally overestimated when compared with the observation. In terms of the average monthly precipitation presented in Figure B-2, the average precipitation that contained the most error was found during the rainy season, in which maximum precipitation occurred. The largest overestimation in terms of average and precipitation variation is evident in the ICHEC product. Meanwhile, the MPI has the small error on average precipitation, which is a slight overestimation, especially during the rainy season. Figure B-3 presented that the error ranges from a minimum of -13.6% to a maximum of 104.9% , which occurred in ICHEC followed by NHRCM and IPSL. The minimum error found in MPI ranged from a minimum of -10.1% to a maximum of 24.5% .

Table B-1 The characteristics of RCMs model

Feature	RCM characteristics			
Research Institute	SEACLID/CORDEX-SEA			Meteorological Research Institute (MRI), Japan
Products	MPI	IPSL	ICHEC	NHRCM
Spatial resolution	25km x 25km	25km x 25km	25km x 25km	5km x 5km
Scenarios	Historical: 1995-2005 RCP4.5: 2020-2039 RCP8.5: 2020-2039	Historical: 1995-2005 RCP4.5: 2020-2039 RCP8.5: 2020-2039	Historical: 1995-2005 RCP4.5: 2020-2039 RCP8.5: 2020-2039	Historical: 1995-2000 RCP8.5: 2020-2039

The results in Figure B-4 suggest that the precipitation from the four RCMs can be captured well at low precipitation (<45 mm/month) when compared with the observation. However, it contains large error in high precipitation. In addition, Figure B-5 illustrated that the MPI also performs best when compared with other RCMs with a R^2 of 0.75. Meanwhile, the R^2 of IPSL, NHRCM, and ICHEC are 0.71, 0.68, and 0.65, respectively. In terms of the RMSEs of RCMs, the MPI provides the best performance with a RMSE of 91 mm followed by IPSL, NHRCM, and ICHEC with RMSEs of 123.3, 152.8, and 159 mm, respectively. Moreover, the MPI model performs well in terms of model accuracy with the NSE of 0.72 followed by IPSL, NHRCM, and ICHEC models with the NSE of 0.61, 0.41, and 0.35, respectively.

The terrain of the NNRB is spatially variable. The upper part of the basin is covered by mountainous area, while the lower part is a plain area. This factor likely influences the performance of the RCMs. A relatively coarse-gridded dataset of the RCM model might not adequately represent highly variable precipitation in this area. The analysis shown in Figure B-1 to Figure B-5 suggested that the MPI model outperforms all other models with the highest R^2 and NSE, lowest RMSE, and error in mean. In conclusion, the MPI model is considered a representative RCM model that used for the analysis of optimizing reservoir operations under climate change scenarios in this research.

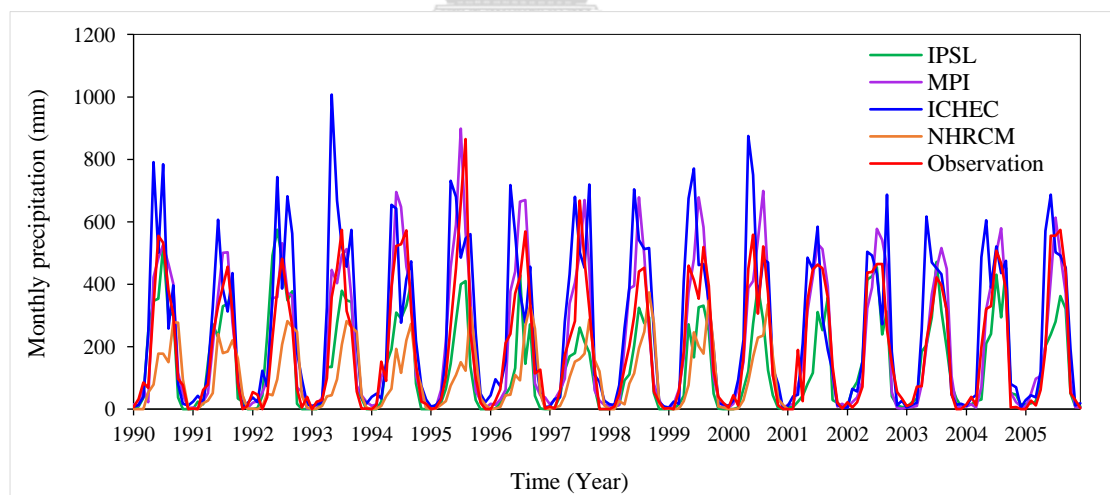


Figure B-1 Comparison of monthly precipitation between RCMs and observation over period of 1990–2005 in NNRB.

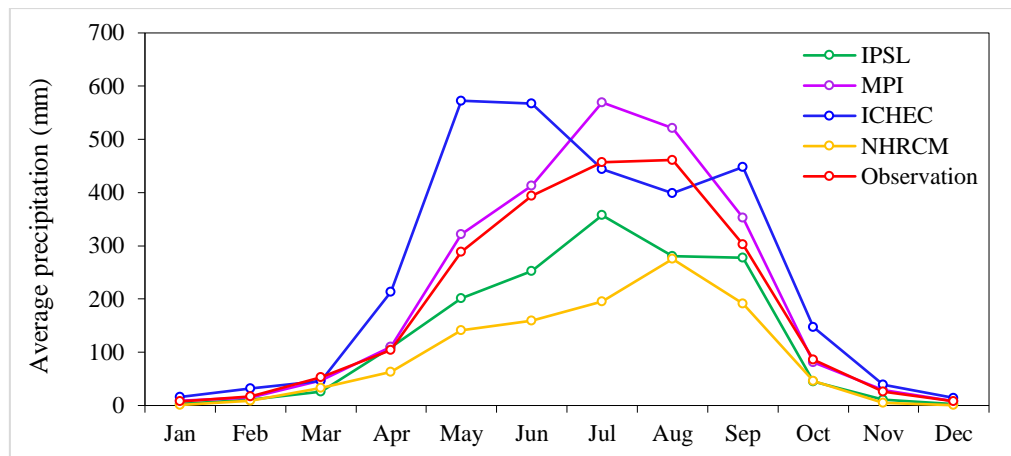


Figure B-2 Comparison of monthly mean precipitation between observation and original RCMs in NNRB (1990–2005).

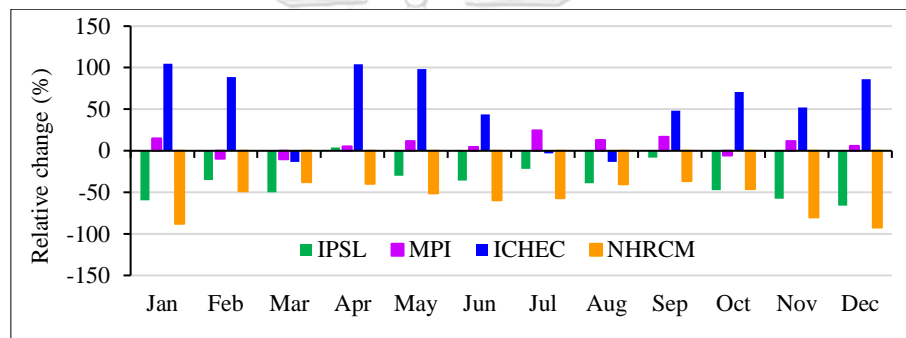


Figure B-3 Relative changes in monthly precipitation from original RCM over the NNRB for the period 1990–2005

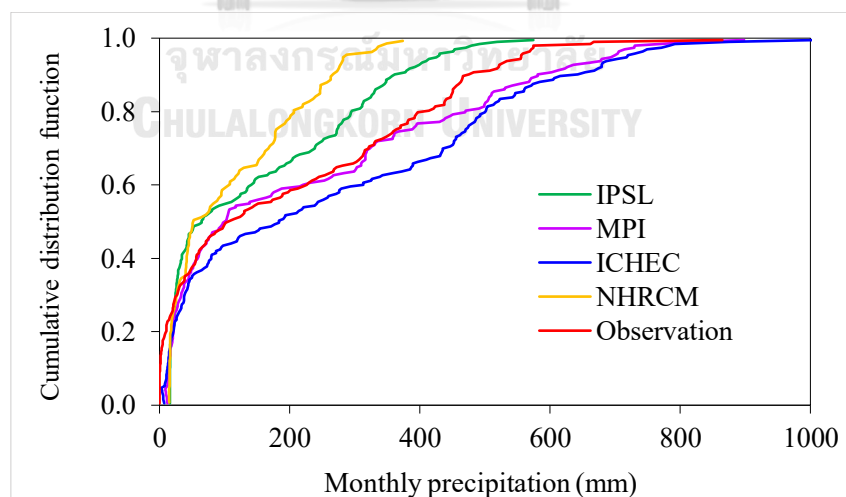


Figure B-4 Cumulative distribution function of monthly precipitation from RCMs and observation during period of 1990–2005

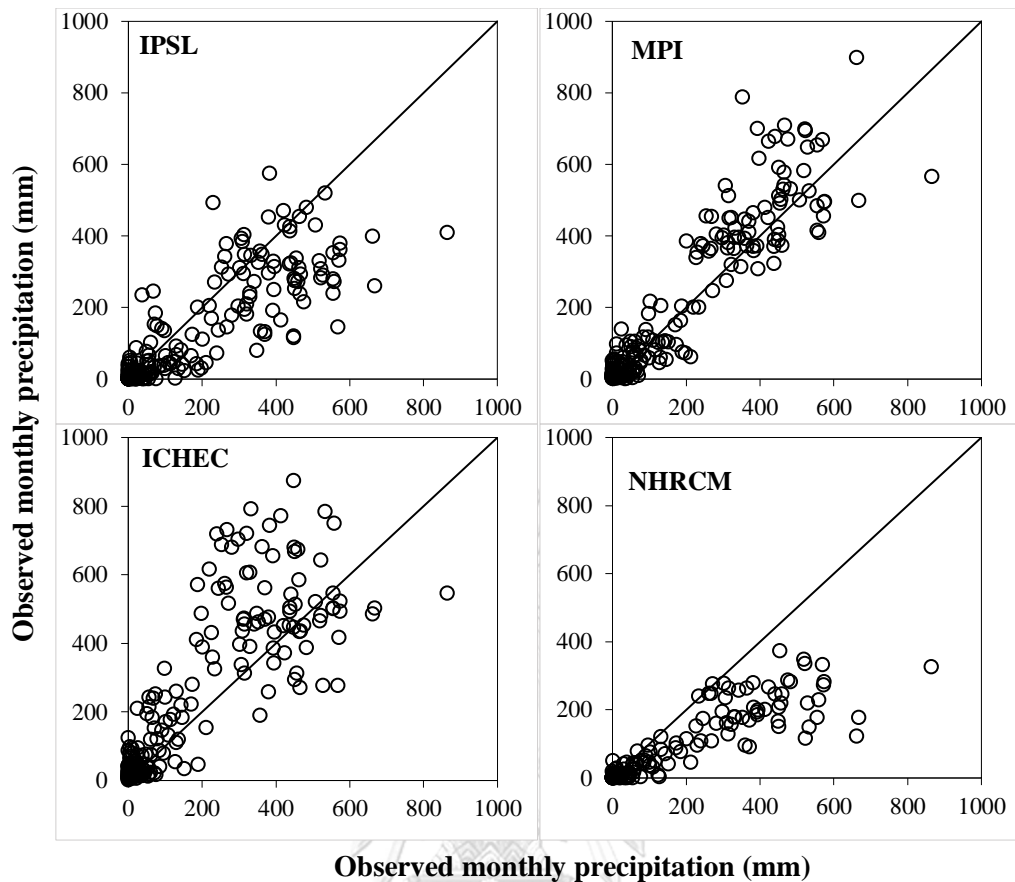


Figure B-5 Relationship between monthly observed and original RCM precipitation in the NNRB over the test period of 1990–2005

B.2. Bias correction

Bias correction is required to reduce systematic bias of climate change projections. In this study, the ratio and quantile mapping (QM) methods were adopted to adjust the bias of precipitation projections in NNRB. Both ratio and QM methods were analyzed in seasonal and monthly time scales. The performance from these two methods were compared on the basis of statistical parameters, including maximum and mean precipitation, R^2 , and NSE. Time series data were divided into four sets: two sets for historical calibration and validation and two sets for future scenarios. The bias correction was tested in the period of 1990–2000. Then, the predictors were used to verify bias precipitation in the period of 2001–2005. The results of bias correction are discussed as follows:

1) Ratio method

In this study, the RCM bias correction using the ratio was classified into seasonal ratio (SR) and monthly ratio (MR). The period used for ratio calculations is 1990–2000. The results show that SR and MR bias correction methods significantly

improve the annual precipitation over the NNRB. The results of SR method presented in Figure B-6 show that precipitation is slightly improved with the reduction of the annual average precipitation by 6.3%. Figure B-7 shows the scatter plot for all months between bias-corrected and observed precipitation. The performance assessed based on R^2 and NSE are 0.75 and 0.71 for dry season and 0.70 and 0.61 for rainy season, respectively. The Figure B-6 also revealed that during dry season (Nov–Apr), the bias correction could reduce errors in mean precipitation, maximum precipitation, and SD by 5.8%, 3.1%, and 4.2%, respectively, when compared with the original RCM. For the rainy season (May–Oct), the bias correction could reduce 6.9% error in mean precipitation, 5.5% for maximum precipitation, and 6.8% for SD. However, the RCM still tends to overestimate monthly precipitation in the NNRB, but some underestimation occurs in May and Jun. These methods still have error in all months when compared with the observed data in the values of RMSE in the dry and wet seasons, which are 24.1 mm and 104.5 mm, respectively. Figure B-6 also illustrated that during the rainy season, the mean, maximum, and SD values of corrected RCM are higher than those of the observation at about 19.0%, 9.6%, and 6.4%, respectively. While in the dry season, the mean, maximum, and SD values of corrected RCM are higher than those of the observation at approximately 13.1%, 6.8%, and 8.7%, respectively. This error might be caused by the limited ability of the ratio method to use too simple scaling factor for wet and dry seasons to capture the bias in highly variable climate regime. The summary of statistical parameter values are presented in Table B-2. The results from the MR method are generally similar to those of the SR method, but with slight improvement. Despite the complexity of the spatial distribution of seasonal precipitation, the bias correction by MR with more values of scaling factor can improve the biased precipitation over NNRB better than the SR method. Figure B-8 shows that the bias correction could reduce error in mean, maximum, and SD of 6.6%, 4.0%, and 6.7%, respectively. Figure B-9 shows the scatter plot for all months between bias-corrected and observed precipitation. In general, the RCM precipitation values are highly similar to the observed values with $R^2 = 0.72$ and $NSE = 0.67$. According to the statistical parameter values shown in Table B-3, the bias correction by MR method is better than the SR method. However, the RCM precipitation still tends to overestimate monthly precipitation.

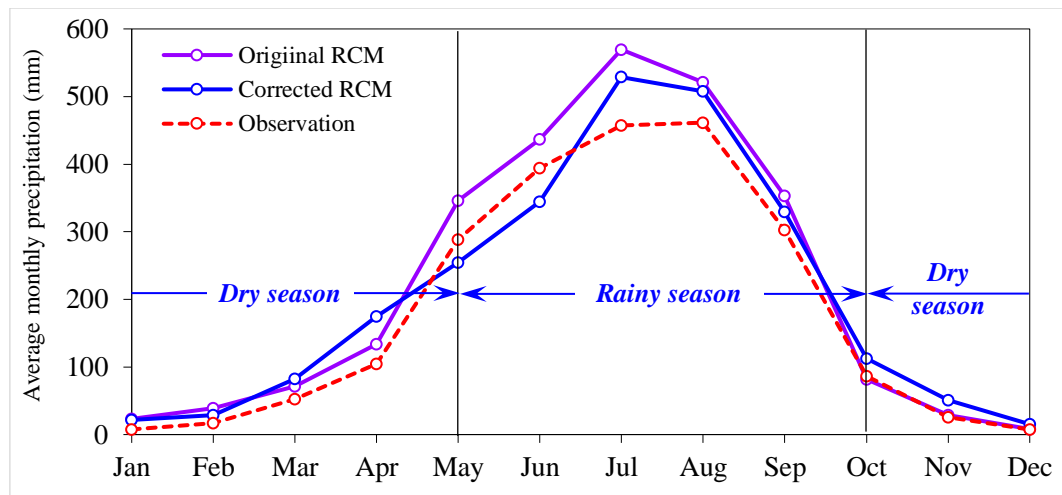


Figure B-6 Comparison of average monthly precipitation from observation, original RCM, and corrected RCM using SR method over the test period of 1990–2000.

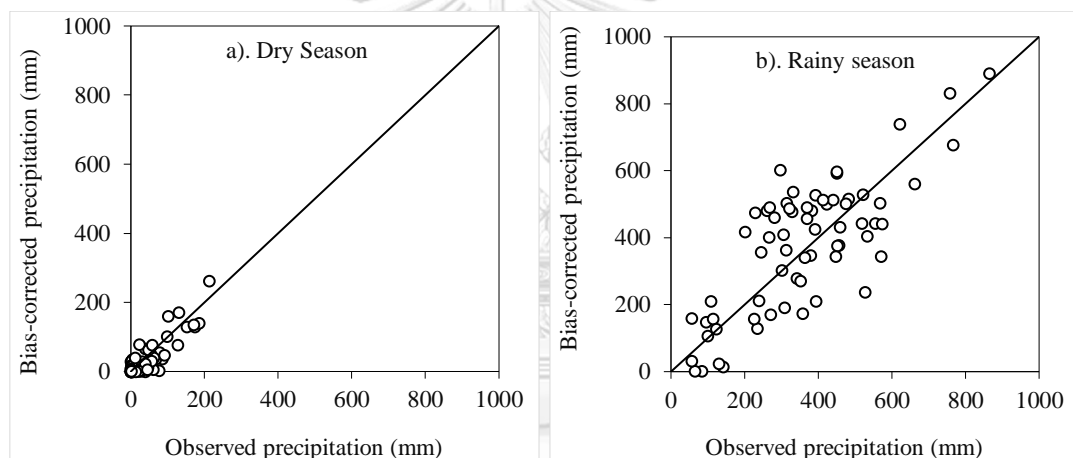


Figure B-7 Relationship between monthly observed precipitation and corrected RCM using SR method over the period of 1990–2000.

Table B-2 Model performance values of SR method over the period of 1990–2000.

Parameter	Observation		Original RCM		Corrected RCM	
	Dry	Rainy	Dry	Rainy	Dry	Rainy
Mean (mm)	38.1	352.4	45.8	450.3	43.1	419.4
Max (mm)	211.9	864.7	233.6	997.3	226.4	942.5
SD (mm)	50.9	162.7	56.6	189.2	54.2	176.4
RMSE (mm)	-	-	30.8	147.7	24.1	104.5
R ²	-	-	0.70	0.62	0.75	0.70
NSE	-	-	0.54	0.48	0.71	0.61

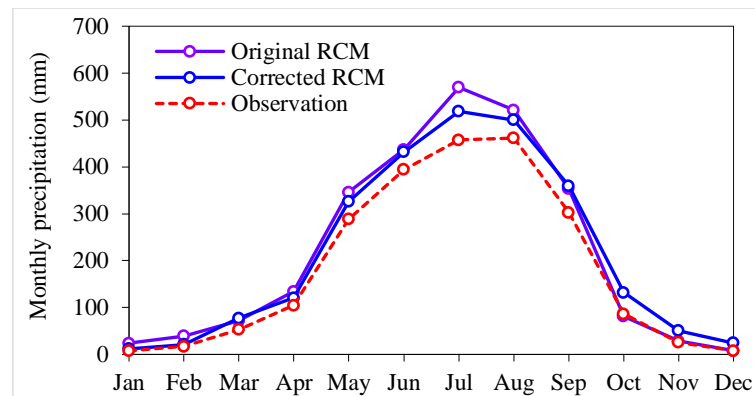


Figure B-8 Comparison of average monthly precipitation from observation, original RCM, and corrected RCM using MR method over the test period of 1990–2000.

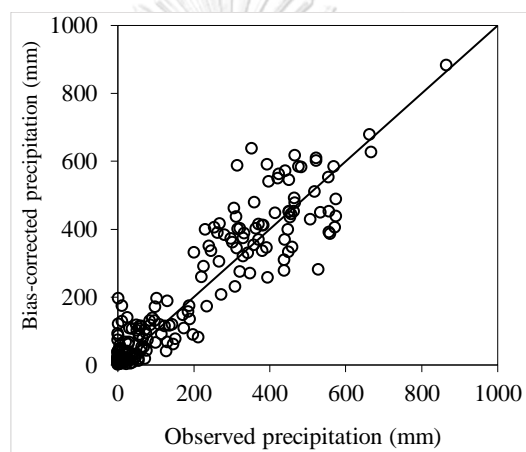


Figure B-9 Relationship between monthly observed precipitation and corrected RCM using MR method over the period of 1990–2000.

Table B-3 Model performance values of MR method over the period of 1990–2000.

Parameter	Observation	Original RCM	Corrected RCM
Mean (mm)	195.3	240.1	223.6
Max (mm)	864.8	895.6	910.2
SD (mm)	198.2	242.9	211.4
RMSE (mm)	-	108.8	83.2
R ²	-	0.64	0.72
NSE	-	0.52	0.67

2) Quantile Mapping (QM) method

QM method was carried out at two timescales, including seasonal QM (SQM) and monthly QM (MQM). The results suggested that both QM methods significantly improved monthly RCM precipitation over the NNRB. The overestimation of the

annual average precipitation could be reduced by both QM methods. The results from SQM are presented in Figure B-10, which shows that RCM precipitation is improved with 6.9% reduction in the annual average precipitation. Figure B-11 shows the relationship between observed and bias-corrected precipitation based on SQM method. The SQM method yielded $R^2 = 0.70$ and $NSE = 0.54$ for dry season and $R^2 = 0.62$ and $NSE = 0.48$ for rainy season. When compared with the original RCM, SQM can reduce biases in mean (7.9%), maximum (5.2%), and SD (5.9%) of precipitation in dry season. For rainy season, SQM reduces 8.8% in mean, 7.2% in maximum, and 7.3% in SD of precipitation. The RMSE values are 22.8 mm/month for dry season and 95.3 mm for rainy season. The results also indicated that during dry and rainy seasons, the mean, maximum, and SD of corrected RCM remain higher than those of observed precipitation, as presented in the Table B-4.

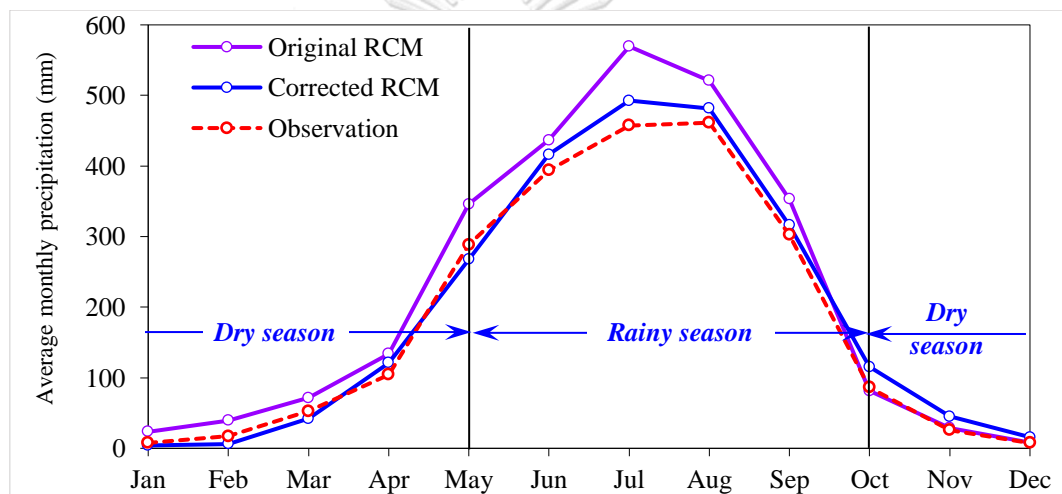


Figure B-10 Comparison of average monthly precipitation from observation, original RCM, and corrected RCM using SQM method over the test period of 1990–2000

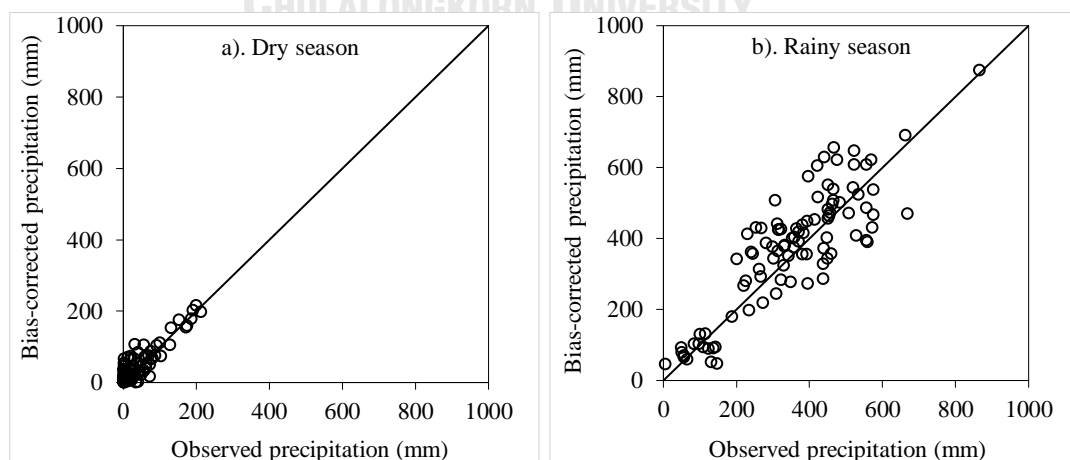


Figure B-11 Relationship between monthly observed precipitation and corrected RCM using SQM method over the period of 1990–2000

Table B-4 Model performance values of SQM method over the period of 1990–2000

Parameter	Observation		Original RCM		Corrected RCM	
	Dry	Rainy	Dry	Rainy	Dry	Rainy
Mean (mm)	38.1	352.4	45.8	450.3	42.2	410.7
Max (mm)	211.9	864.7	233.6	997.3	221.5	925.4
SD (mm)	50.9	162.7	56.6	189.2	53.3	175.4
RMSE (mm)	-	-	30.8	147.7	22.8	95.3
R ²	-	-	0.70	0.62	0.78	0.65
NSE	-	-	0.54	0.48	0.72	0.59

The results obtained from the MQM method are similar to those from the SQM method but with an improvement. The values of $R^2 = 0.72$ and $NSE = 0.67$ when compared with the observation data (Figure B-13). Figure B-13 shows the relationship between observed precipitation and corrected RCM from SQM. Figure B-12 shows that the MQM can reduce the biases in mean, maximum, and SD of 6.6%, 4.0%, and 6.7%, respectively, when compared with the original RCM. The RMSE value is 42.4 mm/month. The results also show that the mean, maximum, and SD of corrected RCM are still higher than the observation in some months, as presented in Table B-5. Table B-5 illustrates that the MQM method slightly outperforms the SQM method in bias reduction.

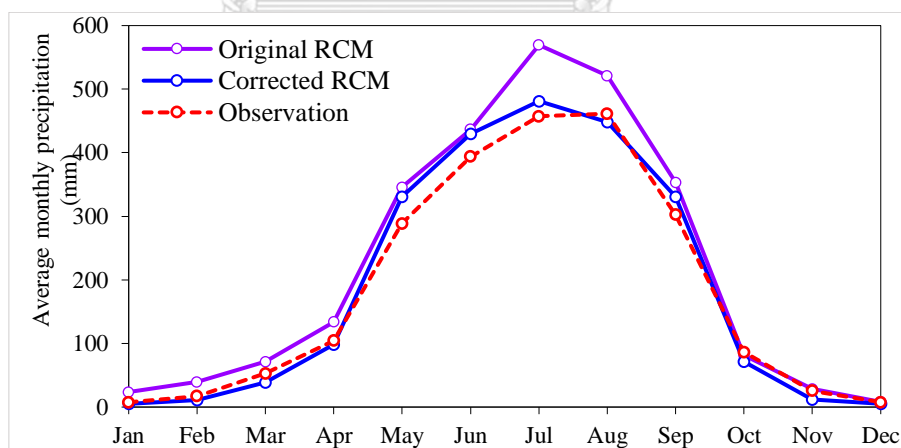


Figure B-12 Comparison of average monthly precipitation from observation, original RCM, and corrected RCM using MQM method over the test period of 1990–2000

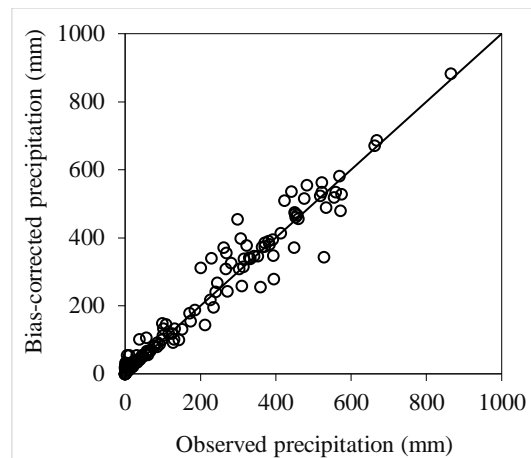


Figure B-13 Relationship between monthly observed precipitation and corrected RCM using MQM method over the period of 1990–2000

Table B-5 Model performance values of MQM method over the period of 1990–2000

Parameter	Observation	Original RCM	Corrected RCM
Mean (mm)	195.3	240.1	201.3
Max (mm)	864.8	895.6	898.9
SD (mm)	198.2	242.9	206.3
RMSE (mm)	-	108.8	42.4
R ²	-	0.64	0.83
NSE	-	0.52	0.75

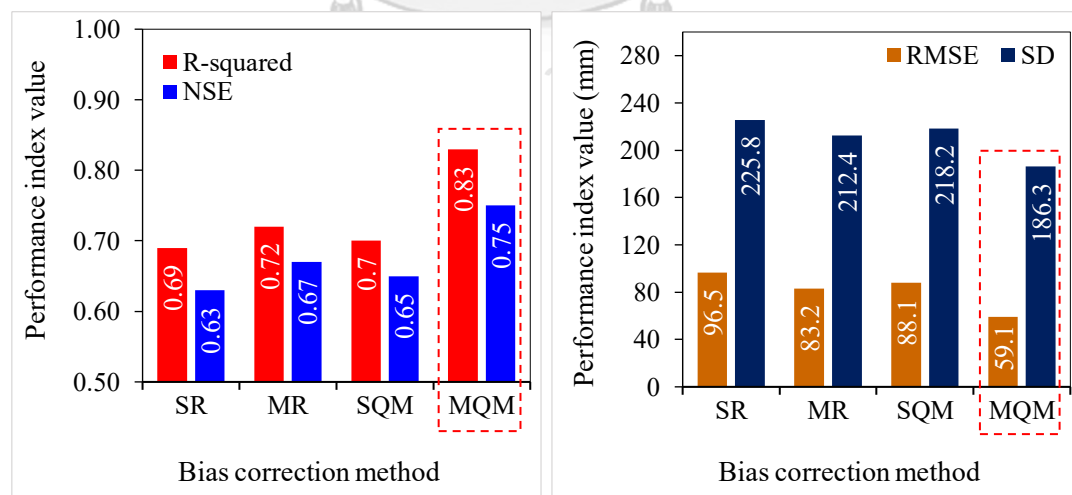


Figure B-14 Comparison of bias correction performances

The precipitation of MPI was bias corrected using four bias correction methods. Different methods show variable performance assessed on the basis of statistical parameters, as shown in Figure B-14. The MQM provided reasonably the best

performance. In conclusion, the MQM method is selected for correcting the bias of future RCM precipitation projections in NNRB because it yielded the highest R^2 and NSE values and the lowest RMSE and SD values.

B.3. MQM verification

To verify the MQM method, the best model predictor set obtained from the test period of 1990–2000 is used to correct the bias precipitation in different periods of 2001–2005. The average monthly corrected bias precipitation between 2001 and 2005 is shown in Figure B-15. The results illustrated that the MQM method could effectively reduce biases in RCM precipitation when compared with the original RCM. Figure B-16 shows the scatter plot for all months between bias-corrected and observed precipitation. In general, the value of RCM precipitation is close to the observation with $R^2 = 0.78$ and $NSE = 0.72$. Notably, the period of data for verification is slightly short and might not cover the variability of high and low precipitation in NNRB. This method must be tested in future precipitation to check the performance and obtain reliable corrected future precipitation. However, the use of MQM verification performance for further analysis is sufficient because its statistical performance indices are similar to the best values obtained during the test period.

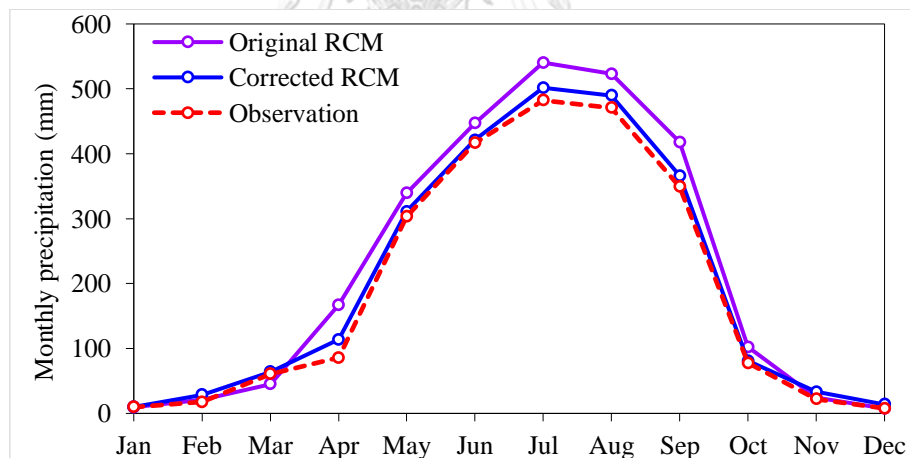


Figure B-15 Comparison of average monthly precipitation from observation, original RCM, and corrected RCM using MQM method over the test period of 2001–2005

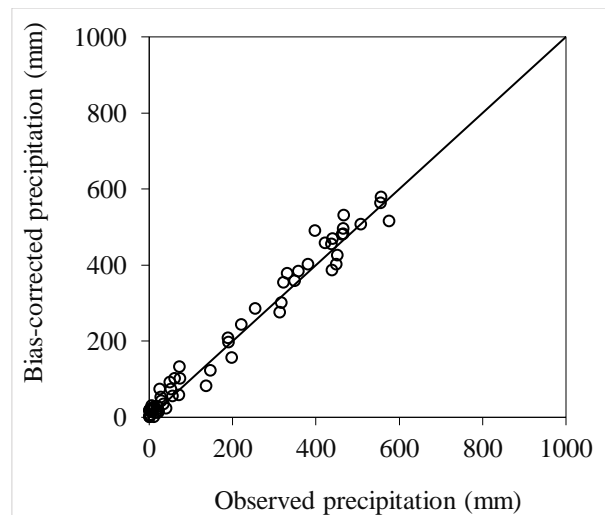


Figure B-16 Relationship between monthly observed precipitation and corrected RCM using MQM method over the period of 2001–2005

Table B-6 Model performance values of MQM method over the period of 2001–2005

Parameter	Observation	Original RCM	Corrected RCM
Mean (mm)	192.0	195.94	213.8
Max (mm)	574.5	578.85	608.8
SD (mm)	196.3	199.19	213.6
RMSE (mm)	-	47.3	30.5
R ²	-	6.82	0.78
NSE	-	5.45	0.72

The MQM method was also applied with near future monthly data under RCP4.5 and RCP8.5 scenarios (Figure B-17). The results from the bias correction method was less than the original RCM data because the bias correction reduced the mean, maximum, and SD precipitation by 22.1mm, 26.3mm, and 19.4 mm for RCP4.5 and by 29.4mm, 35.5mm, and 20.7mm for RCP8.5 scenarios, respectively. The mean, maximum, and SD precipitation in wet months is usually higher than those in the dry months for both scenarios. The error for RCP8.5 is higher than that of RCP 4.5 for all months. However, the future RCM precipitation still tends to overestimate monthly precipitation, especially in wet months, and underestimate in some dry months (Nov to Feb) when compared with the observation data.

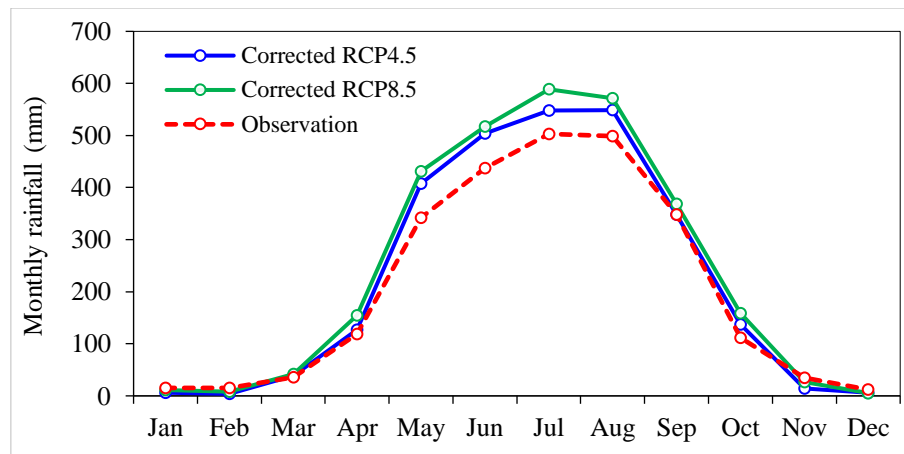


Figure B-17 Comparison of average monthly precipitation from observation and corrected RCM using MQM method over the near future period

Table B-7 Model performance values of MQM method over the near future period

Parameter	RCP4.5		RCP8.5	
	Original	Corrected	Original	Corrected
Mean (mm)	242.6	227.5	263.1	243.7
Max (mm)	784.3	765.2	889.1	862.6
SD (mm)	253.9	239.5	248.5	231.8

B.4. Future precipitation scenarios

MPI model under RCP4.5 and RCP8.5 scenarios during the period of 20 years in the future is selected for this research. The comparison of the total increase in the annual precipitation of RCP4.5 and RCP8.5 between the observed and RCM shows in Figure B-18. In the historical and future time period, the approximate annual precipitation has a five-year cycle change. With regard to the NNRB, RCP4.5 and RCP8.5 climate scenarios revealed that precipitation will increase by 8.2% and 17.4%, respectively. Figure B-19 shows the monthly precipitation in the future period over the NNRB under RCP4.5 and RCP8.5 scenarios. The minimum precipitation of both scenarios is recorded in the first year of near future and tends to increase to the maximum in the 11th year of near future in all time periods. According to Figure B-20, the average monthly precipitation was higher than the observation in nearly all months under both scenarios, except January and December. In terms of seasons, future precipitation during the rainy season period (May–Oct) under RCP4.5 and RCP8.5 was increasing largely. During the dry season period (Nov–Apr), the precipitation is higher than the observed values in Jan and Dec for RCP4.5 and slightly less than the observed precipitation in Mar for RCP8.5. For the maximum

precipitation, the observation and RCPs show similar maximum precipitation in Jul and Aug, especially for observation and RCP4.5. For the SD revealed that the result from RCP8.5 is slightly higher than RCP4.5 scenario when compares to the observation. Figure B-21 presents the near future changes in the monthly mean precipitation of RCM compared with the observation (1990–2015). This figure illustrated that the precipitation in RCP4.5 and RCP8.5 scenarios changes from -12.2% to 19.2% and from -15.6% to 25.0%, respectively. Earlier study found that the differences in the amount of precipitation may be caused by the RCP8.5, which greatly increases the greenhouse gas emissions over time. Generally, RCP8.5 is considered the worst case of climate change and provides the overestimation of projected precipitation. RCP4.5 is characterized as a stabilization scenario of climate change by using climate policy to reduce greenhouse gas emissions (San José et al., 2016).

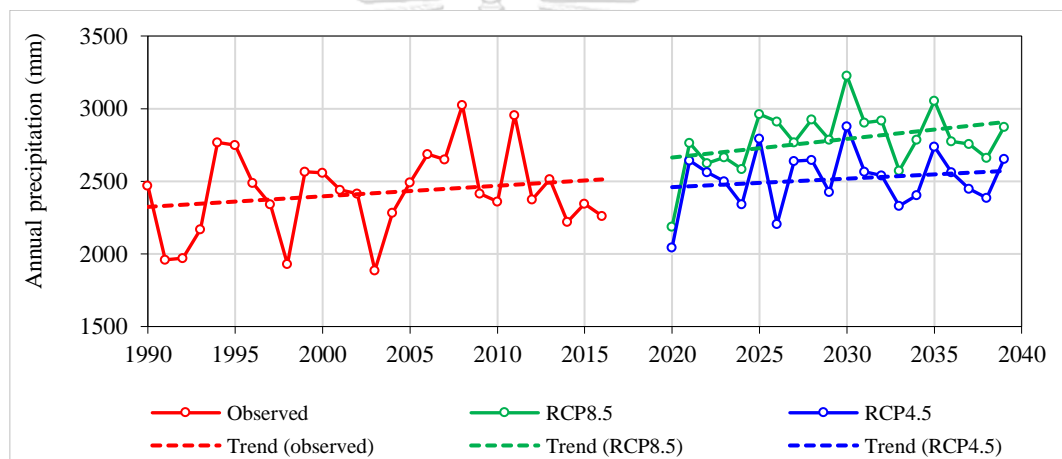


Figure B-18 Comparison of annual precipitation from observation (1990–2015) and future RCM scenarios over the near future period

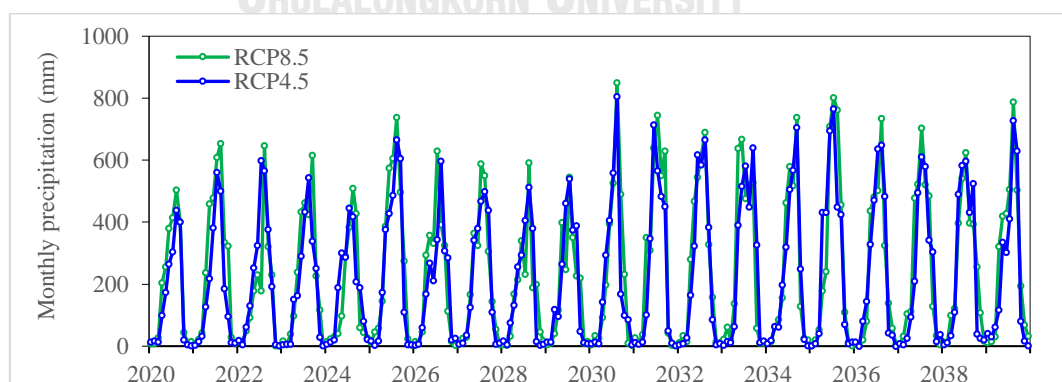


Figure B-19 Monthly precipitation of future RCM scenarios over the near future period

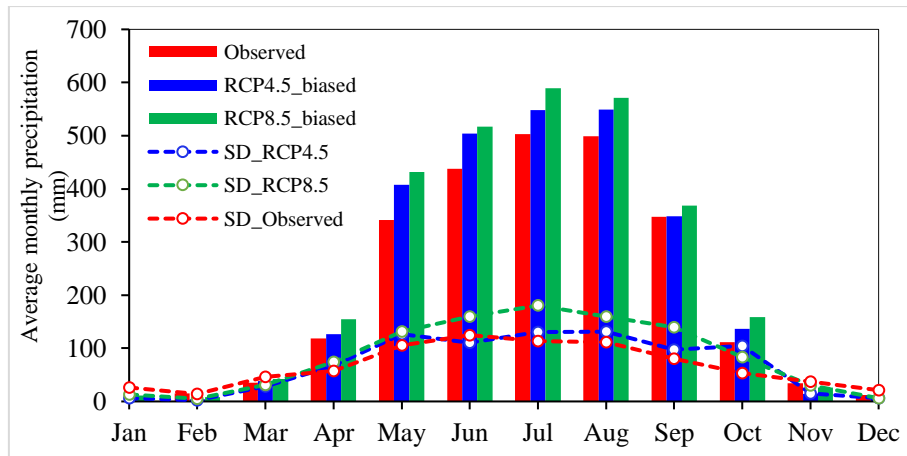


Figure B-20 Comparison of average monthly precipitation from observation (1990–2015) and future RCM over the near future period

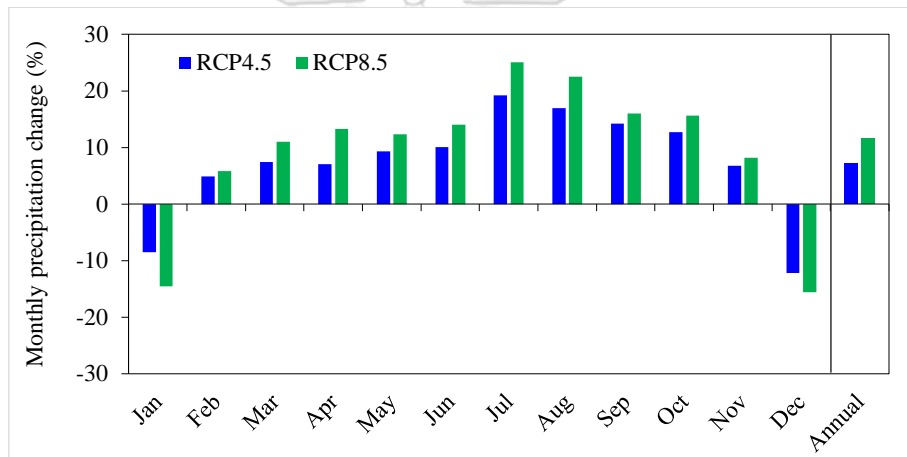


Figure B-21 Future change in monthly mean precipitation of RCM over the near future period compared to observation (1990–2015)

Appendix C

Streamflow prediction

The simulated scenarios are based on the observed rainfall and precipitation from the RCM data to represent the present and future scenarios. The procedure of streamflow prediction is shown in Figure C-1.

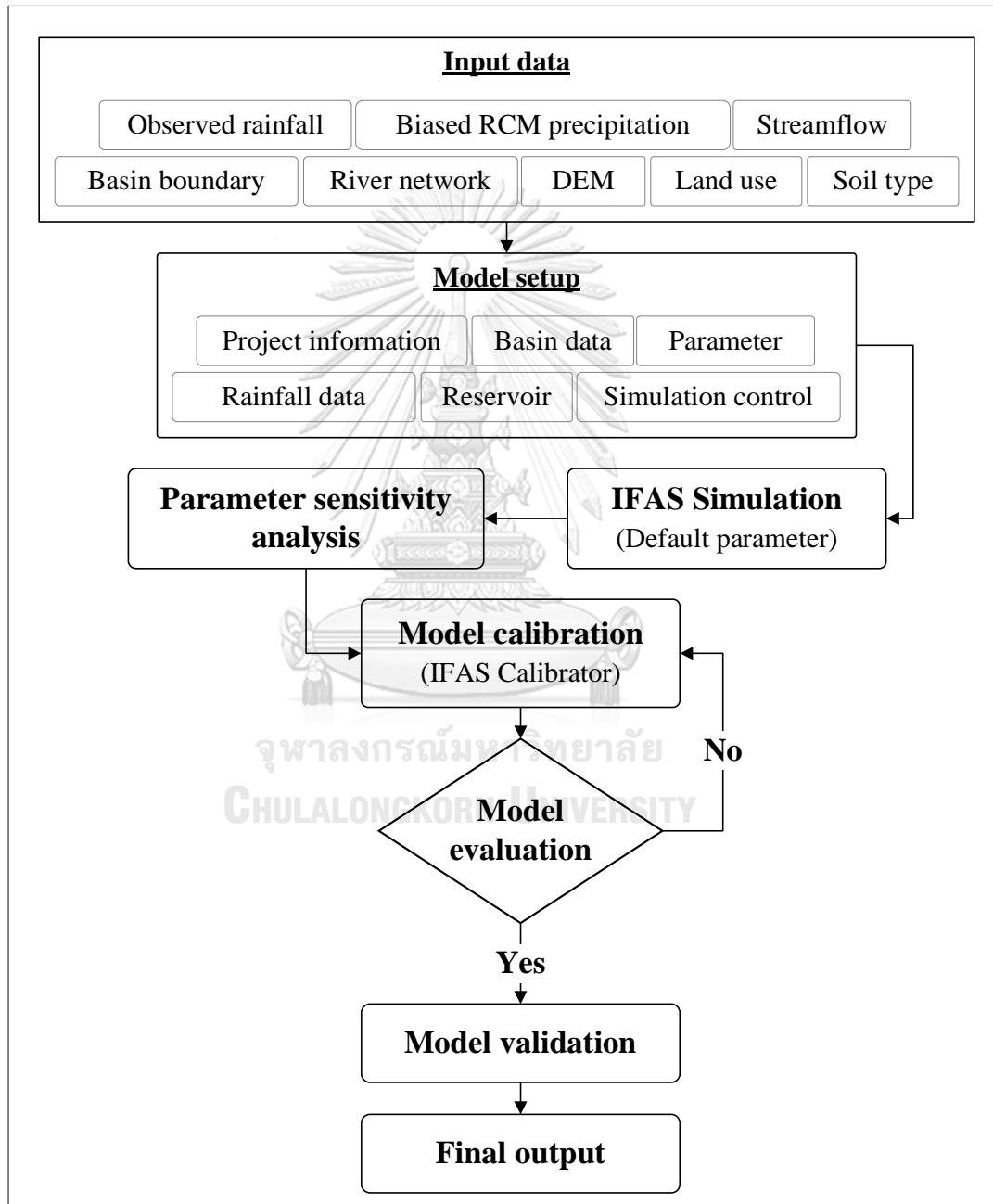


Figure C-1 Streamflow simulation procedure of IFAS model

C.1. Model setup

As mentioned briefly in Chapter 2, IFAS is a physically-based model that requires specific data and information about the study area to represent the complexity of basin hydrological characteristics. Its minimum data requirements include the observed rainfall or precipitation from RCMs or satellite precipitation data, observed streamflow, reservoir fixed outflow rate, land use, soil type, digital elevation model, river network, and basin boundary.

The project information manager comprises the setting part of the target basin information, cell size, and simulation time interval. The DEM and land use data are also included in this part, which can be downloaded using the download function. For this study, the NNRB is selected as the target area, the cell size is a 2 km grid. DEM is based on Hydro 1k obtained from the US Geological Survey, and the land use data are obtained from the global land cover characterization.

The basin data manager creates the basin, sub-basin boundary, and river course network on the basis of the DEM data. The results from this part should be compared with the actual data through the significant function. The grid cell size should be adjusted until the results reach an acceptable agreement. The basin, sub-basin boundary, and river course network are established in Figure C-2.

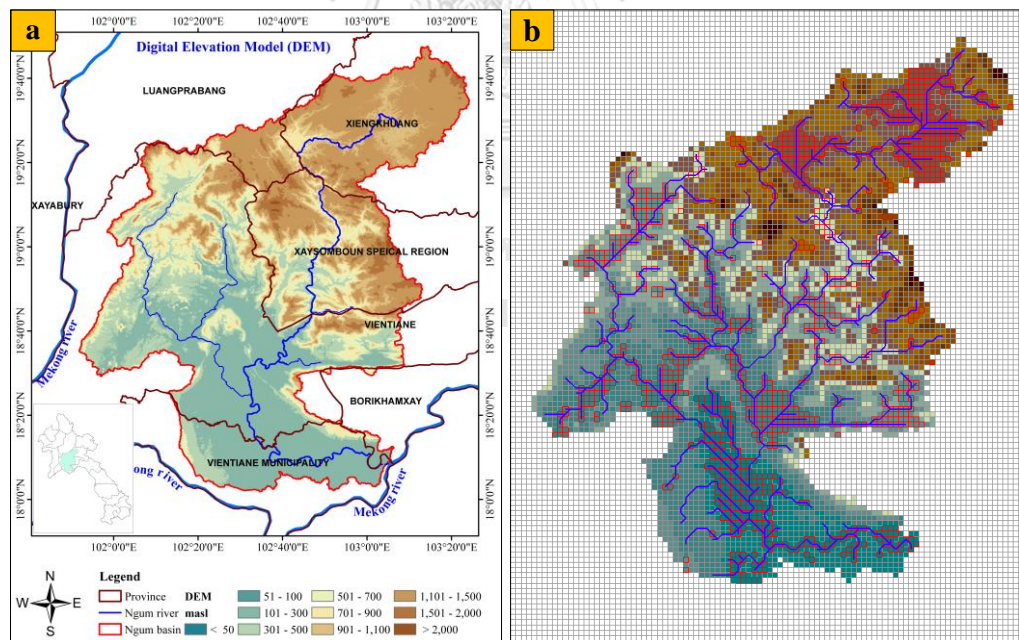


Figure C-2 The basin boundary and river course network of NNRB, a) Actual area from ArcGIS, b) Generated area from IFAS

The rainfall data manager comprises the setting part of the rainfall information. The rainfall data for IFAS can be input by importing observed rainfall data and downloading satellite rainfall data. In this study, the observed rainfall data are selected. The Thiessen polygon method is applied as rainfall interpolation for this research.

The IWRM controller in IFAS refers to the reservoir operation data of each reservoir in the research area. IFAS contains three operation methods: the fixed-rate, fixed value, and combined methods. The fixed value method is selected for the IWRM controller in this study.

The parameter setting part is critical for the runoff calculation analysis. The parameter setting in IFAS contains the surface, aquifer, and river course parameters. These parameters are classified on the basis of the imported geospatial data. IFAS has set the default parameter values, and the parameters can be edited to match with the actual study area.

C.2. Parameter sensitivity analysis

The sensitivity analysis determines the influence of the parameters on the study area streamflow. The analysis of the model parameter sensitivity were tested in 2005. The trial and error method is used as the sensitivity analysis technique in this study. The sensitivity analysis is based on the nine parameters presented in Table C-1. The analysis is done by fixing eight parameter values and adjusting one parameter value by 25% increments from the mean value. Then, a comparison between the streamflow simulation output and the observed data will be performed. The total flow and peak flow will be compared. The same process is performed with the other eight parameters. The sensitivity level can be divided into high, middle, and low. The high sensitivity parameter indicates that the change in the parameter value can increase the streamflow. By contrast, the low sensitivity parameter can decrease the streamflow (Ranatunga et al., 2017).

C.3. Model calibration and validation

After the sensitivity analysis, the most sensitive parameter set related to the streamflow simulation is selected. The parameter values are not optimized. Thus, calibration is necessary to adjust the parameter values. The model calibration process is conducted in daily and monthly time-series from 1990 to 2005. The IFAS calibrator and trial and error techniques determine the optimum values of the model parameters. The model calibration performance is assessed by statistical indices, including R² and NSE. The guideline of the model parameter calibration is listed in Table C-1.

After the model simulated the good results, the optimal parameter values can be applied to validate the streamflow simulation in other periods. The model validation

aims to modify the optimal parameter values from the calibration process. This process is critical to confirm that these values can be used to simulate streamflow in different periods. The model validation process is conducted in daily and monthly time-series from 2006 to 2015 in the same catchment.

Table C-1 Feature for parameter of surface, aquifer, and river course model

Parameter	Description	Range	Unit
Surface tank parameters			
SKF	Final infiltration capacity	0.0001- 0.1	cm/s
SNF	Roughness coefficient of ground surface	0.005-2.0	m ^{-1/3} /s
HFMXD	Maximum water height	0.015- 0.18	m
HFMND	Height where rapid intermediate flow occurs	0.0005- 0.01	m
HFOD	Height where ground infiltration occurs	0.0001-0.005	m
FALFX	Coefficient of rapid intermediate outflow	0.0-1.0	-
Aquifer tank parameters			
AGD	Coefficient of base outflow	0.0001-1.0	1/day
HCGD	Height where slow intermediate flow occurs	0.0-5.0	m
River course tank parameters			
RNS	Manning's roughness coefficient	0.01-0.35	m ^{-1/3} /s

The observed data in the period of 16 years (1990–2005) were used for model calibration, whereas the data in the period of 10 years (2006–2015) were used for model validation. The observed streamflow from the Hinhueb station was used to compare and evaluate the model accuracy. The parameters must be adjusted to obtain the parameter set that is most sensitive to the observed streamflow. The NS catchment was selected for model calibration. Then, the optimal parameters will be verified for the NP, NB, NSan, and NL catchments, which are the sub-basins of the NNRB Figure C-3. Moreover, these parameters were verified to simulate the inflow into NN3 reservoir for future scenarios.

The optimal values of the parameters are also applied to simulate streamflow for a future period. This process aims to assess the impact of climate change on streamflow. The future streamflow simulation process is conducted in daily and monthly time-series of 20 years, which starts from five years ahead from observation data.

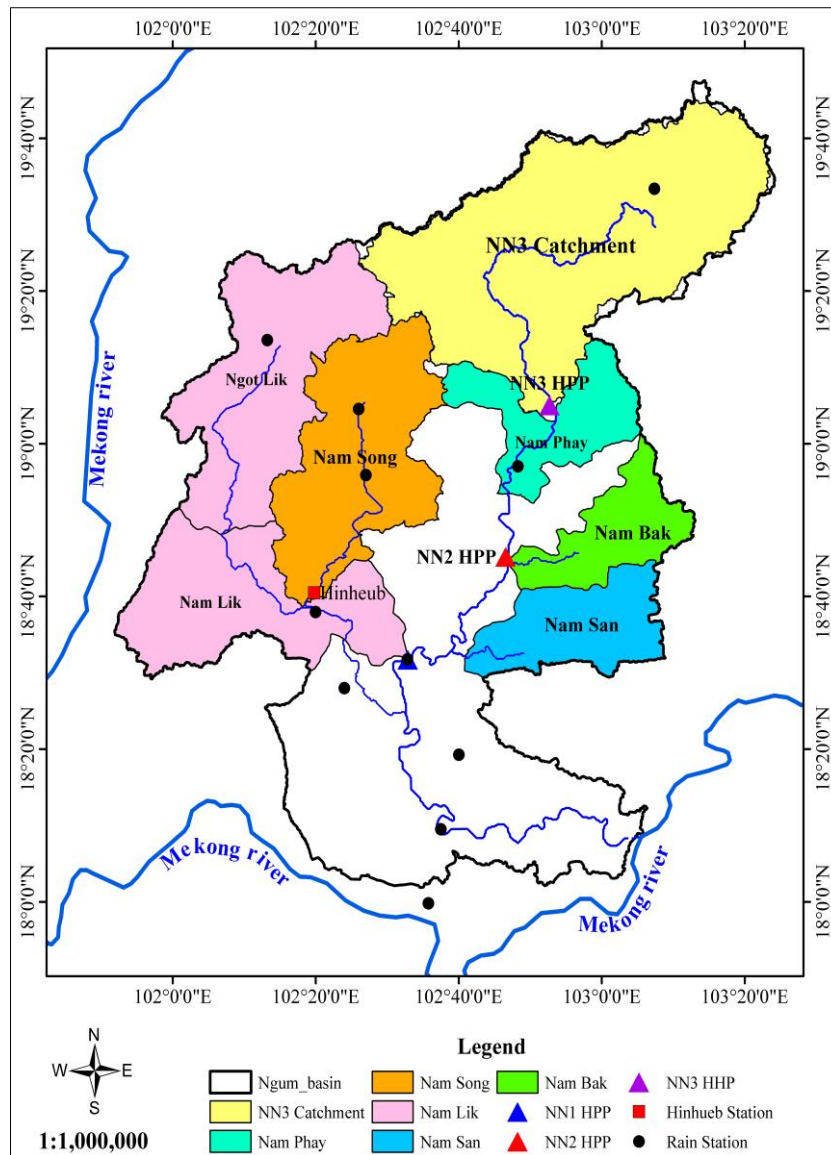


Figure C-3 Sub-catchments diagram in the NNRB.

Table C-2 The guideline of the model parameters calibration of IFAS

Parameter	Change	Guideline
SKF	Increase	Increasing storage height of aquifer layer tank. This is effective in case to increase flood hydrograph in recession period or delaying peak since this increases discharge from aquifer layer tank.
	Decrease	Storage height of surface tank increases. Because of the increased outflow from groundwater tank, it is effective to enlarge the rise of wave form and/or delay the peak.
SNF	Increase	Delaying speed of overland flow. Whether peak discharge decreases or not depends on discharge from the tank and topography and land-use.
	Decrease	Surface outflow becomes fast. Whether or not the peak flow will become big depends on the flow from tank, landform, and land use.
HFMXD	Increase	Surface outflow becomes slow. Whether or not the peak flow will become small depends on the flow from tank, landform, and land use.
	Decrease	Accelerating generation of overland flow. Whether peak discharge increases or not depends on discharge from the tank and topography and land-use.
HFMND	Increase	Decreasing flood hydrograph in increment period. Delaying generation of peak discharge.
	Decrease	Increasing flood hydrograph in increment period. Accelerating generation of peak discharge.
HFOD	Increase	Decreasing overall flood hydrograph. Increasing water volume not to discharge
	Decrease	Increasing overall flood hydrograph. In case of 0, all rainfall exchanges to discharge.
FALFX	Increase	Increasing flood hydrograph in increment period.
	Decrease	Decreasing flood hydrograph in increment period.
AGD	Increase	Increasing base flow.
	Decrease	Decreasing base flow.
HCGD	Increase	Decreasing flood hydrograph in recession period. Delaying peak discharge.
	Decrease	Increasing flood hydrograph in recession period. Accelerating peak discharge.
RNS	Increase	Decreasing amount of flow in river channel
	Decrease	Increasing amount of flow in river channel

Table C-3 Hydraulic conductivity values by bed material group

Bed material group	Bed material characteristics	Hydraulic conductivity (mm/hr.)
Very high loss rate	Very clean gravel and large sand	> 127
High loss rate	Clean sand and gravel, field conditions	51 - 127
Moderate high loss rate	Sand and gravel mixture with low silt-clay content	25 - 76
Moderate loss rate	Sand and gravel mixture with high silt-clay content	6 - 25
Insignificant to loss rate	Consolidated bed material; high silt-clay content	0.025 - 2.5

Source: (Xu, 2016)

Table C-4 Hydraulic conductivity by soil texture

Soil texture	Hydraulic conductivity (m/day)
Gravel coarse sand	10 - 50
Medium sand	1 - 5
Sandy loam, fine sand	1 - 3
Loam, clay loam, clay (well structured)	0.5 - 2
Very fine sandy loam	0.2 - 0.5
Clay loam, clay (poorly structured)	0.002 - 0.2
Dense clay (no cracks, pores)	< 0.002

Source: (Merli and Capatti, 2016)

Table C-5 Hydraulic conductivity by material types

Material type	Hydraulic conductivity (cm/s)
Clay	$10^{-9} - 10^{-6}$
Silt, sand silts, clayey sand, till	$10^{-6} - 10^{-4}$
Silt sands, fine sands	$10^{-5} - 10^{-3}$
Well-sorted sands, glacial outwash	$10^{-3} - 10^{-1}$
Well-sorted gravel	$10^{-2} - 1$

Source: (Merli and Capatti, 2016)

Table C-6 Hydraulic conductivity by material types

Material type	Hydraulic conductivity (cm/s)
Gravel, coarse	150
Gravel, medium	270
Gravel, fine	450
Sand, coarse	45
Sand, medium	12
Sand, fine	2.5
Silt	0.08
Clay	0.0002
Sandstone, fine-grained	0.2
Sandstone, medium-grained	3.1
Limestone	0.49
Dolomite	0.001
Dune sand	20
Loess	0.08
Peat	57
Schist	0.2
Slate	0.00008
Till, predominantly sand	0.49
Till, predominantly gravel	30
Tuff	0.2
Basalt	0.01
Gabbro, weathered	0.2
Granite, weathered	14

Source: (Zhang, 2005)

Table C-7 Manning's n values for channel flow

Type of channel	Minimum	Normal	Maximum
Natural streams - minor streams (top width at flood stage < 100 ft)			
1. Main Channels			
clean, straight, full stage, no rifts or deep pools	0.025	0.03	0.033
same as above, but more stones and weeds	0.03	0.035	0.04
clean, winding, some pools and shoals	0.033	0.04	0.045
same as above, but some weeds and stones	0.035	0.045	0.05
same as above, lower stages, more ineffective slopes and sections	0.04	0.048	0.055
with more stones	0.045	0.05	0.06
sluggish reaches, weedy, deep pools	0.05	0.07	0.08
very weedy reaches, deep pools, or floodways with heavy stand of timber and underbrush	0.075	0.1	0.15
2. Mountain streams, no vegetation in channel, banks usually steep, trees and brush along banks submerged at high stages			
a. bottom: gravels, cobbles, and few boulders	0.03	0.04	0.05
b. bottom: cobbles with large boulders	0.04	0.05	0.07
3. Floodplains			
a. Pasture, no brush			
short grass	0.025	0.03	0.035
high grass	0.03	0.035	0.05
b. Cultivated areas			
no crop	0.02	0.03	0.04
mature row crops	0.025	0.035	0.045
mature field crops	0.03	0.04	0.05
c. Brush			
scattered brush, heavy weeds	0.035	0.05	0.07
light brush and trees, in winter	0.035	0.05	0.06
light brush and trees, in summer	0.04	0.06	0.08
medium to dense brush, in winter	0.045	0.07	0.11
medium to dense brush, in summer	0.07	0.1	0.16
d. Trees			
dense willows, summer, straight	0.11	0.15	0.2
cleared land with tree stumps, no sprouts	0.03	0.04	0.05
same as above, but with heavy growth of sprouts	0.05	0.06	0.08
heavy stand of timber, a few down trees, little undergrowth, flood stage below branches	0.08	0.1	0.12
same as 4. with flood stage reaching branches	0.1	0.12	0.16

Table C-8 Manning's n values for channel flow (cont.)

Type of channel	Minimum	Normal	Maximum
4. Excavated or Dredged Channels			
a. Earth, straight, and uniform			
clean, recently completed	0.016	0.018	0.02
clean, after weathering	0.018	0.022	0.025
gravel, uniform section, clean	0.022	0.025	0.03
with short grass, few weeds	0.022	0.027	0.033
b. Earth winding and sluggish			
no vegetation	0.023	0.025	0.03
grass, some weeds	0.025	0.03	0.033
dense weeds or aquatic plants in deep channels	0.03	0.035	0.04
earth bottom and rubble sides	0.028	0.03	0.035
stony bottom and weedy banks	0.025	0.035	0.04
cobble bottom and clean sides	0.03	0.04	0.05
c. Dragline-excavated or dredged			
no vegetation	0.025	0.028	0.033
light brush on banks	0.035	0.05	0.06
d. Rock cuts			
smooth and uniform	0.025	0.035	0.04
jagged and irregular	0.035	0.04	0.05
e. Channels not maintained, weeds and brush uncut			
dense weeds, high as flow depth	0.05	0.08	0.12
clean bottom, brush on sides	0.04	0.05	0.08
same as above, highest stage of flow	0.045	0.07	0.11
dense brush, high stage	0.08	0.1	0.14
5. Lined or Constructed Channels			
a. Cement			
neat surface	0.01	0.011	0.013
mortar	0.011	0.013	0.015
b. Wood			
planed, untreated	0.01	0.012	0.014
planed, creosoted	0.011	0.012	0.015
unplanned	0.011	0.013	0.015
plank with battens	0.012	0.015	0.018
lined with roofing paper	0.01	0.014	0.017
c. Concrete			
trowel finish	0.011	0.013	0.015
float finish	0.013	0.015	0.016
finished, with gravel on bottom	0.015	0.017	0.02
unfinished	0.014	0.017	0.02
good section	0.016	0.019	0.023
wavy section	0.018	0.022	0.025
on good, excavated rock	0.017	0.02	
on irregular excavated rock	0.022	0.027	

Table C-9 Manning's n values for channel flow (cont.)

Type of channel	Minimum	Normal	Maximum
d. Concrete bottom float finish with sides of:			
dressed stone in mortar	0.015	0.017	0.02
random stone in mortar	0.017	0.02	0.024
cement rubble masonry, plastered	0.016	0.02	0.024
cement rubble masonry	0.02	0.025	0.03
dry rubble or riprap	0.02	0.03	0.035
e. Gravel bottom with sides of:			
formed concrete	0.017	0.02	0.025
random stone mortar	0.02	0.023	0.026
dry rubble or riprap	0.023	0.033	0.036
f. Brick			
glazed	0.011	0.013	0.015
in cement mortar	0.012	0.015	0.018
g. Masonry			
cemented rubble	0.017	0.025	0.03
dry rubble	0.023	0.032	0.035
h. Dressed ashlar/stone paving			
	0.013	0.015	0.017
i. Asphalt			
smooth	0.013	0.013	
rough	0.016	0.016	
j. Vegetal lining			
	0.03		0.5

Source: (Chow, 1959 cited by (Seree Chanyotha, 2013))

Table C-10 Manning's n values for overland flow

Channel characteristics	Median	Range
Fall, no residue	0.010	0.008 - 0.012
Conventional tillage, no residue	0.090	0.06 - 0.12
Conventional tillage, residue	0.190	0.16 - 0.22
Chisel plow, no residue	0.090	0.06 - 0.12
Chisel plow, residue	0.130	0.1 - 0.16
Fall disking, residue	0.400	0.3 - 0.5
No till, no residue	0.070	0.04 - 0.1
No till, 0.5-1 t/ha residue	0.120	0.07 - 0.17
No till, 2-9 t/ha residue	0.300	0.17 - 0.47
Rangeland, 20% cover	0.600	0.45 - 0.73
Shot grass prairie	0.150	0.1 - 0.2
Dense grass	0.240	0.17 - 0.3
Bermuda grass	0.410	0.3 - 0.48

Source: (Milad Jajarmizadeh, 2012)

Table C-11 Manning's n values for channel flow

Channel characteristics	Median	Range
Excavated or dredged		
Earth, straight and uniform	0.025	0.016 - 0.333
Earth, winding and sluggish	0.35	0.023 - 0.050
Not maintained, weeds and brush	0.075	0.040 - 0.140
Natural streams		
Few tree, stone or brush	0.05	0.025 - 0.065
Heavy timber and brush	0.1	0.050 - 0.150

Source: (Ayvaz, 2013)

C.4. Results of streamflow prediction

C.4.1. Parameter sensitivity analysis

Sensitive parameters on total flow and peak flow for sensitivity value change of $\geq 0.05\%$ was selected. The results of changes in the sensitivity values of parameters were presented in Table C-12. The seven most sensitive parameters influenced the total flow and peak flow in the NNRB, except HFMND and HFOD. The most sensitive parameters for streamflow prediction were SKF, RNS, and SNF. AGD, HFMXD, and HCGD were characterized as middle sensitive compared with SKF, RNS, and SNF but more sensitive than FALFX, which was characterized as low sensitive. The summary of the final sensitive parameters on total flow and peak flow are listed in Table C-13.

Table C-12 Sensitive parameter on total flow and peak flow

Parameter	Unit	Parameter range	Parameter (mean)	25% Increment	Change (%)	
					Total flow	Peak flow
RNS	$m^{-1/3} / s$	0.01-0.35	0.170	0.213	-24.8	-15.2
SKF	cm/s	0.0001-0.1	0.050	0.062	-8.33	-11.7
SNF	$m^{-1/3} / s$	0.005-2.0	0.998	1.247	-7.47	-9.35
AGD	1/day	0.0001-1.0	0.050	0.062	4.10	3.82
HFMXD	m	0.1-1.0	0.450	0.563	2.35	2.13
HCGD	m	0.0-5.0	2.500	3.125	-1.82	-1.51
FALFX	-	0.0-1.0	0.500	0.625	0.88	1.24
HFMND	m	0.0005-0.01	1.000	1.250	-0.02	-0.01
HFOD	m	0.0001-0.005	0.002	0.003	0.00	0.00

Table C-13 Final parameter sensitivity from for streamflow calibration

Parameter	Description	Sensitive level
RNS	Manning's roughness coefficient	high
SKF	Final infiltration capacity	high
SNF	Roughness coefficient of ground surface	high
AGD	Coefficient of base outflow	middle
HFMXD	Maximum storage height	middle
HCGD	Height where intermediate outflow occurs	middle
FALFX	Coefficient of rapid intermediate outflow	low

C.4.2. Model calibration results

After the sensitivity analysis, the most sensitive parameter sets related to the streamflow prediction were selected, the model calibration process were conducted in daily and monthly timeseries for a period of 1990–2005. The daily mean areal rainfall over the NNRB was estimated using Thiessen polygon method based on the time series data recorded by 11 rain gauges. Two methods, namely, automatic calibration using IFAS calibrator and manual calibrations, were adopted to carry out the optimum values of the model parameters.

1) Daily streamflow prediction

The daily streamflow prediction in NNRB was calibrated with the dataset of 1995, 1996, and 2004 wet years. The reason is that the results of the optimum values of parameters will be applied to obtain the future high streamflow, which is inputted into the optimization model under flood condition. The hydrograph of daily observed versus simulated streamflow was presented in Figure C-4. The model can simulate daily streamflow in wet years with a good match with the observed daily streamflow at the basin outlet, especially in high streamflow. The scatter plot between daily observed and simulated streamflow given in Figure C-5 demonstrated that the model successfully simulates daily streamflow at the basin outlet with reasonable accuracy. The statistical indicators presented a regression between daily observed and simulated streamflow with NSE of 0.69 and R^2 of 0.75. However, the results illustrated that the model has slightly overestimated the streamflow. This phenomenon may probably be due to the land-use changes in this period, which contributed to why the rainfall came faster than usual, and that the river has a small baseflow. The optimal values of the parameter set from daily calibration given in Table C-14 will be applied for the daily streamflow validation of NP, NB, NSan, NL, and NN3 catchments.

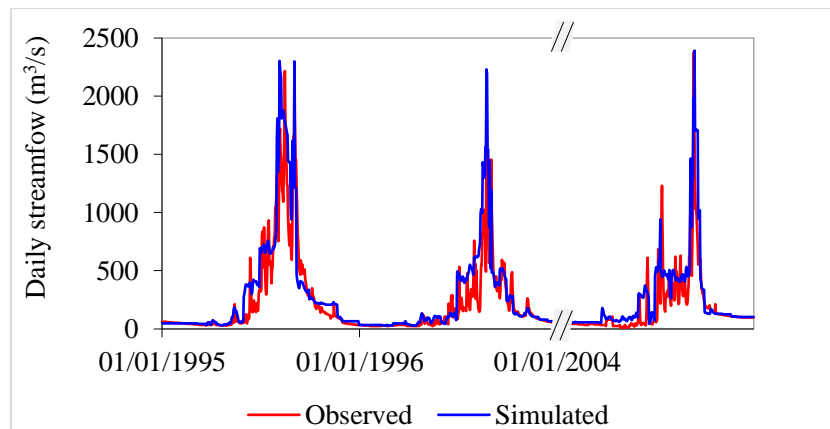


Figure C-4 Daily streamflow from IFAS model calibration compares with observation at Hinhueb station.

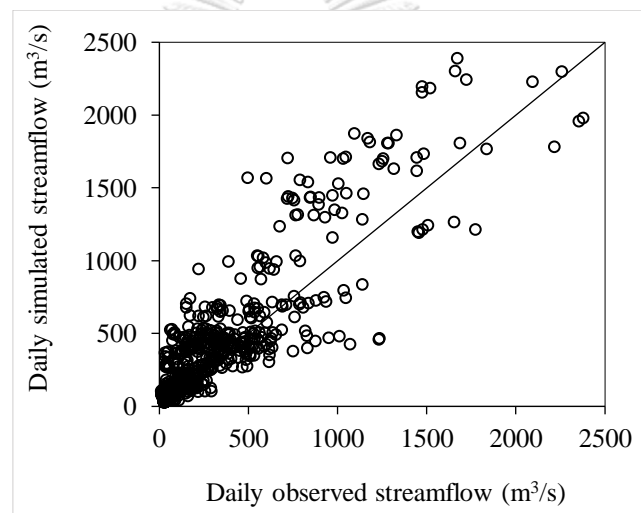


Figure C-5 Correlation between simulated and observed daily streamflow of calibration at Hinhueb station.

Table C-14 Optimal parameter values of daily streamflow calibration

Parameter	Description	Parameter range	Optimal value	Unit
RNS	Manning's roughness coefficient	0.01- 0.35	0.035	$m^{-1/3} /s$
SKF	Final infiltration capacity	0.0001- 0.1	0.051	cm/s
SNF	Roughness coefficient of ground surface	0.01- 2.0	0.58	$m^{-1/3} /s$
AGD	Coefficient of base outflow	0.0001- 1.0	0.0035	1/day
HFMXD	Maximum storage height	0.1- 1.0	0.01	m
HCGD	Height where slow intermediate outflow occurs	0.0 - 5.0	0.285	m
FALFX	Regulation coefficient of rapid intermediate outflow	0.0 - 1.0	0.001	-

2) Monthly streamflow prediction

The monthly streamflow prediction in NNRB was calibrated with 16 years dataset of 1990–2005. Figure C-6 presented that the observed and simulated hydrographs of monthly streamflow followed the pattern similar to the daily simulation, and low flow was better. The result given in Figure C-6 also demonstrated that the monthly streamflow prediction was better with the improvement of NSE and R^2 to 0.78 and 0.84, respectively. The scatter plot between monthly observed and simulated streamflow given in Figure C-7 showed very good agreement. However, the model has slightly failed to capture the peak flow in few years during the calibration period. The optimal values of the parameter set from the monthly calibration given in Table C-15 will be applied for the monthly streamflow validation of NB and NSan catchments.

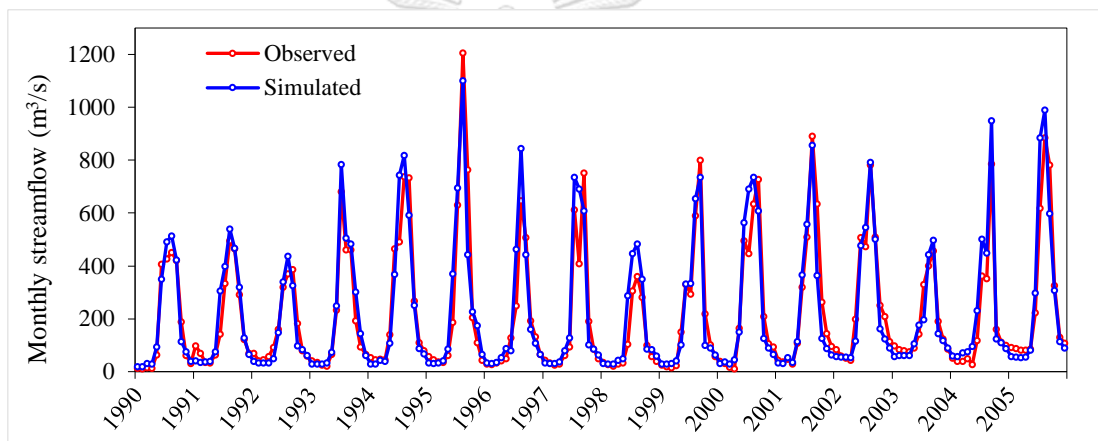


Figure C-6 Monthly streamflow from IFAS model calibration compares with observation at Hinhueb station

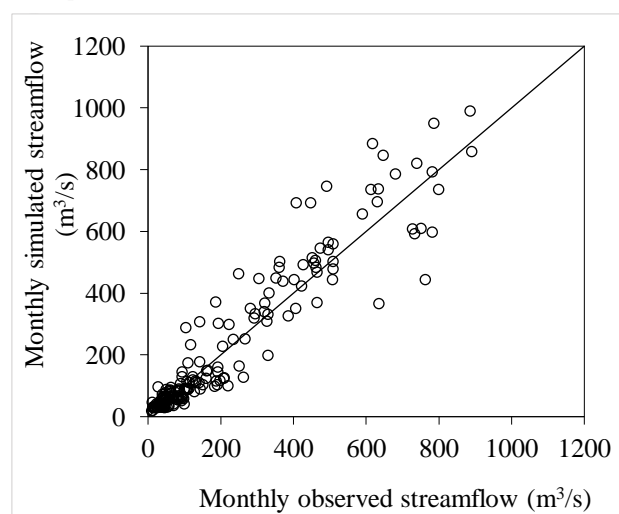


Figure C-7 Correlation between simulated and observed monthly streamflow of calibration at Hinhueb station

Table C-15 Optimal parameter values of monthly streamflow calibration

Parameter	Description	Parameter range	Unit	Optimal value
RNS	Manning's roughness coefficient	0.01- 0.35	m ^{-1/3} /s	0.035
SKF	Final infiltration capacity	0.0001- 0.1	cm/s	0.055
SNF	Roughness coefficient of ground surface	0.01- 2.0	m ^{-1/3} /s	0.65
AGD	Coefficient of base outflow	0.0001- 1.0	1/day	0.0035
HFMXD	Maximum storage height	0.2- 1.0	m	0.01
HCGD	Height where slow intermediate outflow occurs	0.0 - 5.0	m	0.285
FALFX	Regulation coefficient of rapid intermediate outflow	0.0 - 1.0	-	0.001

C.4.3. Model validation results

Daily and monthly calibrated model parameters from Table C-14 and Table C-15 were validated with other observed streamflow time series of 2006–2015. The model validation results of daily and monthly streamflow predictions at the basin outlet were discussed as follows:

1) Daily streamflow prediction

The daily streamflow prediction was validated with the wet years dataset of 2008 and 2011, wherein large flood occurred in the center of Laos. The daily streamflow validation result presented in Figure C-8 showed that the model could simulate daily streamflow with a good match with the observed daily streamflow at the basin outlet in high and low streamflow. Figure C-9 shows the scatter plot between daily observed and simulated streamflow. The model successfully simulates daily streamflow reliably. The result also demonstrated that the model validation was acceptable based on NSE and R² of 0.68 and 0.71, respectively.

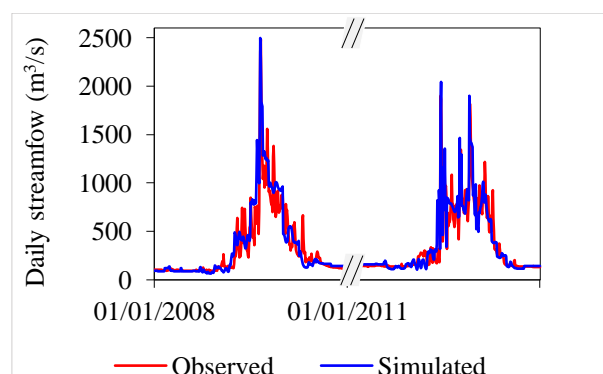


Figure C-8 Daily streamflow from IFAS model validation compares with observation at Hinhueb station

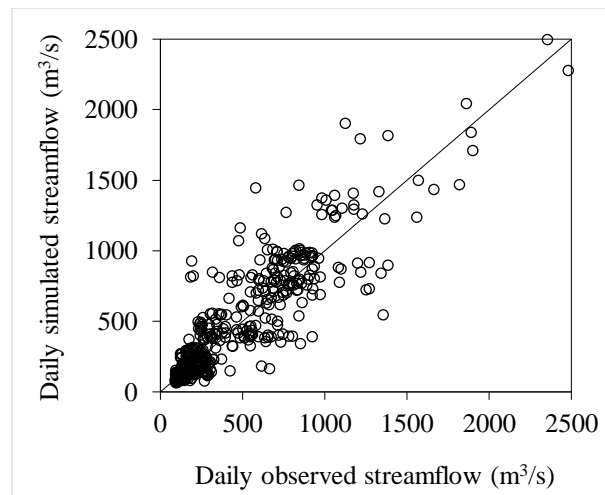


Figure C-9 Correlation between simulated and observed daily streamflow of validation at Hinhueb station

2) Monthly streamflow prediction

The monthly streamflow prediction at the basin outlet was calibrated with 10 years dataset of 2006–2015. The monthly streamflow prediction result was satisfied because the values of statistical indicators, namely, NSE and R^2 are all acceptable with values of 0.72 and 0.81, respectively. The observed and simulated hydrographs of the monthly streamflow (Figure C-10) and the scatter plot between the monthly observed and simulated streamflow (Figure C-11) also showed very good agreement. However, the result showed some overestimation in normal streamflow. Moreover, the observed streamflow data measured during the validation period with large flood occurred in 2008 and 2011. The result in Figure C-10 also revealed that IFAS performs well in flood years, which occurred in 2008 and 2011.

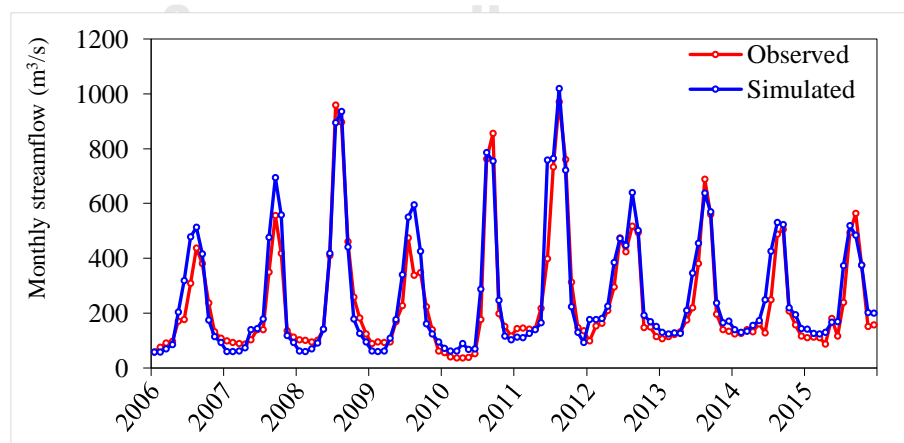


Figure C-10 Monthly streamflow from IFAS model validation compares with observation at Hinhueb station

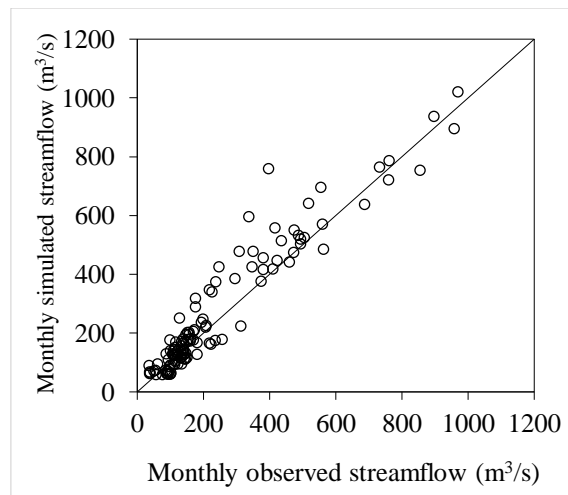


Figure C-11 Correlation between simulated and observed monthly streamflow of validation at Hinhueb station

C.4.4. Model application

1) Daily streamflow prediction

The model parameters from the calibration and validation of daily streamflow were applied for NB and NSan rivers in the years of 2008 and 2011. The simulated streamflow of NB and NSan results were presented in Figure C-12. The Figure 5-33 showed that the daily streamflow during the years of 2008 and 2011 varied from minimum to maximum of 8.3 mm to 193.5 mm, respectively, whereas the daily average was measured as 32.5 mm. For the NSan river, the result showed that daily streamflow were higher than the NB river with the minimum, maximum, and average of 22.6, 355.2, and 68.0 mm, respectively. Moreover, the streamflow in 2008 was slightly higher than that in 2011. This phenomenon may be due to the fact that the large flood occurred in 2008.

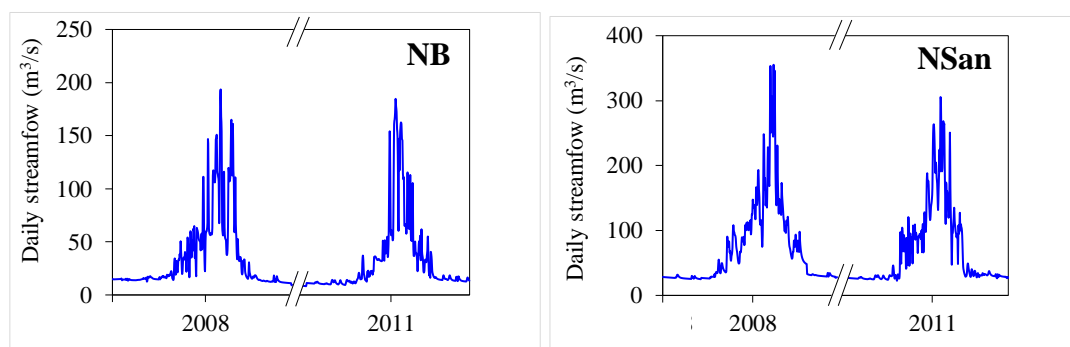


Figure C-12 Daily simulated streamflow of NB river and NSan river for flood years in 2008 and 2011

2) Monthly streamflow prediction

The model parameters from the calibration and validation of monthly streamflow were also applied for NB and NSan rivers in the period of 2012–2015. The total monthly streamflow of NB and NSan was compared with the streamflow calculated from the water balance equation (Figure C-13). The model validation shows good performance with $NSE = 0.78$ and $R^2 = 0.86$. The high level of NSE and R^2 values have been linked to the ability of IFAS model to capture the streamflow in NB and NSan catchments during the validation period. This finding indicated the acceptable performance of the IFAS model at a monthly time scale in limited data catchment.

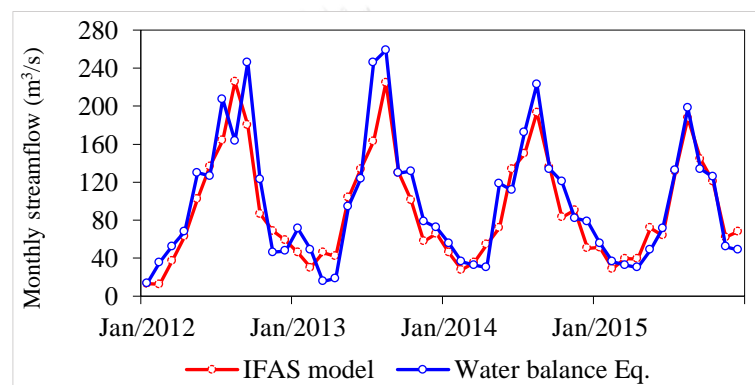


Figure C-13 Comparison between monthly streamflow from water balance equation and IFAS model (total NB and NSan)

Therefore, the IFAS model could be used to simulate the monthly streamflow in ungauged catchment, such as NB and NSan. However, the calculated streamflow for 2014 is slightly higher than that simulated by IFAS. Such discrepancy may be ascribed to the fact that the infiltration loss term is not considered in the water balance equation because of data limitation, thereby increasing the streamflow in some months.

C.4.5. Future streamflow scenarios

The rainfall–runoff model for future streamflow prediction was conducted using IFAS model. Daily streamflow was simulated over the wet years of the 6th, 7th, 11th, and 16th years, whereas monthly streamflow was simulated for 20 years under RCP4.5 and RCP8.5 scenarios. The daily streamflow was validated at the NP, NB, NSan, NL, and NN3 catchment outlets, whereas the monthly streamflow validated nearly the same catchments, except NL catchment. The NL is out of network for optimal reservoir operation simulation. The model application results of future daily and monthly streamflow predictions at the basin outlet were discussed as follows:

The result in the daily future streamflow prediction of all rivers under RCP4.5 and RCP8.5 scenarios is presented in Figure C-14. The future streamflow under RCP8.5 scenario is mostly higher than that under RCP4.5 scenario, especially in high streamflow period. Clearly, in Figure C-14, the future streamflow during wet years resulted in a similar trend of precipitation under RCP4.5 and RCP8.5 scenarios. The streamflow in the future period increased continuously and reduced after reaching the maximum streamflow in the 11th year under both RCPs scenarios. The result also illustrated that during the wet years, the large variation of daily streamflow occurred in the 11th year and followed by 16th year.

Figure C-15 illustrates the average monthly future streamflow during 2020–2039 under RCP4.5 and RCP8.5 scenarios. The result shows that the ranges of simulated streamflow in corresponding months for RCP4.5 scenario are 22.8–514.5 m³/s for NN3, 2.1–30.8 m³/s for NP, 10.8–108.8 m³/s for NB, 4.6–161.7 m³/s for NSan, and 4.3–141.0 m³/s for NS. For the RCP8.5 scenario ranges from 18.3–545.9 m³/s for NN3, 2.8–32.8 m³/s for NP, 8.1–114.5 m³/s for NB, 6.0–169.2 m³/s for NSan, and 4.5–147.3 m³/s for NS. The streamflow projection is similar to the projected precipitation pattern. High monthly streamflow is simulated over a time period for RCP8.5 compared with the RCP4.5 scenario for all rivers, except that some years are slightly less in low streamflow. Moreover, the future streamflow projection for NN3, NP, NB, NSan, and NS rivers for RCP4.5 scenario is predicted to increase by 4.8%, 2.9%, 3.5%, 3.2%, and 3.8%, respectively, while RCP8.5 scenario is predicted to increase by 5.3%, 3.1%, 4.7%, 4.9%, and 5.1%, respectively.

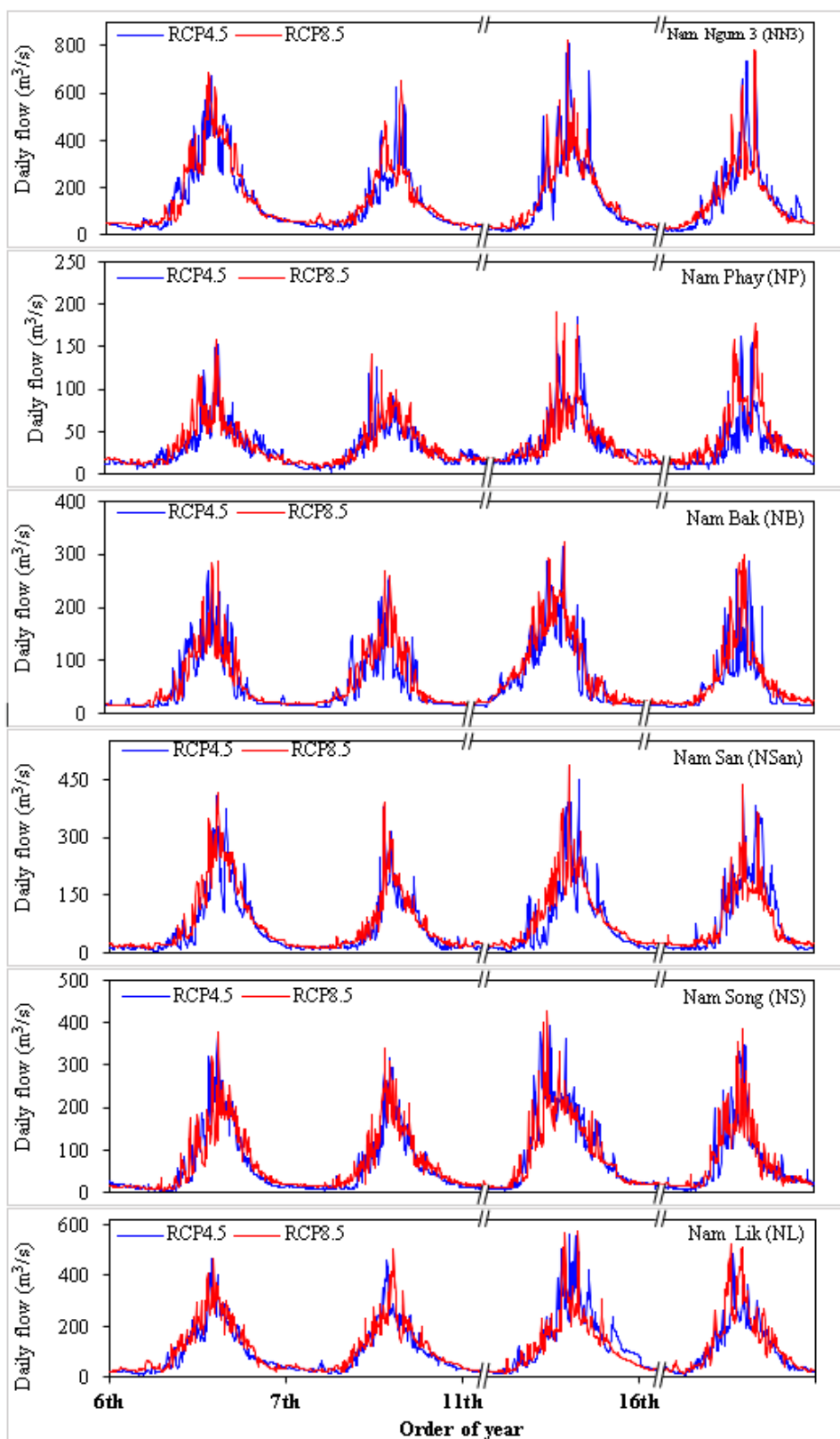


Figure C-14 Hydrograph of future daily streamflows of NN3, NNP, NB, NSan, NS, and NL rivers under RCP4.5 and RCP8.5 scenarios

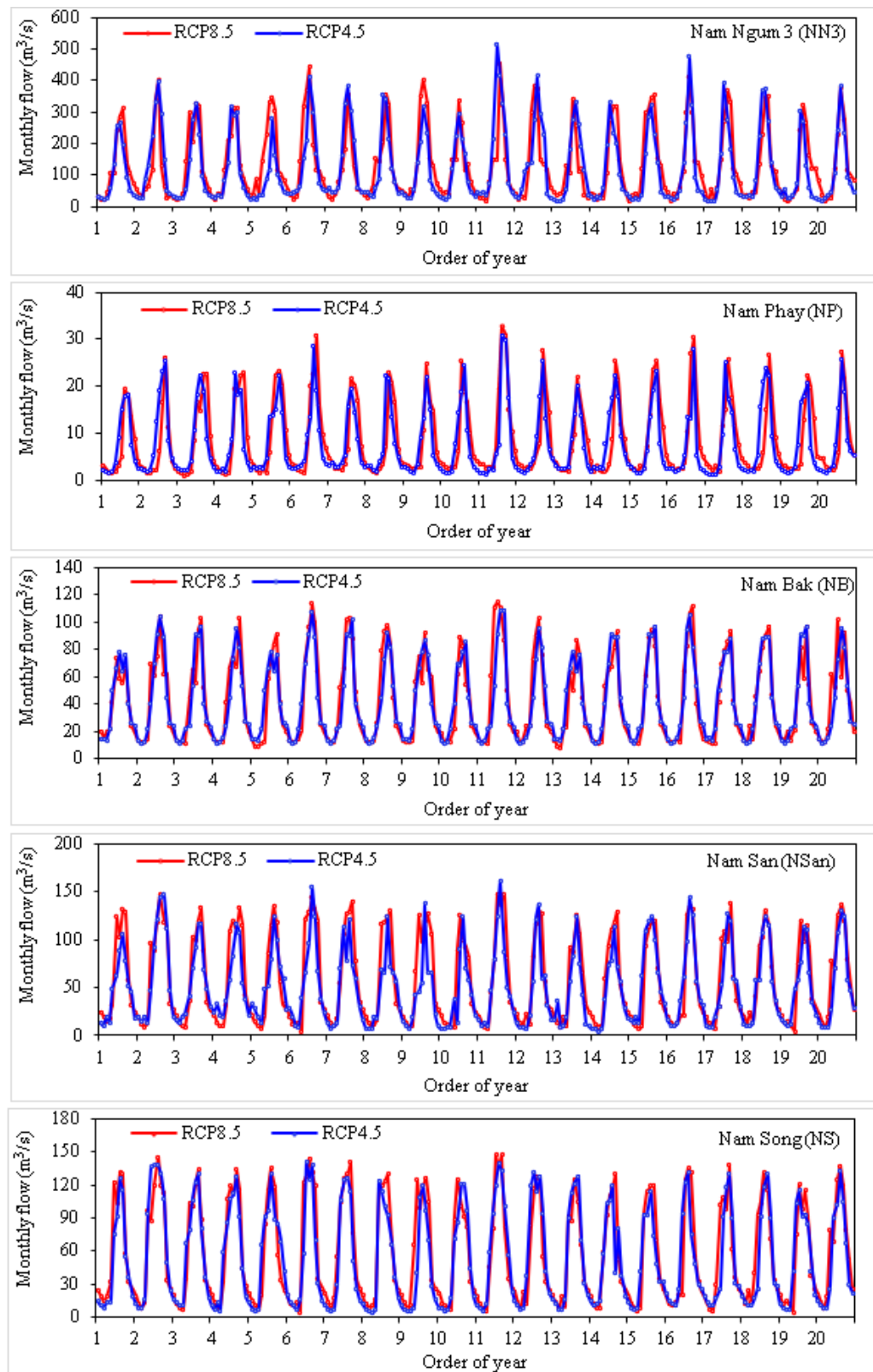


Figure C-15 Hydrograph of future monthly streamflows of NN3, NNP, NB, NSan, and NS rivers simulated using IFAS model under RCP4.5 and RCP8.5 scenarios

VITA

NAME Bounhome Kimmany

DATE OF BIRTH 03 March 1990

PLACE OF BIRTH Phongsaly, Laos

INSTITUTIONS ATTENDED Department of Water Resources Engineering, Faculty of Engineering, Chulalongkorn University

HOME ADDRESS Department of Meteorology and Hydrology, Faculty of Water Resources, National University of Laos

PUBLICATION

Kimmany, B., Sriariyawat, A., and Visessri, S. "Effectiveness of hydrologic models for streamflow simulation in the Nam Song River Basin". The 21st National Convention on Civil Engineering. 28 – 30 June 2016, Songkla, Thailand.

Kimmany, B., and Visessri, S. "Assessment of rainfall-runoff models for streamflow prediction in Nam Song River Basin". THA 2017 International Conference on "Water Management and Climate Change Towards Asia's Water-Energy-Food Nexus". 25 – 27 January 2017, Bangkok, Thailand.

Kimmany, B., and Visessri, S. "Optimal reservoir operation under inflow scenarios in Nam Ngum River Basin using Mixed-Integer Nonlinear Programming". THA 2019 International Conference on "Water Management and Climate Change Towards Asia's Water-Energy-Food Nexus and SDGs". 23 – 25 January 2019, Bangkok, Thailand.

Kimmany, B., Ruangrassamee, P., and Visessri, S. "Optimal multi-reservoir operation under inflow scenarios in Nam Ngum River Basin". Engineering Journal, vol. 24, no. 5, pp. 1-13, 2020.